Energy-efficient cooperative relay protocols for wireless sensor networks

Le-Quang-Vinh Tran

N° d'ordre : ANNÉE 2012

THÈSE / UNIVERSITÉ DE RENNES 1
sous le sceau de l'Université Européenne de Bretagne

pour le grade de

DOCTEUR DE L'UNIVERSITÉ DE RENNES 1

Mention : Traitement du Signal et Télécommunications

École doctorale MATISSE

présentée par

Le-Quang-Vinh TRAN

préparée à l'unité de recherche UMR6074 IRISA
Institut de recherche en informatique et systèmes aléatoires - CAIRN
École Nationale Supérieure des Sciences Appliquées et de Technologie

---

Energy-efficient cooperative relay protocols for wireless sensor networks

Thèse à soutenir à Lannion
Décembre 2012

devant le jury composé de :

GORCE Jean-Marie
Professeur à l'INSA Lyon / rapporteur

DIOURIS Jean-François
Professeur à Polytech Nantes / rapporteur

DENEIRE Luc
Professeur à l'Université de Nice / examinateur

MARY Philippe
Maître de conférences à l'INSA Rennes / examinateur

SENTIEYS Olivier
Professeur à l'Université de Rennes 1 / directeur de thèse

BERDER Olivier
Maître de Conférences à l'Université de Rennes 1/ co-directeur de thèse

Abstract

Wireless sensor networks (WSNs) consist of a large number of sensor nodes which are usually battery-powered and designed to operate for a long period of time. Consequently, minimizing the energy consumption is a very important design consideration in WSNs. In this thesis, based on cooperative relay techniques, a novel cooperative transmission protocol (i.e. the fully distributed space-time coded (fDSTC) protocol) and an energy efficient cooperative MAC protocol (i.e. RIC-MAC) are proposed and considered to minimize the total energy consumption for WSNs.

Recently, cooperative relay techniques (e.g. repetition-based or distributed space-time code based (DSTC-based) protocols) are increasingly of interest as one of the advanced techniques to mitigate the fading effects of transmisison channel. The fDSTC protocol is firstly proposed and compared with the conventional distributed space-time coded (cDSTC) protocol. Then, the thorough comparison of the fDSTC and cDSTC protocols in case of non-regenerative relays (NR-relays) and regenerative relays (R-relays) are considered in terms of error performance, outage probability, diversity order and energy consumption via both numerical simulations and mathematical analysis. In addition, the fDSTC protocol is verified via multi-antenna systems and shown to be more energy-efficient than the cDSTC protocol using either a typical energy model widely-used in the literature or a real energy model based on the PowWow platform. Besides, a mathematical analysis in terms of energy consumption is complementarily given to show how to choose the best cooperative models to prolong the lifetime of WSNs.

The aforementioned works consider the energy efficiency of the cooperative relays techniques under the view of ideal medium access control (MAC) protocol. However, the MAC protocol is responsible for regulating the shared wireless medium access of the networks, therefore, it has great influences on the total energy consumption of the networks. That leads to a big motivation to design cooperative MAC protocols, RIC-MAC and adaptive RIC-MAC, by combining preamble sampling and cooperative relay techniques.

The analytic results still confirm the interest of using cooperative relay techniques. However, the energy efficiency of the cooperative relay systems may be affected by the MAC protocol design, the traffic loads of the networks and the desired latency.

"We must not forget that when radium was discovered no one knew that it would prove useful in hospitals. The work was one of pure science. And this is a proof that scientific work must not be considered from the point of view of the direct usefulness of it. It must be done for itself, for the beauty of science, and then there is always the chance that a scientific discovery may become like the radium a benefit for humanity."

–Marie Curie–

Contents

Acronyms

ASEP	Average Symbol Error Probability
AF	Amplify and Forward
AWGN	Additive White Gaussian Noise
AGC	Automatic Gain Control
ARQ	Automatic Repeat-reQuest
ADC	Analog to Digital Converter
BER	Bit Error Rate
BPSK	Binary Phase-Shift Keying
cDSTC	conventional Distributed Space-Time Coded
CC	Coded Cooperation
CF	Compress and Forward
CSI	Channel State Information
CTS	Clear to Send
CTMRS	CSI-Timer Mapping Relay Selection
CDF	Cumulative Distribution Function
DSTC	Distributed Space-Time Coded
DMT	Diversity Multiplexing Tradeoff
DF	Decode and Forward
DAC	Digital to Analog Converter
DSP	Digital Signal Processing
EADST	Error Aware Distributed Space-Time
ECC	Error Correction Code
fDSTC	fully Distributed Space-Time Coded
GIRS	Geographic Information based Relay Selection
HARQ	Hybrid Automatic Repeat reQuest
ISI	Interference Inter-Symbol
ITRS	Incremental Transmission Relay Selection
LTE-Advanced	Long Term Evolution-Advanced
LOS	Line Of Sight

MAC	Medium Access Control
MIMO	Multi-Input Multi-Output
MRC	Maximum Ratio Combining
MGF	Moment Generating Function
MGFs	Moment Generating Functions
ML	Maximum Likelihood
MTP	Minimum Transmission Power
MRE	Maximum Residual Energy
MEI	Maximal Energy-efficiency Index
MOP	Minimum Outage Probability
MABC	Multiple-Access BroadCast
MSCR	MIMO Simple Cooperative Relay model
MNCR	MIMO Normal Cooperative Relay model
MFCR	MIMO Full Cooperative Relay model
NR-relays	Non Regenerative relays
OPA	Optimum Power Allocation
ORLF	Opportunistic Relay with Limited Feedback
OORS	Outage-Optimal Relay Selection
PDF	Probability Density Function
PARS	Power-Aware Relay Selection
PEP	Pairwise Error Probability
PA	Power Amplifier
PSD	Power Spectral Density
PAR	Peak-to-Average Ratio
PRCSMA	Persistent Relay Carrier Sensing Multiple Access
QoS	Quality of Service
R-relays	Regenerative relays
RTS	Request-to-Send
RF	Radio Frequency
SISO	Single-Input Single-Output
SNR	Signal to Noise Ratio
SER	Symbol Error Rate
SRS	Simple Relay Selection
SENS	Switched-and-Examined Node Selection
TDBC	Time Division BroadCast
WSNs	Wireless Sensor Networks

Notations

h_{ij}	channel coefficient of the link between terminal i and terminal j
Ω_{ij}	variance of h_{ij}
z_{ij}	AWGN noise of the link between terminal i and terminal j
N_ij	variance of noise z_{ij}
y_{ij}	the received signal at terminal j from terminal i
γ_{ij}	SNR of the link between terminal i and terminal j
γ_{sjd}	SNR of the source-destination link via relay j
$\bar{\gamma}_{ij}$	average SNR of γ_{ij}
y_d	the final combined signal at destination
γ_d	post-detection SNR at destination
γ_j	post-detection SNR at relay j
γ_d^U	upper bound of γ_d
γ_d^L	lower bound of γ_d
P_{γ_d}	error probability at destination
$P_{\gamma_d}^L$	lower bound on error probability at destination
$P_{\gamma_d}^U$	upper bound on error probability at destination
ϵ_s	source transmit power
ϵ_j	transmit power of relay j
x	transmit signal of source
G_j	amplifying factor of relay j
$M_{\gamma_{ij}}$	moment generating function of the link between terminal i and terminal j
$E_1(.)$	exponential integral function
P^{out}	outage probability
M_r	number of relays
$\boldsymbol{h_{ij}}$	channel coefficient vector of the link between terminal i and terminal j
$\boldsymbol{U}$	forwarded signal matrix of relays
$\boldsymbol{z_{ij}}$	AWGN noise vector of the link between terminal i and terminal j
u_j	forwarded signal of relay j
$Re\{.\}$	real part of a complex number

P_{PA}	power consumption of power amplifier
P_{DAC}	power consumption of DAC
P_{ADC}	power consumption of ADC
P_{IFA}	power consumption of IFA
P_{syn}	power consumption of frequency synthesizer
P_{filt}	power consumption of active filters at transmission side
P_{filr}	power consumption of active filters at receiver side
P_{mix}	power consumption of mixer
P_{LNA}	power consumption of LNA
L_s	system loss factor
N_0	single-sided thermal noise power spectral density
λ_c	carrier wavelength
G_t	transmitter antenna gain
G_r	receiver antenna gain
f_c	carrier frequency
P_{needed}^{Tx}	needed transmission power
P_c	power consumption of all circuit blocks
d_{sd}	transmission distance
pl	power loss factor
R_b	bit rate
R	spectral efficiency
M_{tx}	number of transmit antenna
M_{rx}	number of receive antenna
P_c^{tx}	circuit power consumption of transmitter
P_c^{rx}	circuit power consumption of receiver
E^b	total energy consumption per bit
P_T	total power consumption for transmitting
P_R	total power consumption for receiving
$P_{desired}^{Rx}$	desired receive power
N_f	noise figure
p_{2k}^j	conditional error probability at relay j on $x[2k]$
r	relative distance of relays
rr	relative inter-distance of relays
g	multiplexing gain
$d(g)$	diversity gain
R_b	bit rate
η	drain efficiency of RF power amplifier
ξ	peak-to-average ratio

M_{tx}	number of transmit antennas
M_{rx}	number of receive antennas
p_G	BER of good state
p_B	BER of bad state
p_{GB}	transition probability from good to bad state
p_{BG}	transition probability from bad to good state
π_G	average probability of being in good state
π_B	average probability of being in bad state
P_{tx}	power consumption level of transmit state
P_{rx}	power consumption level of receive state
P_{aq}	power consumption level of acquire state
P_{mn}	power consumption level of monitor state
P_{sp}	power consumption level of sleep state
T_{RTS}	time (second) to transmit RTS
T_{CTS}	time (second) to transmit CTS
T_{DATA}	time (second) to transmit DATA
T_{ACK}	time (second) to transmit ACK
T_{BZ}	time (second) to transmit BZ
δ_{tx}	average time of transmit state
δ_{rx}	average time of receive state
δ_{aq}	average time of acquire state
δ_{mn}	average time of monitor state
δ_{sp}	average time of sleep state
$E[N_{WB}]$	expected number of wakeup beacon
$E[N_{BZ}]$	expected number of BZ
p_{co}	collision rate
p_{WB}	probability that a wakeup beacon fails to be received
p_{RTS}	probability that an RTS is successfully responded with a CTS
L	average latency of a successful transmission
M	number of RTS slots
p_{f5}	handshake failure rate
n	number of neighbor nodes
T	wakeup period

List of Figures

List of Tables

Introduction

Energy is really not only a crucial factor for economic competitiveness and employment but also a vital key for human life. In fact, adequate and affordable energy supplies are significant to economic development and energy is indispensable to most industrial and commercial wealth. It is a sign for relieving poverty, improving human welfare and raising living standard. However, like the other resources (e.g. water, minerals, etc.) energy is limited. In addition, that energy needs nowadays increase quickly leads to many problems such as greenhouse effects, resource depletion, etc. Consequently, scientists have recently focused on the sustainable development (i.e. development that meets the needs of the present without promising the ability of future generations to meet their own needs). Therefore, sustainable energy defined as energy which is replenishable within a human lifetime and causes no long-term damage to the environment is a very hot topic. It includes renewable energy and energy efficiency. Renewable energy terminology (i.e. green energy) focuses on the ability of an energy source to continue providing energy without any significant negative impact to the environment. On the other hand, moving towards energy sustainability will require changes not only in the way energy is supplied, but in the way it is used with the objective of reducing the amount of required energy. It relates to energy efficiency that represents the main interest of this thesis.

In wireless communication network design and operation, financial and environmental considerations have motivated a trend to minimize the amount of energy consumption. Such a trend is referred to as green radio communications. In green radio communications, a main network design objective is to reduce the amount of energy consumption while maintaining satisfactory quality of service (QoS). Although silicon technology is progressing exponentially, doubling about every two years [1], processor power consumption is also increasing by 150% every two years [2]. In contrast, the improvement in

battery technology is much slower, increasing a modest 10% every two years [3], leading to an exponentially increasing gap between the demand for energy and the battery capacity offered. Futhermore, the shrinking device sizes are also imposing an ergonomic limit on the available battery capacity. Hence, energy efficiency is becoming more and more important for battery-driven wireless communication. Energy consumption is affected by all layers of system design, ranging from physical to application layers. In this thesis, we will focus on improving the energy efficiency of transmission and medium access control (MAC) protocols for resource-constrained networks such as wireless sensor networks (WSNs).

Multiple-input and multiple-ouput (MIMO) techniques have been shown to be capable to improving wireless system capacity and spectral efficiency [4]. In addition, it is also shown that further energy efficiency improvement is achievable by adapting multi-antenna encoding to channel conditions [5] (e.g. precoders, space-time codes, etc.). However, that a wireless sensor node can typically support only one antenna due to the limited size and cost makes the direct application of multi-antenna technique to distributed WSNs impractical. Fortunately, the sensor nodes can cooperate with each others to deploy a virtual MIMO transmission (i.e. cooperative MIMO) [6, 7] or exploit the spatial diversity (i.e. cooperative relay) [8]. Cooperative relay techniques, in which the neighbor nodes serve as the relay nodes to forward different faded signals to destination, are shown to be able to increase spectral efficiency [9] and provide significant energy efficiency improvement [10]. Thanks to these advantages, the cooperative relay techniques will be considered in this thesis as energy-efficient transmission protocols to achieve energy efficiency.

The advantages of cooperative relay techniques come with a signalling overhead and additional energy consumption. In addition, cooperation can also cause collisions that may affect throughput adversely and thus decrease energy efficiency due to its complicated transmission protocol. Therefore, MAC protocol has significant influences on the energy efficiency of the cooperative relay techniques. Since MAC layer is responsible for regulating the shared wireless medium access of the networks, the energy-efficient MAC protocols for cooperative strategies will be thoroughly designed and considered in this thesis in order to further improve the benefits of the cooperative relay techniques and reduce their inconveniences such as delay, collision, etc.

Thesis contributions

In this thesis, based on existing cooperative relay techniques in the literature, a new energy-efficient cooperative relay technique, called fully distributed space-time coded (fDSTC) protocol is proposed to improve the performances of cooperative relay systems [a]. The fDSTC protocol in which relays will use distributed space-time codes (DSTC) to forward their received signals to destination belongs to DSTC-based cooperative relay techniques. However, unlike conventional DSTC (cDSTC) protocol existing in the literature, in the fDSTC protocol the relays will exchange their data with each other before the forwarding phase.

Besides energy efficiency which is the main concern of this thesis, the error performance, spectral efficiency and diversity order of the fDSTC protocol, using non-regenerative relays (NR-relays) and regenerative relays (R-relays), are also thoroughly considered and compared with the cDSTC protocol. It is proved in this thesis through mathematical analysis and numerical simulations that the fDSTC protocol outperforms the cDSTC protocol in terms of error performance, spectral efficiency, diversity order and of course energy efficiency [b].

The fDSTC protocol is then exploited in MIMO systems to show the interest of the association between cooperative relay techniques and MIMO techniques to further improve the performances of wireless systems [c]. In addition, two precise energy models, one based on an artificial energy model widely used in the literature, the other based on real energy model developed by CAIRN/IRISA, are presented to accurately evaluate the energy consumption of the systems [d,e].

Finally, new MAC protocols for cooperative relay systems are proposed to completely consider the energy efficiency of cooperative relay systems from physical to MAC layers [f]. RIC-MAC, i.e. cooperative MAC protocol based on fixed relay, is shown to be able to gain energy as compared to single-input single-output (SISO) systems and multi-hop SISO systems. Moreover, adaptive RIC-MAC, i.e. RIC-MAC with relay selection technique, is shown to further increase the energy efficiency of the cooperative relay systems.

Structure of the thesis

Chapter 1: Cooperative relay techniques

In this chapter, most of the existing works concerning cooperative relay techniques are re-presented. Cooperative relay techniques are classified into two main categories based on the method that relays forward their signals to destination, i.e. repetition-based and DSTC-based cooperative relay techniques. Moreover, some advanced techniques such as relay selection, power allocation and two-way relays are shown to be able to combine with cooperative relay techniques to further improve the performances of cooperative relay systems. At the end of this chapter, some numerical results are figured out to illustrate the outperformance of cooperative relay techniques with or without the combination with the advanced techniques.

Chapter 2: Fully distributed space-time codes

The fDSTC protocol is firstly proposed and considered using both NR-relays and R-relays. In terms of error performance, the average symbol error probability (ASEP) is explicitly derived to verify the numerical simulations. In addition, outage probability of the protocols is also thoroughly given through mathematical approximation and numerical simulations. Then, the diversity multiplexing trade-off (DMT) and maximum diversity order of the protocols are derived. In terms of energy efficiency, two energy models (i.e. typical and real energy models) used to evaluate the energy consumption of the cooperative systems throughout this thesis are also re-presented. Besides, the best power allocation among the transmitters is also considered through simulations to further increase the BER performance of the fDSTC protocol.

Chapter 3: MIMO cooperative relay systems

In this chapter, the fDSTC and cDSTC protocols are once again considered, however in the context of MIMO systems. The association of cooperative relay techniques and MIMO techniques are shown to further increase the system performance in terms of error performance and energy efficiency. Besides, a thorough analysis on energy consumption of cooperative relay systems is given to show the best cooperative strategy. In addition, the

effect of synchronization error on the bit error rate (BER) performance is also thoroughly considered.

Chapter 4: MAC protocols for low-power cooperative sensor networks

This chapter proposes MAC protocols for low-power cooperative sensor networks. Detailedly, MAC protocols based on preamble sampling or low power listening techniques, well-known as energy efficient techniques, are designed for cooperative relay systems. RIC-MAC, a cooperative MAC protocol using receiver initiated techniques [11], is considered for fixed relay networks in terms of average energy consumption per packet and latency. The total energy consumption is derived through mathematical analysis with the help of two energy models presented in Chapter 2. The effect of traffic load on the energy consumption and latency is also considered. In addition, adaptive RIC-MAC, association RIC-MAC with relay selection technique, is shown to be able to further increase the energy efficiency of RIC-MAC.

Finally, the conclusions and perspectives are given individually at the end of this thesis.

Publications

[a] L.Q.V. Tran, O. Berder, and O. Sentieys, "Non-Regenerative Full Distributed Space Time Codes in Cooperative Relaying Model", IEEE Wireless Communications & Networking Conference (WCNC), 28-31/03/2011, pp. 1529-1533.

[b] L.Q.V. Tran, O. Berder, and O. Sentieys, "On the performance of fully distributed space-time coded protocol", submitted to EURASIP Journal on Wireless Communications and Networking.

[c] L.Q.V. Tran, O. Berder, and O. Sentieys, "Spectral Efficiency and Energy Efficiency of Distributed Space-Time Relaying models", in Proceedings of IEEE Consumer Communications & Networking Conference (CCNC), 09-12/01/2011, pp. 1088-1092.

[d] L.Q.V. Tran, O. Berder, and O. Sentieys, "Energy Efficiency of Cooperative Strategies in Wireless Sensor Networks", in Proceedings of IEEE Conference on Advanced Technologies for Communications (ATC), 20-22/10/2010, pp. 29-32.

[e] L.Q.V. Tran, O. Berder, and O. Sentieys, "Efficacité Spectrale et Energétique des Systèmes de Relais", Actes du Gretsi, 5-8/09/2011, Bordeaux, France.

[f] L.Q.V. Tran, O. Berder, and O. Sentieys, "RIC-MAC: a MAC Protocol for Low-Power Cooperative Wireless Sensor Networks", to be submitted to IEEE Transactions on Vehicular Technology (Correspondence).

Chapter 1

Cooperative Relay Techniques

1.1 Introduction

In wireless communications, the quality of a received signal is attenuated by not only additive noise, but also path-loss and multi-path fading effects. These challenges can be traditionally overcome by high reliable transmission, e.g. sophisticated coding, which leads to complicated signal processing. However, it is not suitable for small-device and resource-constrained wireless networks such as wireless sensor networks (WSNs). Recently, new solutions to exploit the multi-path propagation, i.e. cooperative communications, are proposed to combat fading effects [8, 12]. In fact, cooperative communications are considered to exploit spatial diversity gains via cooperation of user terminals without the need of multiple antenna transceiver. Two well-known cooperative communication techniques are cooperative MIMO and cooperative relay. In cooperative MIMO, two neighbor terminals collaborate in the first transmission phase and serve as a virtual MIMO antenna array [10]. In cooperative relay, the terminals acting as relays do not have data to transmit. They only forward copied versions of data to destination to achieve the spatial diversity, thus increasing performance of the original transmission (i.e. source-destination transmission) [12].

Although cooperative MIMO is also well-known as an advanced technique to replace traditional MIMO [6, 7], the inter-communication between neighbor nodes is assumed to be free error or the distance [6, 7] between neighbor nodes is considered as much

smaller than the transmission distance [10]. That limits the application range of cooperative MIMO in reality. On the other hand, in cooperative relay techniques, relays can be placed anywhere, but in the communication range between source and destination. In WSNs, sensor nodes are randomly distributed. The hard constraint of the distance between neighbor nodes, therefore, may not be satisfied. Considering the general WSNs, in this thesis, we only focus on cooperative relay techniques. Based on the transmission protocol at relays, we can classify them into two main categories: repetition-based and distributed space-time code-based (DSTC-based) cooperative relay techniques [9]. In repetition-based cooperative relay techniques, each relay after receiving signal from source will consecutively forward the signal to destination. Each transmitted signal (including the original one transmitted from source to destination) is passed through multiple independent paths and thus, the probability that the signal fails to reach the destination is significantly reduced. In contrast to repetition-based cooperative relay techniques, in DSTC-based cooperative relay techniques, the relays will take advantages of distributed space-time coded (DSTC) protocol to simultaneously forward the signal to the destination and hence, the spectral efficiency of the system is increased.

Besides, it is also claimed that advantages of cooperation can be further exploited by applying some advanced techniques in the cooperative relay systems such as power allocation, relay selection, two-way relay, etc. [13–15]. On the one hand, without knowing the channel conditions, each terminal is given a fair opportunity of utilizing the cooperative relaying channel. However, if the channel conditions (i.e. channel state information (CSI)) are available to the terminals, the resource usage or traffic load can be redistributed to improve the communication efficiency [13]. On the other hand, optimal relay selection is also important for reaping the performance benefit of cooperative relay techniques [14]. Recently, bidirectional relays or two-way relays are also investigated to improve bandwidth efficiency of cooperative relay systems [15].

The rest of this chapter is organized as follows. Section 1.2 will present the repetition-based cooperative relay techniques. The DSTC-based cooperative relay techniques will be presented in Section 1.3. Then, in Section 1.4, some advanced techniques for cooperative relay systems are presented to further exploit the best performance of cooperative relay techniques. The performance of the cooperative relay systems will be re-simulated to once again confirm their advantages over SISO system in Section 1.5. Finally, conclusion is given in Section 1.6.

1.2 Repetition-based cooperative relay techniques

Based on signal processing at relays before the relays forward signal to the destination, the relays can be classified as non-regenerative (NR) or amplify-and-forward (AF) relays, regenerative (R) or decode-and-forward (DF) relays, coded cooperation (CC) relays, and compress-and-forward (CF) relays. For NR-relays, the relays simply amplify the received signal from the source and forward it directly and consecutively to the destination without decoding. For R-relays, the relays will firstly decode the received signal and then forward the decoded signal to the destination. When the decoded signal is additionally encoded to provide additional error protection to the original signal, it is referred to the case of CC-relays. On the other hand, in CF-relays, the relays retransmit a quantized or compressed version of the received signal, exploiting the statistical dependencies between the signal received at the relays and that received at the destination. Among these relays, NR-relays and R-relays are the most popular one due to their simplicity and intuitive designs. Therefore, they will be considered in this thesis. In order to evaluate the

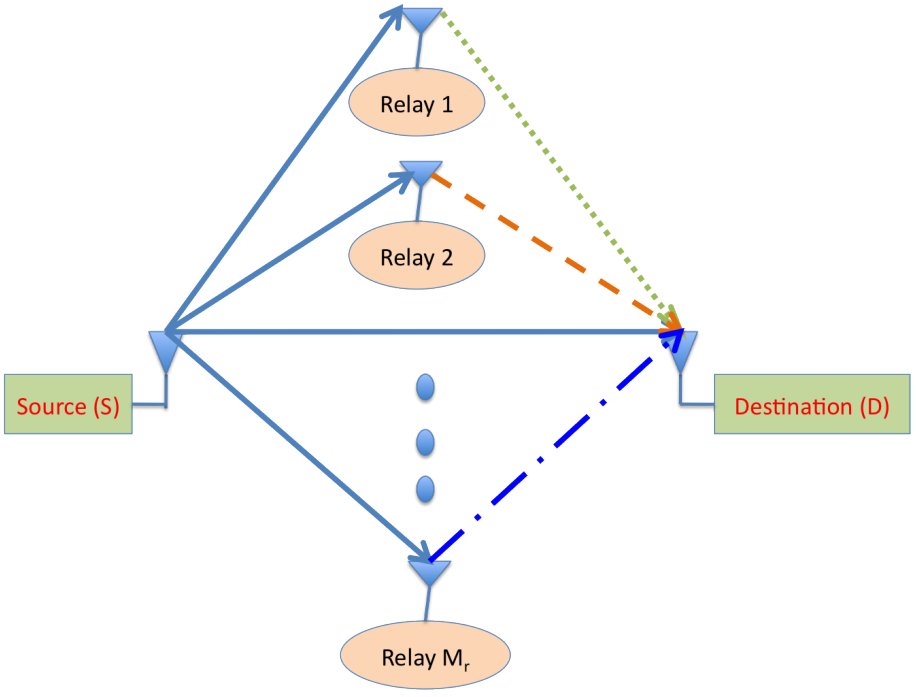

FIGURE 1.1: Repetition-based cooperative relay system

performance of the repetition-based cooperative relay techniques, the system with one source, M_r relays and one destination which all equipped with one antenna is considered (Fig. 1.9). In repetition-based cooperative relay techniques, the transmission protocol is composed of two phases. In the first phase, the source will simultaneously transmit its

signal to the relays and the destination. The received signal at the destination, y_{sd} is

$$y_{sd} = \sqrt{\epsilon_s} h_{sd} x + z_{sd}, \tag{1.1}$$

and the received signal at the relay j, y_{sj} is represented as

$$y_{sj} = \sqrt{\epsilon_s} h_{sj} x + z_{sj}, \quad j \in \{r_1, r_2, ..., r_{M_r}\}, \tag{1.2}$$

where h_{sd}, h_{sj} are the channel coefficients of the transmission link from the source to the destination and the relay j respectively; z_{sd} and z_{sj} are the noise at the destination and the relay j and ϵ_s is the source transmit power.

1.2.1 NR-relays

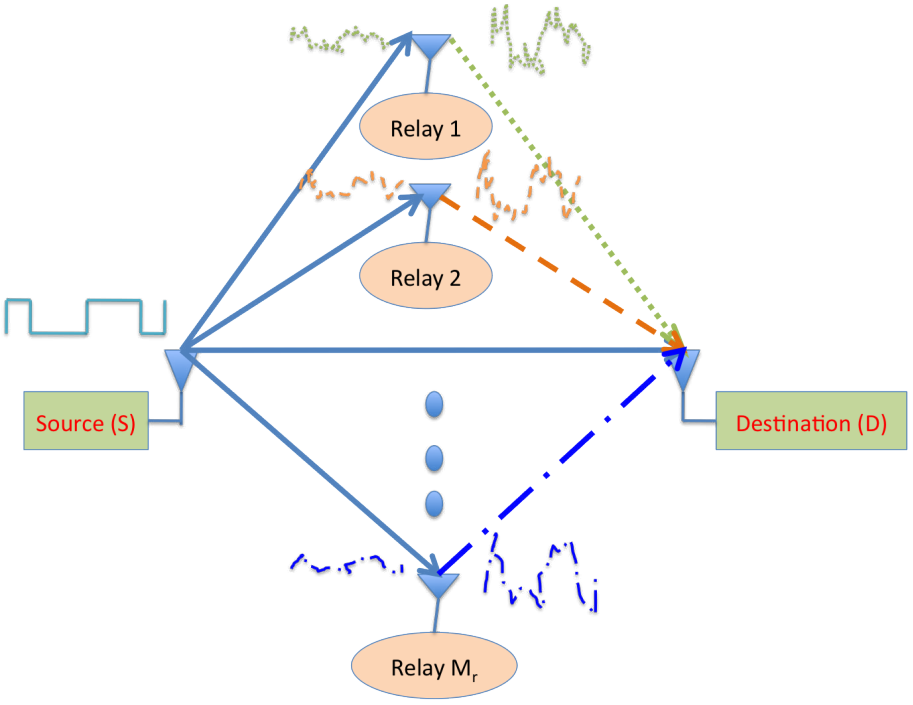

FIGURE 1.2: Repetition-based cooperative relay system using NR-relays

With NR-relays, after receiving a noisy version of the signal transmitted from the source, the relays just amplify and then consecutively retransmit this noisy version to the destination (Fig. 1.2). The signal received at the destination from the relay j is expressed as

$$y_{jd} = G_j h_{jd} x + z_{jd}, \quad j \in \{r_1, r_2, ..., r_{M_r}\}, \tag{1.3}$$

with h_{jd} and z_{jd} the channel and noise coefficients of the link between the relay j and the destination respectively and $G_j = \sqrt{\frac{\epsilon_j}{|h_{sj}|^2\epsilon_s+N_{sj}}}$ the amplifying factor [12] of the relay j where ϵ_j is the transmit power of the relay j and N_{sj} is the variance of the additive noise z_{sj}.

The destination firstly combines the signals received from the source and the relays by using the maximal ratio combining (MRC) technique and then makes a final decision. Although the noise is also amplified at the NR-relays, the destination node receives $M_r + 1$ independently faded versions of the transmit signal. Therefore, it can exploit the diversity gain to make a more precise decision on the final combined signal. Using the MRC technique, the combined signal at the destination is given by

$$y_d = \frac{\sqrt{\epsilon_s}h_{sd}^*}{N_{sd}}y_{sd} + \sum_{j\in\{r_1,r_2,\ldots,r_{M_r}\}} \frac{h_{jd}^* G_j^* h_{sj}^*}{|h_{jd}|^2|G_j|^2N_{jd} + N_{sj}}y_{jd}. \tag{1.4}$$

Then the total signal to noise ratio (SNR) at the destination can be derived as

$$\begin{aligned}\gamma_d &= \gamma_{sd} + \sum_{j\in\{r_1,r_2,\ldots,r_{M_r}\}} \frac{\gamma_{sj}\gamma_{jd}}{\gamma_{sj}+\gamma_{jd}+1}, \\ &= \gamma_{sd} + \sum_{j\in\{r_1,r_2,\ldots,r_{M_r}\}} \gamma_{sjd},\end{aligned} \tag{1.5}$$

where $\gamma_{sj} = \frac{\epsilon_s|h_{sj}|^2}{N_{sj}}$ is the SNR of the link between the source and the relay j, $\gamma_{jd} = \frac{\epsilon_j|h_{jd}|^2}{N_{jd}}$ is the SNR of the link between the relay j and the destination, $\gamma_{sd} = \frac{\epsilon_s|h_{sd}|^2}{N_{sd}}$ is the SNR of the source-destination link, and γ_{sjd} is the SNR of the transmission from the source to the destination via the relay j.

The average symbol error probability (ASEP) of the repetition-based cooperative relay system using NR-relays based on moment generating function based (MGF-based) approach of [16, Eq. 9.12] for BPSK simulation can be derived as

$$P_{\gamma_d} = \frac{1}{\pi}\int_0^{\pi/2} \frac{\prod_{j\in\{r_1,r_2,\ldots,r_{M_r}\}} M_{\gamma_{sjd}}(-\frac{g_{BPSK}}{sin^2\theta})}{1+\frac{g_{BPSK}\overline{\gamma_{sd}}}{sin^2\theta}}d\theta, \tag{1.6}$$

where $M_{\gamma_{sjd}}$ [17, Eq. 13] is the moment generation function of the source-destination link via the relay j, $g_{BPSK} = 1$ [16] and $M_{\gamma_{sd}} = \left(1+\frac{g_{BPSK}\overline{\gamma_{sd}}}{sin^2\theta}\right)^{-1}$ [16, Tab 9.1]. The

moment generating function (MGFs) of $\{\gamma_{sjd}\}_{j\in\{r_1,r_2,...,r_{M_r}\}}$ are found in [17]

$$M_{\gamma_{sjd}}(s) = \frac{\bar{\gamma}_{1,j}\bar{\gamma}_{2,j} - 4\bar{\gamma}_{3,j}}{\bar{\gamma}_{4,j}^2} - \frac{s\bar{\gamma}_{3,j}\big(\bar{\gamma}_{4,j} + 2\bar{\gamma}_{3,j}\big)}{\bar{\gamma}_{4,j}^3} e^{\frac{\bar{\gamma}_{2,j}-\bar{\gamma}_{4,j}}{2\bar{\gamma}_{3,j}}} E_1\Big(\frac{\bar{\gamma}_{2,j}-\bar{\gamma}_{4,j}}{2\bar{\gamma}_{3,j}}\Big) \\ \frac{s\bar{\gamma}_{3,j}\big(\bar{\gamma}_{4,j} - 2\bar{\gamma}_{3,j}\big)}{\bar{\gamma}_{4,j}^3} e^{\frac{\bar{\gamma}_{2,j}+\bar{\gamma}_{4,j}}{2\bar{\gamma}_{3,j}}} E_1\Big(\frac{\bar{\gamma}_{2,j}+\bar{\gamma}_{4,j}}{2\bar{\gamma}_{3,j}}\Big), \tag{1.7}$$

where $\bar{\gamma}_{1,j} = \bar{\gamma}_{sj} + \bar{\gamma}_{jd}$, $\bar{\gamma}_{3,j} = \bar{\gamma}_{sj}\bar{\gamma}_{jd}$, $\bar{\gamma}_{2,j} = \bar{\gamma}_{1,j} - \bar{\gamma}_{3,j}s$, $\bar{\gamma}_{4,j} = \sqrt{\bar{\gamma}_{2,j}^2 - 4\bar{\gamma}_{3,j}}$, $\bar{\gamma}_{sj}$ and $\bar{\gamma}_{jd}$ are respectively the mean of the random variable γ_{sj} and γ_{jd} which have exponential distribution and $E_1(.)$ is the exponential integral function defined in [18, Eq. 5.11]. The proof of (1.7) is given in [17, Appendix A].

With the assumption that $\epsilon_s = \epsilon_j$ and $N_{sd} = N_{sj} = N_{jd} = N_0, \forall j$, the outage probability of the system in high SNR region can be approximated as [19, Eq. 32]

$$P^{out} \sim \frac{1}{(M_r+1)!}\frac{1}{\Omega_{sd}^2} \prod_{j\in\{r_1,r_2,...,r_{M_r}\}} \frac{\Omega_{sj}^2 + \Omega_{jd}^2}{\Omega_{sj}^2\Omega_{jd}^2}\Big(\frac{2^{(M_r+1)R}-1}{SNR}\Big)^{M_r+1}, \tag{1.8}$$

where Ω_{sd}^2, Ω_{sj}^2 and Ω_{jd}^2 are the variances of the channel coefficient h_{sd}, h_{sj} and h_{jd} respectively, R is the spectral efficiency and $SNR = \epsilon_s/N_0$. Therefore, the maximum diversity order of the system can be illustrated to be equal to $M_r + 1$.

1.2.2 R-relays

In the second phase of the repetition-based cooperative relay techniques, instead of just amplifying the analog received signal as in NR-relays, the R-relays will attempt to decode the received signal and then retransmit the detected signal to the destination as shown in Fig. 1.3. Let $\hat{x_j}$ is the detected signal at the relay j, the received signal at the destination from the relay can be expressed as

$$y_{jd} = \sqrt{\epsilon_j}h_{jd}\hat{x}_j + z_{jd}, \quad j \in \{r_1, r_2, ..., r_{M_r}\}. \tag{1.9}$$

The combined signal using the MRC technique is

$$y_d = \frac{\sqrt{\epsilon_s}h_{sd}^*}{N_{sd}}y_{sd} + \sum_{j\in\{r_1,r_2,...,r_{M_r}\}} \frac{\sqrt{\epsilon_j}h_{jd}^*}{N_{jd}}y_{jd}. \tag{1.10}$$

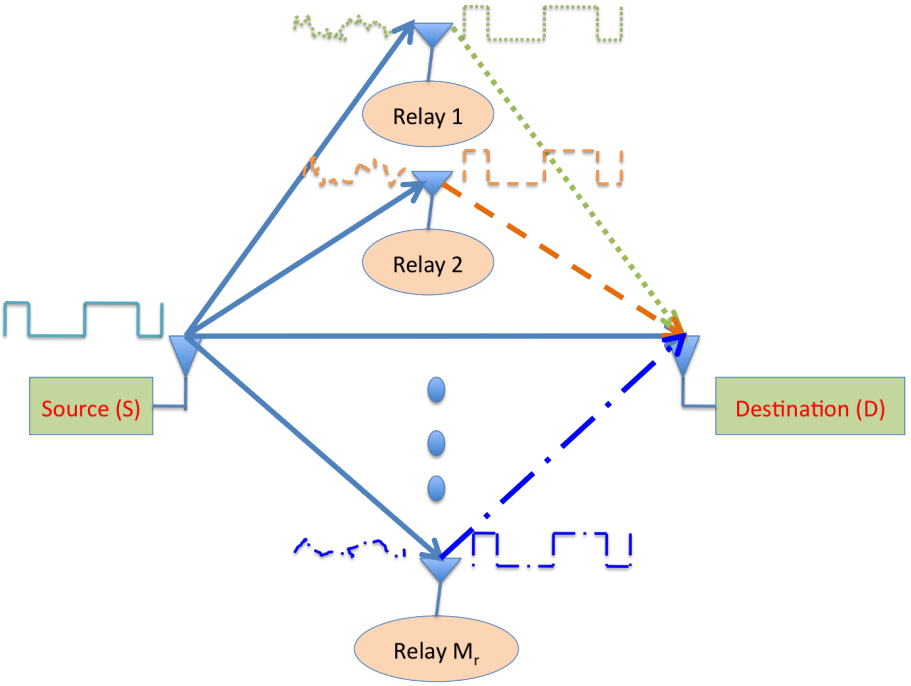

FIGURE 1.3: Repetition-based cooperative relay system using R-relays

If the signal is perfectly decoded at the relays, the total SNR at the destination is given by

$$\gamma_d = \gamma_{sd} + \sum_{j \in \{r_1, r_2, \ldots, r_{M_r}\}} \gamma_{jd}. \tag{1.11}$$

By using the R-relays, the noise amplification drawback of the NR-relays can be eliminated. As we see, if there is no error decoding at the R-relays, the total SNR at the destination is greater than that in case of NR-relays. However, if the detection at the R-relays is not reliable, the performance of the MRC combination at the destination may be quickly degraded which leads to a worse performance in comparison with NR-relays.

Due to the nonlinear characteristic of the maximum likelihood (ML) decoder at the relays, exact analysis in terms of error performance of the cooperative relay systems with R-relays is considered as a challenging problem. However, in [20] the authors gave an attempt to derive exact expressions for the BER of the cooperative system employing a single R-relay. Then these results are extended to the case of multiple R-relays for the piecewise linear combiner, known to be a close approximation of the ML detector.

Besides, the outage probability of the cooperative relay system with one R-relay in high SNR region is shown in [9] as

$$P^{out} \sim \frac{1}{\Omega_{sr_1}^2} \frac{2^{2R}-1}{SNR}. \tag{1.12}$$

The result in (1.12) indicates that the cooperative relay system with R-relays does not offer maximum diversity gains for high SNR, because requiring the R-relays to fully decode the source signal limits the performance of R-relays to that of direct transmission between the source and relays. To exploit full spatial diversity and overcome the shortcomings of the R-relays in the cooperative relay system, the relay selection technique will be used as presented in Section 1.4.

1.3 DSTC-based cooperative relay techniques

The DSTC-based cooperative relay techniques are also composed of two phases of communication. The first phase is the signal broadcast from the source to the relays and the destination. In the second phase, instead of the consecutive signal transmission of each relay to the destination, all the relays will simultaneously forward the received signal to the destination using a space-time block code [5, 21] (e.g. Alamouti or Tarokh, etc.) as shown in Fig. 1.4. That leads to more bandwidth efficiency or spectral efficiency in comparison with the repetition-based cooperative relay model.

The received signals at the destination and the relays in the broadcast phase are illustrated in (1.1) and (1.2) respectively. We assumed that the channel coefficients remain the same for M_r consecutive time intervals. Then, the signals received at the destination from the relays, $\boldsymbol{y_{rd}}$ are given by

$$\boldsymbol{y_{rd}} = \boldsymbol{U}\boldsymbol{h_{rd}} + \boldsymbol{z_{rd}}, \tag{1.13}$$

where $\boldsymbol{h_{rd}} = \begin{bmatrix} h_{r_1 d} & h_{r_2 d} & \dots & h_{r_{M_r} d} \end{bmatrix}^T$ is the Rayleigh channel coefficient vector, $\boldsymbol{z_{rd}}$ is the AWGN noise vector at the destination and $\boldsymbol{U}$ is the forwarded signal matrix. The dimension of $\boldsymbol{y_{rd}}$ and $\boldsymbol{z_{rd}}$ vectors depends on the dimension of the $\boldsymbol{U}$ matrix. Based on the type of relays (i.e. NR-relays or R-relays), the components of $\boldsymbol{U}$ matrix will be correspondently designed.

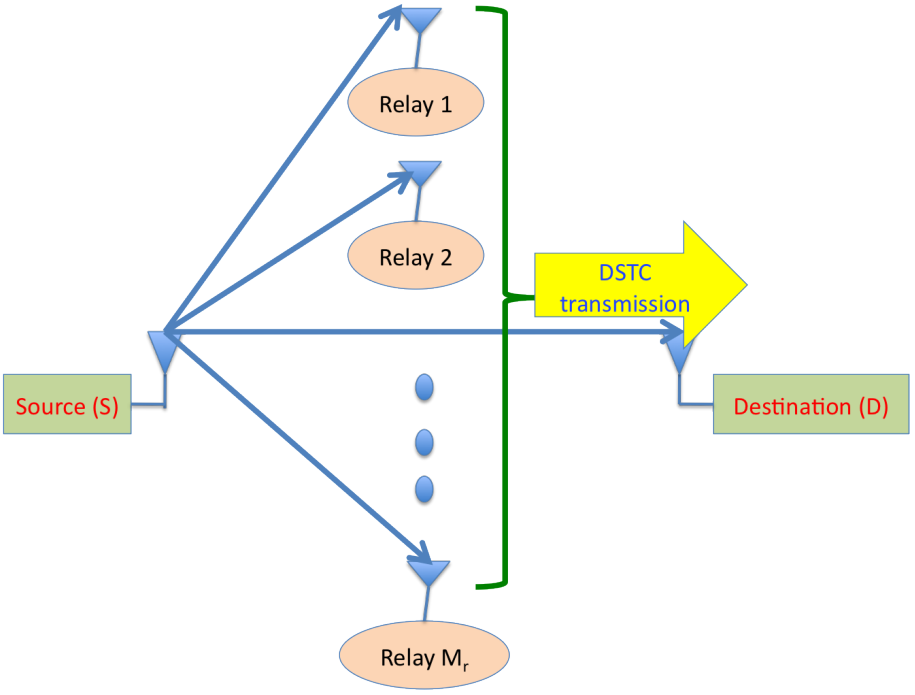

FIGURE 1.4: DSTC-based cooperative relay system

1.3.1 NR-relays

In case of NR-relays, the $\boldsymbol{U}$ matrix is designed using orthogonal space time block code [21] based on the basic component of u_j which is the forwarded signal at the relay j, $j \in \{r_1, r_2, ..., r_{M_r}\}$ and is given by

$$u_j = G_j y_{sj}, \tag{1.14}$$

with G_j the amplifying factor of the relay j.

Based on different assumptions on channel state information (CSI) knowledge at the relays, several amplifying factors are chosen to satisfy an average output energy constraint per symbol.

- Case 1: when there is no instantaneous CSI at the relays, but statistical CSI is available, G_j is given by [22]

$$G_j = \sqrt{\frac{\epsilon_j}{\epsilon_s \Omega_{sj}^2 + N_{sj}}}. \tag{1.15}$$

This amplifying factor ensures that an average output energy per symbol is maintained, but allows the instantaneous output power to be much larger than the average.

- Case 2: if the relays know backward channel coefficients h_{sj}, the following amplifying factor can be used [23]

$$G_j = \sqrt{\frac{\epsilon_j}{\epsilon_s \Omega_{sj}^2 + N_{sj}}} \frac{h_{sj}^*}{|h_{sj}|}. \tag{1.16}$$

  Although in this case, the instantaneous output power may be larger than the average, unlike case 1, all existing space-time block codes can be used.

- Case 3: to prevent saturating the relay amplifier, automatic gain control (AGC) adjusts the input power to the amplifier and facilitates controlling the instantaneous output power of each relay so that it remains constant. An appropriate amplifying factor for this case is given by [17]

$$G_j = \frac{h_{sj}^*}{|h_{sj}|} \sqrt{\frac{\epsilon_j}{\epsilon_s |h_{sj}|^2 + N_{sj}}}. \tag{1.17}$$

The Alamouti receiver is used at the destination to process the signals received from the relays. In order to recover the original transmit signal, the output of the Alamouti receiver is combined with the signal received from the source $\boldsymbol{y_{sd}}$ using MRC technique. As a result, the post-detection SNR at the destination can de derived as

$$\gamma_d = \gamma_{sd} + \frac{\epsilon_s \left(\sum_{j \in \{r_1, r_2, \ldots, r_{M_r}\}} |h_{sj} G_j h_{jd}|^2 \right)^2}{\sum_{j \in \{r_1, r_2, \ldots, r_{M_r}\}} N_{sjd} |h_{sj} G_j h_{jd}|^2}, \tag{1.18}$$

where $N_{sjd} = |h_{jd} G_j|^2 N_{sj} + N_{jd}$. If N_{sjd} is constant $\forall j$, [24, Eq. 13] can be re-found

$$\gamma_d = \gamma_{sd} + \frac{\epsilon_s \sum_{j \in \{r_1, r_2, \ldots, r_{M_r}\}} |h_{sj} G_j h_{jd}|^2}{\sum_{j \in \{r_1, r_2, \ldots, r_{M_r}\}} \left(|h_{jd} G_j|^2 N_{sj} + N_{jd} \right)}. \tag{1.19}$$

If the amplifying factor of case 1 and case 2 is used, the post-detection SNR at the destination can be expressed as

$$\begin{aligned}\gamma_d &= \gamma_{sd} + \sum_{j\in\{r_1,r_2,\ldots,r_{M_r}\}} \frac{\frac{\epsilon_s\epsilon_j}{\epsilon_s\Omega_{sj}^2+N_{sj}}}{\sum_{j\in\{r_1,r_2,\ldots,r_{M_r}\}} \frac{\epsilon_j}{\epsilon_s\Omega_{sj}^2+N_{sj}}\Omega_{jd}^2 N_{sj} + N_{jd}} |h_{sj}h_{jd}|^2 \\ &= \gamma_{sd} + \sum_{j\in\{r_1,r_2,\ldots,r_{M_r}\}} \mu_{sjd}|h_{sj}h_{jd}|^2 \\ &= \gamma_{sd} + \sum_{j\in\{r_1,r_2,\ldots,r_{M_r}\}} \gamma_{sjd}.\end{aligned} \tag{1.20}$$

Then, the MGFs of $\{\gamma_{sjd}\}_{j\in\{r_1,r_2,\ldots,r_{M_r}\}}$ are derived as shown in [24]

$$M_{\gamma_{sjd}}(s) = \frac{1}{s\mu_{sjd}\Omega_{sj}^2\Omega_{jd}^2} e^{\frac{1}{s\mu_{sjd}\Omega_{sj}^2\Omega_{jd}^2}} E_1\Big(\frac{1}{s\mu_{sjd}\Omega_{sj}^2\Omega_{jd}^2}\Big). \tag{1.21}$$

The BER of the DSTC-based cooperative relay system employing BPSK modulation and using NR-relays and amplifying factor as in case 1 and case 2 is given by (1.6) where $M_{\gamma_{sjd}}$ is shown in (1.21).

On the other hand, if the AGC is used at the relays, the post-detection SNR at the destination (1.19) becomes

$$\gamma_d = \gamma_{sd} + \sum_{j\in\{r_1,r_2,\ldots,r_{M_r}\}} \frac{\frac{\epsilon_s\epsilon_j}{\epsilon_s|h_{sj}|^2+N_{sj}}}{\sum_{j\in\{r_1,r_2,\ldots,r_{M_r}\}} \frac{\epsilon_j}{\epsilon_s|h_{sj}|^2+N_{sj}}|h_{jd}|^2 N_{sj} + N_{jd}} |h_{sj}h_{jd}|^2. \tag{1.22}$$

Because of the summation terms in the denominator of (1.22) consisting of another rational function, obtaining the corresponding probability density function (PDF) is very complicated. Therefore, the upper bound of (1.22) is analyzed

$$\gamma_d \le \gamma_d^U = \gamma_{sd} + \sum_{j\in\{r_1,r_2,\ldots,r_{M_r}\}} \gamma_{sjd}, \tag{1.23}$$

where $\gamma_{sjd} = \frac{\epsilon_s|h_{sj}G_jh_{jd}|^2}{N_{sjd}}$. If $\Omega_{sj} = \Omega_{jd}$, $N_{sj} = N_{jd}$ and $\epsilon_j = \epsilon$, $\forall j$, γ_{sjd} becomes

$$\gamma_{sjd} = \frac{\gamma_{sj}\gamma_{jd}}{\gamma_{sj}+\gamma_{jd}+1}. \tag{1.24}$$

As a result, the lower bound on ASEP of the DSTC-based cooperative relay system

using NR-relays and employing BPSK modulation is the same as ASEP of repetition-based cooperative relay systems as given by (1.6).

The DSTC-based cooperative relay system is shown to achieve full diversity order (i.e. $M_r + 1$) with amplifying factor of case 1 and case 2 by mathematical analysis [24]. However, it is claimed in [24] by simulation that in case of AGC at the relays, the system can not get full diversity order.

Moreover, in order to get higher rate, instead of using distributed orthogonal space-time code [21] at the relays, in [22], the authors considered the distributed linear dispersion [25] at the relays while the distributed GABBA space time codes (full-rate code) is used in [26]. These prior works focused on two-hop models. Recently, the DSTC-based cooperative relay system are considered with communications having more than two hops in [27].

1.3.2 R-relays

Unlike NR-relays, with R-relays, the relays firstly detect the signal received from the source and then form the space time coded signal matrix $\boldsymbol{U}$. Therefore, the components of $\boldsymbol{U}$ depend on the decoded signal $\hat{x}_j$ at the relay j. Like in case of NR-relays, the matrix $\boldsymbol{U}$ can be designed based on orthogonal space-time block codes or GABBA space-time codes or linear dispersion codes.

Recall that, the DSTC-based transmission at the relays will induce the inter-symbol interference (ISI) due to the error detection at the relays. If the ISI can be removed, the DSTC-based cooperative relay system can achieve the same error performance as the repetition-based cooperative relay system. Therefore, if the source-relay links are error-free [28], the total SNR at the destination is given in (1.11). For BPSK modulation, the average error performance over the channel realizations is derived as shown in [29]

$$P_b = \frac{1}{2}\prod_{j\in\{r_1,r_2,\ldots,r_{M_r}\}}\frac{\gamma_{jd}}{\gamma_{jd}-\gamma_{sd}}\Big(1-\sqrt{\frac{\gamma_{sd}}{1+\gamma_{sd}}}\Big)+\frac{1}{2}\sum_{j\in\{r_1,r_2,\ldots,r_{M_r}\}}\pi_{jd}\Big(1-\sqrt{\frac{\gamma_{jd}}{1+\gamma_{jd}}}\Big), \tag{1.25}$$

where $\pi_{jd} = \prod_{i,j\in\{r_1,r_2,\ldots,r_{M_r}\},i\neq j}\frac{\gamma_{id}}{\gamma_{id}-\gamma_{jd}}$.

Otherwise, if the effect of intermediate decision errors at the relays is taken into account, the overall performance of the DSTC-based cooperative relay system will be degraded

as a consequence of the ISI. Since the repetition-based cooperative relay system is not affected by the ISI, it outperforms the DSTC-based cooperative relay system in terms of BER performance. Nevertheless, if the quality of the source-relay link increases, translating to less errors at the relays, the performance gap between the repetition-based and DSTC-based cooperative relay systems is expected to diminish.

In the presence of the error detection at the relays, the optimal maximum-likelihood (ML) and suboptimal scalar detectors are considered in [30] to derive closed form on BER of the DSTC-based cooperative relay system. When using an ML detector, the destination must have perfect knowledge of the error probability vectors, occurring at the relay. This requires an exchange of information between the relays and the destination. In addition, this information has to be updated with a rate depending on the channel coherence time. If this information is not available at the destination, a sub-optimum scalar detector can be implemented instead of the ML detector. In this case, the decision on the transmitted signal $x[n]$ can be simply detected as

$$\hat{x}[n] = sign\{Re\{y_d[n]]\}\}, \tag{1.26}$$

where $Re\{x\}$ stands for the real part of a complex number and $y_d[n]$ is the received signal at the destination after using MRC technique to combine the signal received from the source and the relays. The closed form error probability with ML and sub-optimum scalar detectors for DSTC-based cooperative relay system using two R-relays (i.e. $M_r = 2$) are given in [30]. Because of the complexity of these expressions, the closed form error probability in the case of M_r relays is not derived here, but can be reserved for future works.

Using two R-relays, it is claimed in [31] that the DSTC-based cooperative system does not collect the full diversity with suboptimal scalar detector. Furthermore, the highest diversity achieved by the DSTC-based cooperative relay system is the diversity of the source-relay channel. Even though, the ML receiver has the potential to collect diversity, it still can not collect the full diversity of the DSTC-based cooperative relay system as a result of the ISI channel induced by the error detection at the R-relays. In order to collect the full diversity of the ISI channel, the receiver needs full (deterministic) information about all channel taps and not just statistical information, which is the case when error probability at the R-relays is available at the destination.

The novel error aware distributed space-time (EADST) system with two R-relays relying on feedback from the destination is proposed in [31]. Based on the minimum error probability at the destination, it is demonstrated to be able to overcome the loss of diversity of DSTC-based cooperative relay system by switching between cooperation using the DSTC-based transmissions and one-hop transmissions [31]. The feedback-free EADST system which improves on DSTC-based cooperative relay system by allowing the amplification at the relays to depend on the relays' own error rate is also considered in [31].

In EADST system with feedback from the destination. First, the destination has to know the error probability at the R-relays to determine the amplifying factor since the BER performance of whole system depends on the error probability of not only the source-relay link but also the relay-destination link [31, Eq. 13]. Second, the amplifying factor has to be transmitted from the destination to the relays. In contrast, in feedback-free EADST system, the amplifying factor will be approximated at the relays depending only on the error probability at the relay [31, Eq. 14]. The simulations in [31] showed that without knowledge of the relays' error probability at the destination, the error performance of the DSTC-based cooperative relay system performs poorly (i.e. the diversity order of the system is only one). The feedback-free EADST system is shown to lose diversity at high SNR regions while the EADST system with feedback always gets full diversity.

1.4 Advanced techniques in cooperative relay systems

In comparison with traditional multi-input multi-output (MIMO) systems, the cooperative relay systems suffer a considerable degradation in terms of BER performance due to the noise amplification of NR-relays or the error detection of R-relays. As a result, many advanced techniques such as relay selection, power allocation, two-way relays, etc. are considered together with cooperative relay systems to improve BER performance, diversity order, spectral efficiency and energy efficiency.

1.4.1 Relay selection or opportunistic relay

The cooperative transmission protocol models using relays can be either repetition-based or DSTC-based depending on how the received signals at the relays are forwarded to the

destination. However, in many practical scenarios, all the nodes in the network do not simultaneously participate in the transmission; therefore, the suitable nodes based on different constraints will be selected as the relays for cooperative transmission. The relay selection methods can be classified into two main categories: relay selection with or without feedback from the destination as shown in Fig 1.5. Relay selection techniques have been extensively studied in the literature [13, 32–40]. However, only some well-known techniques are presented here as the examples of relay selection techniques.

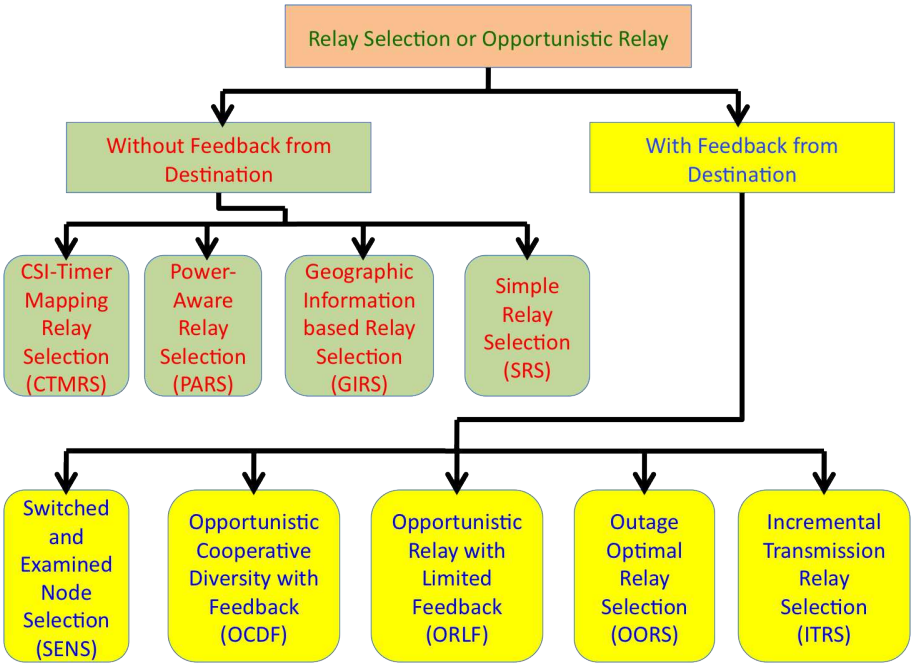

FIGURE 1.5: Classification of distributed relay selection schemes

1.4.1.1 Relay selection without feedback from the destination

1.4.1.1.a CSI-Timer Mapping Relay Selection (CTMRS)

A distributed relay selection scheme that does not require global topology information is proposed in [13]. In the CTMRS scheme, all potential relays (e.g. M_r) can deduce the channel quality (h_{sj}, h_{jd}) from the strength of the received request-to-send (RTS) or clear-to-send (CTS) sequences and derive a timeout from it. The timeout serves as a back off and node with the earliest timeout becomes the cooperating relay. The initial timer value for node j is proportionally inversed of g_j where g_j is defined based on one of the two following policies.

Policy I: the minimum of (h_{sj}, h_{jd}) is selected

$$g_j = min\{|h_{sj}|^2, |h_{jd}|^2\}. \tag{1.27}$$

Policy II: the harmonic mean of the source-relay and relay-destination links is used

$$g_j = \frac{2|h_{sj}|^2|h_{jd}|^2}{|h_{sj}|^2 + |h_{jd}|^2}. \tag{1.28}$$

A node being the best candidate as a relay has its timer reduced to zero first. When the timer of a potential relay expires, it broadcasts a flag packet to inform itself as a relay if the channel is free. Then the other potential nodes stop their timers and back off. It is claimed by the work in [13] that the achieved diversity of CSI-Timer mapping relay selection scheme is on the order of the number of cooperating terminal (e.g. $M_r + 1$) even though only one relay forwards the received signal.

1.4.1.1.b Power-Aware Relay Selection (PARS)

The power-aware relay selection (PARS) is considered in [32] to maximize network lifetime by combining the optimal transmit power and the residual power level of the source and potential relay. The algorithm consists of two phases.

- Firstly, each potential relay performs the optimal power allocation (OPA) algorithm to get the optimal transmit power for both the source and each potential relay at the given transmission rate.
- Secondly, the PARS derives a timeout based on the optimal transmit power and the residual power level of each pair of source and potential relay.

In addition, PARS is shown to be able to extend the network lifetime by about 100% as compared to [13].

1.4.1.1.c Geographic Information based Relay Selection (GIRS)

A simple geographic-based relay selection in which the best relay can be efficiently determined by using the geographical information among nodes is proposed in [34]. In this algorithm, the distance information is assumed to be perfectly known at each node and the goal is to select the best relay to maximize the cooperation gain, and hence minimize

the symbol error probability (SEP) at the destination. The source chooses the best relay (e.g. relay $j*$) which has the minimum selection metric Δ_j as follows

$$j* = \underset{j\in\{r_1,r_2,...,r_{M_r}\}}{\arg\min} \{\Delta_j\}, \quad \Delta_j = c_1^2 d_{sj}^{\alpha} + c_2 d_{jd}^{\alpha}, \tag{1.29}$$

where c_1 and c_2 are two parameters based on modulation scheme [34] and d_{sj} and d_{jd} are the distances of source-relay and relay-destination respectively. Then, the source broadcasts a message to indicate which node is chosen as a relay for its transmission. The simulation results show the improvement and outperformance of this scheme over random relay selection protocol in terms of SEP.

1.4.1.1.d Simple Relay Selection (SRS)

The authors in [37] consider a network having a set $\mathcal{M}$ of m nodes. Each node $s \in \mathcal{M}$ has data to transmit to its own destination $d(s) \notin \mathcal{M}$, and acts as a relay for other nodes in $\mathcal{M}$. The SRS scheme works as follows

- Firstly, each node broadcasts its data to its respective destination and decodes the data from the other $m-1$ sources. Then, it determines if it can be a relay for the source s_i (i.e. correct detection of the signal received from s_i). After that, it declares itself as a member of relay set $\mathcal{D}(s_i)$ which is transmitted to each source s_i
- Secondly, the source s_i will pick in its relay set $\mathcal{D}_{s_i}$ the relay which has the highest instantaneous SNR for the cooperative transmission.

Through analysis and simulation, it is shown that the SRS scheme achieves full diversity order.

1.4.1.2 Relay selection with feedback from the destination

1.4.1.2.a Switched-and-Examined Node Selection (SENS)

The relay selection scheme based on timeout can lead to collision when the timer of two or more potential relays expires at the same time. Furthermore, that all potential nodes need to listen to channel all the time wastes energy. In [33], an algorithm using the

idea of switched diversity with post selection is proposed. First, an arbitrary node j is selected as a relay. If the SNR of the source-relay link is greater than a target threshold (e.g $\gamma_{sj} > \gamma_T$), the relay node requests the CSI from the destination. If the estimated SNR of the relay-destination link is higher than the threshold (e.g. $\gamma_{jd} > \gamma_T$), this potential relay will confirm it as a relay. Otherwise, the procedure loops through the list of potential relays. The SENS scheme is shown to achieve the same performance as the CTMRS scheme [13], but with less collision and more energy efficiency.

1.4.1.2.b Opportunistic Relay with Limited Feedback (ORLF)

The protocol of ORLF scheme consists of two phases [36].

- In the first phase, source transmits data to both destination and potential relays. The potential relays will indicate success or failure of the signal detection to the destination via one bit of data.
- In the second phase, the destination selects the best relay based on the estimated relay-destination SNR and announces its decision with one bit feedback per relay.

The analysis results show that this scheme can get the same diversity-multiplexing trade-off achieved by space-time coded protocol [36].

1.4.1.2.c Opportunistic Cooperative Diversity with Feedback (OCDF)

In [35], the automatic repeat request (ARQ) technique is combined with opportunistic relay to achieve a remarkable performance gain. The relay selection algorithm is totally the same as in [13]. However, the selected relay will not transmit the received message until it receives a single-bit feedback from the destination, indicating that the message has not been correctly decoded in the first phase. That means when the destination successfully receives the message from the source, the relay-destination transmission is unnecessary.

1.4.1.2.d Incremental Transmission Relay Selection (ITRS)

In [38], an incremental transmission relay selection (ITRS) where the source itself is also considered in the selection procedure is proposed. The source broadcasts signal in the first phase. If destination can not successfully decode the signal, it will identify and pick up the best potential node from among successful relays and the source for

retransmission after performing a limited hand-shake like [35] in the second phase. The diversity multiplexing trade-off of ITRS is shown to improve the system performance in comparison with [13].

1.4.1.2.e Outage-Optimal Relay Selection (OORS)

A relay selection combined with feedback and adaptive forwarding, called outage-optimal relay selection (OORS), is proposed in [40]. If the cooperation is necessary (i.e. the source-destination transmission is failed), a decision threshold is introduced. Each relay independently evaluates its potentiality for cooperation and forms a set of cooperative nodes. The destination will select a node in this set that has the maximum instantaneous mutual information as a relay. If the set is null, the source will be chosen for retransmission. Simulation results show that OORS outperforms ORLF [35] and ITRS [38] in terms of outage probability.

1.4.2 Power allocation

Besides relay selection techniques, the advantages of cooperative communications in resource constrained networks (e.g. WSNs) can be made more efficient with suitable power allocation. Different power allocation schemes have been proposed in the literature [14, 41–44] depending on the desired gain as shown in Fig. 1.6, e.g. minimization of transmit power, guaranty of a required data rate, maximization of network lifetime, etc. In [14], the power allocation expression for a two hop non-regenerative cooperative relay

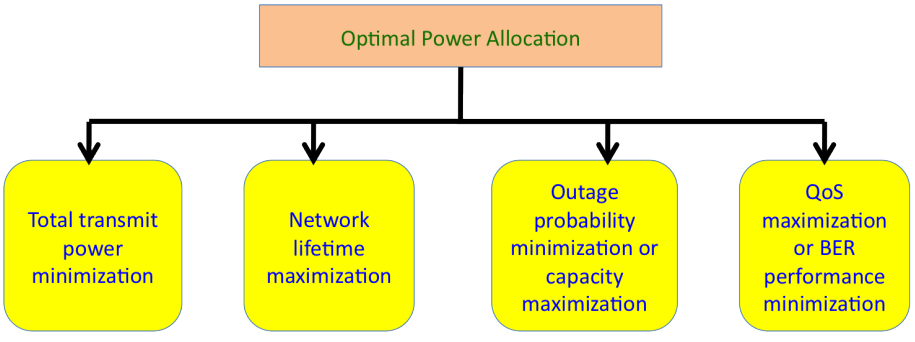

FIGURE 1.6: Optimal power allocation schemes

system is derived to maximize the channel capacity under power constraint. Based on BER performance analysis, the optimum power allocation for the regenerative cooperative relay system is derived when CSI is available at the destination [41]. It is shown

that the optimum power allocation does not depend on the direct link between source and destination, it depends only on the channel links related to the relay. Besides, when only mean channel gain information is available at the transmitters, the power allocation problem for regenerative cooperative relay system with random node locations is considered in [42] to minimize outage probability under total transmit power constraint. On the other hand, for energy-limited wireless networks such as WSNs, maximizing the network lifetime is more important for uninterrupted data transmission without replenishing batteries frequently [43]. Therefore, in [43] four power-allocation strategies, namely, the minimum transmission power (MTP), maximum residual energy (MRE), maximal energy-efficiency index (MEI), and minimum outage probability (MOP) strategies, to prolong network lifetime are proposed. Furthermore, a strategy to minimize the total transmit power in a regenerative user cooperative uplink, such that each user satisfies its quality-of-service (QoS) at fixed data rate is considered in [44].

1.4.3 Two-way relays

In traditionally unidirectional cooperative relay systems, several relays assist in the source-destination communication in order to achieve spatial diversity [8, 9, 12]. However, the half-duplex constraint of the relays induces a severe loss of bandwidth efficiency due to occupying more time slots for one-round information. In order to overcome the performance loss in the use of spectral resources, a novel transmission scheme referred as bidirectional cooperative networks or two-way relay networks have been recently studied in the literature. In contrast to conventional schemes, fewer transmission cycles are required in two-way relay transmission, which consequently provides improvement in the performance of spectrum efficiency [45]. In fact, in two-way relay transmission one or multiple relays are deployed to establish a reliable bidirectional communication between the two transceivers. The key idea with the two-way relay communication is that each terminal can cancel the interference (generated by its own transmission) from the signal received from the relay to recover the signal transmitted from the other terminal. Currently, according to the required time slots, the two-way relay transmission can be grouped into the time division broadcast (TDBC) (i.e. three phase communication protocol) [15] and the multiple-access broadcast (MABC) (i.e. two-phase communication protocol) [46].

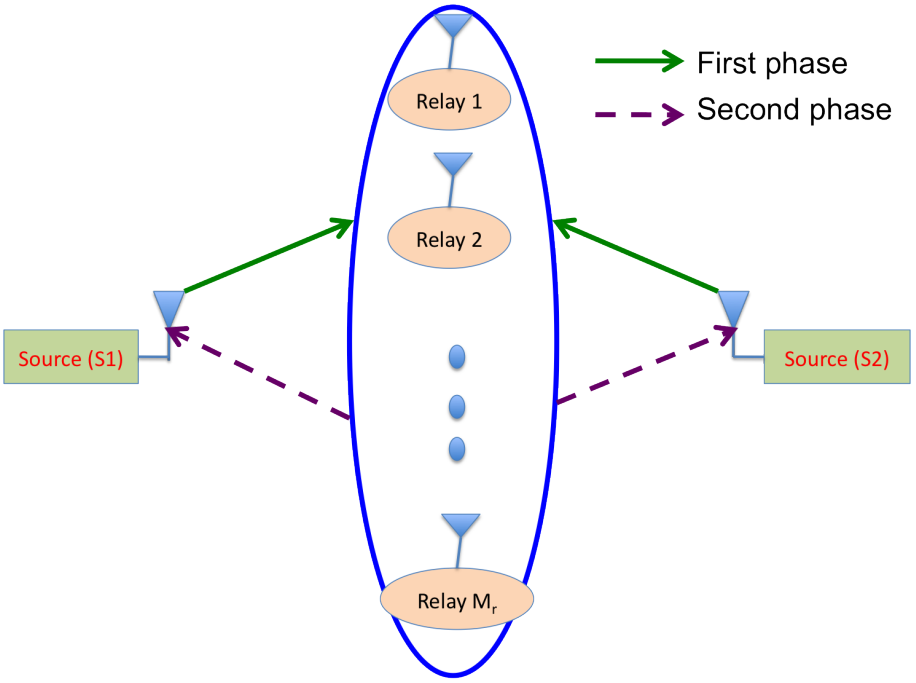

FIGURE 1.7: MABC protocol

1.4.3.1 MABC protocol

The MABC tranmission protocol consists of two phases as shown in Fig. 1.7. In the fist phase, two sources $S1$ and $S2$ transmit simultaneously their symbol x_1 and x_2 to the relays respectively. The NR-relays or R-relays then broadcast their received signal to $S1$ and $S2$ using repetition-based or DSTC-based cooperative relay protocols. Since $S1$ and $S2$ know their own symbol x_1 and x_2, the self-interference at $S1$ and $S2$ can be removed. Therefore, $S1$ and $S2$ can obtain interference-free signals.

1.4.3.2 TDBC protocol

The TDBC protocol needs three time-slots for a complete communication between two terminals with the help of relays depicted in Fig. 1.8. At the first time slot, $S1$ will transmit x_1 to the relays and $S2$ at the same time. Similarly, $S2$ simultaneously transmits x_2 to $S1$ and the relays. Finally, after combining the two received signals (i.e. x_1 and x_2), the NR-relays or R-relays will broadcast the combined signal to $S1$ and $S2$ using repetition-based or DSTC-based cooperative relay protocols.

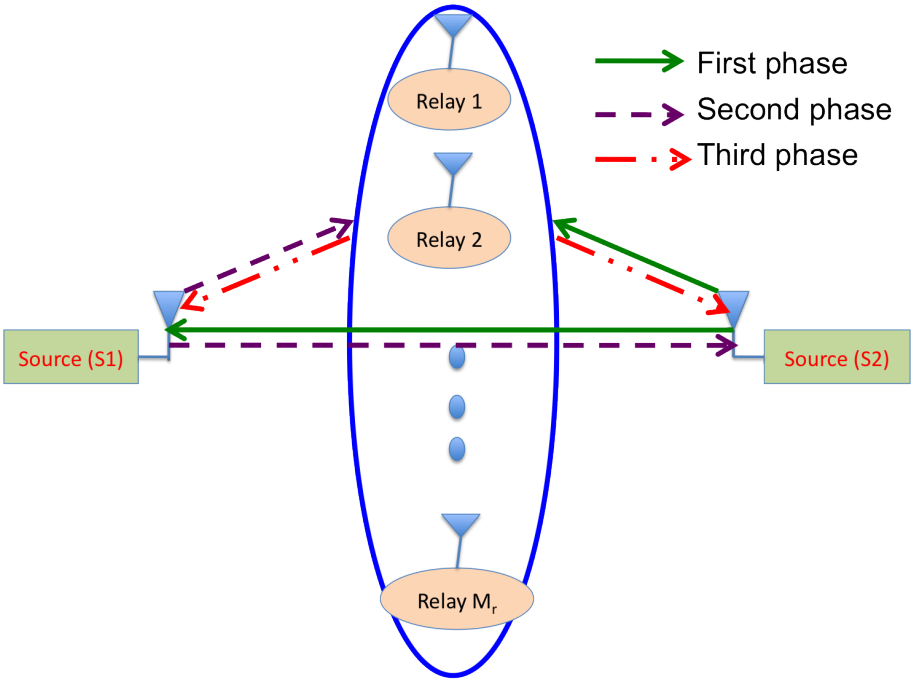

FIGURE 1.8: TDBC protocol

1.4.3.3 MABC vs TDBC

Due to the different required temporal phases, the main characteristic for both protocols can be summarized as follows [46]

1. MABC
   - The MABC protocol needs only two time slots for two data flows. Therefore the channel resources are used more efficiently
   - That both sources simultaneously access the channel leads to interference
   - The MABC can not utilize the direct transmission between the two sources. Thus, it only achieves the first diversity order ($M_r = 1$).
2. TDBC
   - The TDBC protocol requires three time slots for two data flows which results in suboptimal utilization of the channel resources.
   - The relay deals with a single transmission at each time; therefore there is no interference.
   - In the TDBC protocol, the direct transmission between the two sources is taken into account. Thus it can get the second diversity order ($M_r = 1$).

1.4.4 Association between the advanced techniques

The above advanced techniques are shown to be able to increase the performance of cooperative relay systems in terms of BER, spectral efficiency and energy efficiency. Moreover, the suitable association between these techniques (i.e. relay selection, power allocation and two-way relay) are recently illustrated to further improve the system performance. In [15], a bidirectional relay networks based on MABC and TDBC, consisting of two different end-sources and multiple NR-relays, is considered together with relay selection technique. The outage probability is shown to be minimized through a max-min criterion. On the other hand, relay selection techniques for two-way R-relay systems based on MABC are proposed to get benefits in terms of outage probability and diversity gain [46]. Besides, the combination of relay selection and optimal power allocation techniques are considered in [47, 48]. In [48], a relay selection and power allocation scheme for R-relays is proposed and shown to be able to extend the network lifetime while an adaptive power control for the selected R-relay is considered in [47] in order to satisfy the given data rate requirement.

In addition, an optimal joint relay selection and power allocation scheme for two-relay networks is considered in [49]. In [50], the proposed two-way relay system with relay selection and optimal power allocation is shown to have considerable performance improvement over equal power allocation scheme. Recently, an energy-efficient relay selection and power allocation scheme is studied for TDBC networks in [51] with the objective of minimizing transmit power consumption at required end-to-end rates.

1.5 Simulation Results

In this section, the BER performance of repetition-based and DSTC-based cooperative relay systems is re-simulated with or without using the advanced techniques. For a fair comparison between the cooperative relay systems and SISO system, the total transmit powers of all the systems are the same. That means if in SISO, source transmits signal to destination with the transmit power of P, in cooperative relay systems, the total transmit power of all terminals must be equal to P (i.e. $\epsilon_r + \sum_{j\in\{r_1,r_2,\ldots,r_{M_r}\}} \epsilon_j = P$). Unless otherwise stated, for the following simulations the transmit power of all terminals

(relays and source) will have equal allocation (i.e. $\epsilon_s = \epsilon_j = \epsilon, \forall j$). The relays are assumed to be in the middle of the source and the destination.

1.5.1 Repetition-based cooperative relay systems

The BER performance of repetition-based cooperative relay systems using BPSK modulation is shown in Fig. 1.9 when the number of relays changes from 1 to 4. Fig. 1.9a shows the performance for NR-relays while the performance of R-relays is shown in Fig. 1.9b. The simulation results are well-matched with the previous results illustrated in the literature [8, 13]. With NR-relays, the diversity order of the system is M_r. That means when the number of NR-relays increases the diversity order of the system will increase proportionally. Otherwise, with R-relays, because of error detection at the relays, the diversity order of the system will always be one although how many R-relays are used in the cooperative system.

1.5.2 DSTC-based cooperative relay systems

The BER performance of DSTC-based cooperative relay systems with NR-relays and R-relays is shown in Fig. 1.10. For the simplicity, this simulation is only done for the case $M_r = 2$. As shown in the figure, the BER performance of R-relays is considerable with SISO system. Therefore, the diversity order of the system with R-relays is only one. For NR-relays, the BER performance is simulated depending on different amplifying factor used at the relays. It is claimed through the simulation that using AGC (1.16) (case 3), the system can get second diversity order. However, with the amplifying factor in (1.16) (case 2) the system is shown to be able to achieve full diversity order (i.e. 3). The results are totally well-matched with the results in [24].

1.5.3 DSTC-based vs repetition-based cooperative relay systems

Fig. 1.11 shows the BER comparison between repetition-based and DSTC-based cooperative relay systems in case of NR-relays and R-relays. Instead of using 3 time slots to transmit a signal from source to destination via two relays like repetition-based cooperative relay systems, in DSTC-based cooperative relay systems (e.g. $M_r = 2$), it only

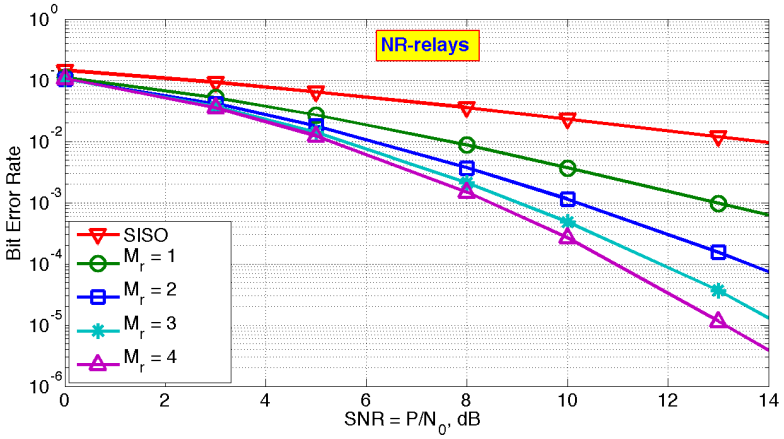

(a) NR-relays

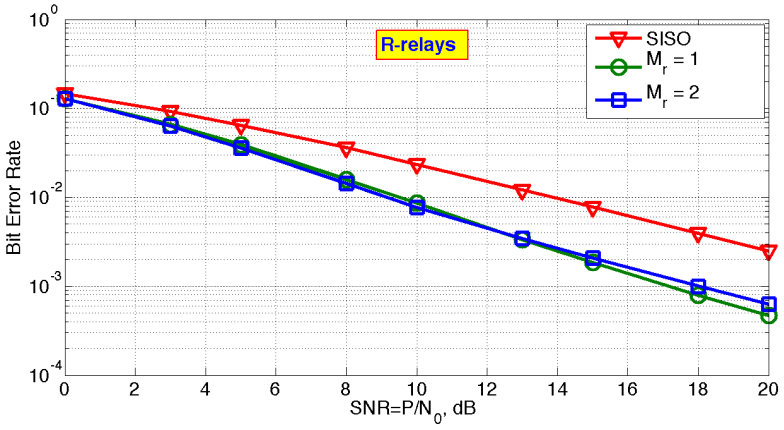

(b) R-relays

FIGURE 1.9: BER performance of repetition-based cooperative relay system

needs 2 time slots. Although having more bandwidth efficiency than repetition-based cooperative relay systems, DSTC-based cooperative relay systems have worse performance than repetition-based cooperative relay systems in terms of BER as shown in Fig. 1.11. To prevent the saturation at relays, AGC is used in cased of NR-relays.

1.5.4 Relay selection

One can also wonder about the benefits of relay selection technique in improving the BER performance of cooperative relay system. The performance of repetition-based cooperative system with relay selection technique is shown in Fig. 1.12. In this simulation, the CTMRS technique [13] with the relay selection policy based on the harmonic mean of the source-relay and relay-destination links (1.28), mentioned CTMRS in the figure,

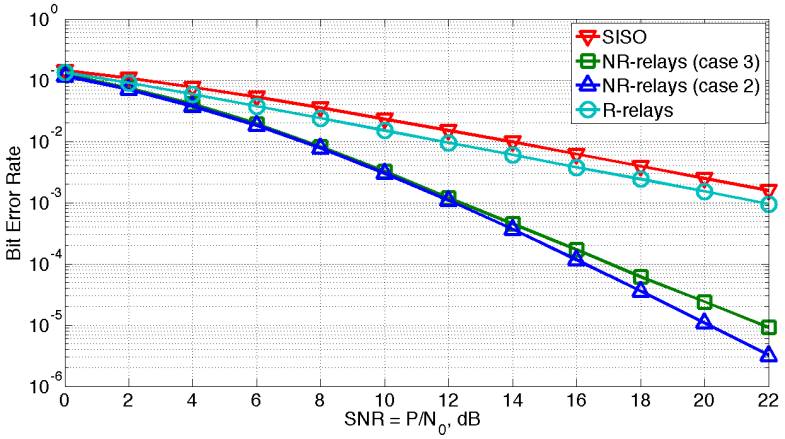

FIGURE 1.10: BER performance of DSTC-based cooperative relay system

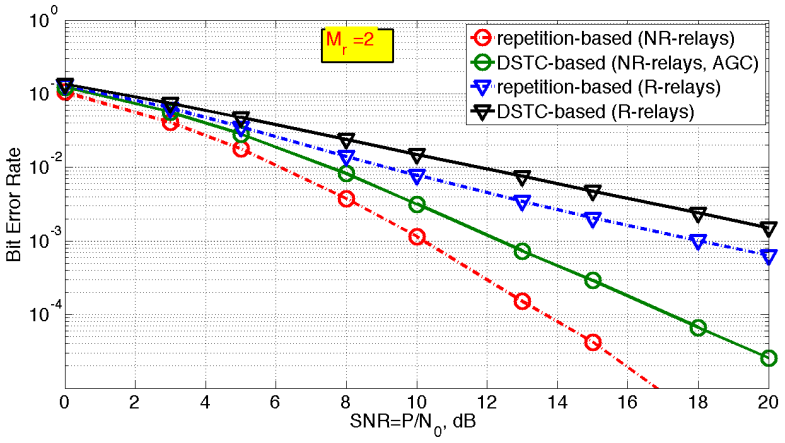

FIGURE 1.11: BER performance comparison of DSTC-based and repetition-based cooperative relay systems

is used. The results without mentioning CMTRS are reserved for the BER performance of the system without using relay selection technique. Although in the relay selection technique, there is only one best relay forwarding signal to destination, it is illustrated to further improve the performance of the system using NR-relays. Besides, for the system using R-relays, the relay selection technique is shown to be able to improve the diversity order of the system. Instead of one, the system can fully achieve the diversity order of M_r.

1.5.5 Power allocation

Finally, the effect of optimal power allocation on the BER performance of repetition-based and DSTC based cooperative systems is also shown in Fig. 1.13. In this simulation the transmit power of the terminals is no way equal allocation. Instead of this we have

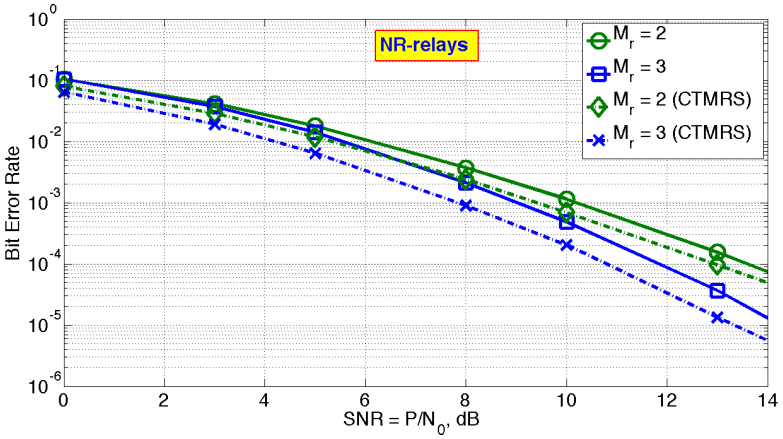

(a) NR-relays

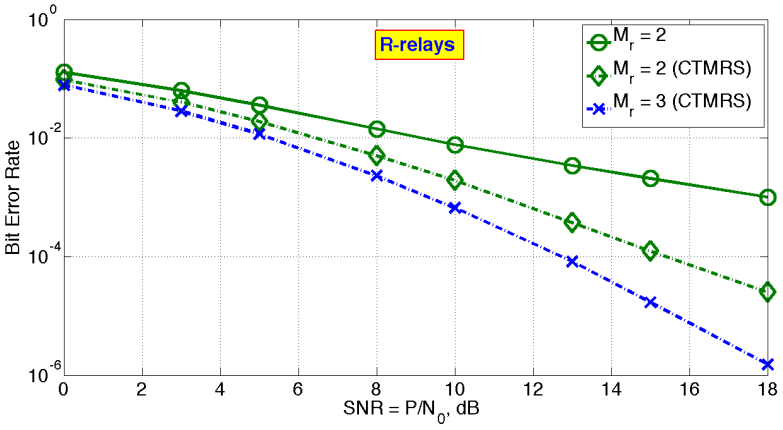

(b) R-relays

FIGURE 1.12: BER performance of repetition-based cooperative relay system with relay selection technique (CTMRS)

$\epsilon_s + M_r\epsilon_r = P$ ($\epsilon_j = \epsilon_r \, \forall j$) where $\epsilon_s = c_P P$ and $\epsilon_r = (1-c_P)P/M_r$. Fig. 1.13a shows the SNR required as a function of c_P when the BER desired is equal to 10^{-4} for repetition-based cooperative relay systems. The optimal power allocation for NR-relays happens when $c_P = 0.6$ while for R-relays, the system will need the less SNR required when $c_P = 0.7$. On the other hand, the optimal power allocation for DSTC-based cooperative relay systems is shown in Fig. 1.13b when $BER = 10^{-3}$. As shown in the figure, for NR-relays, the best performance is achieved when $c_P = 0.7$. In contrast, for R-relays, $c_P = 0.9$ is the optimal power allocation ratio.

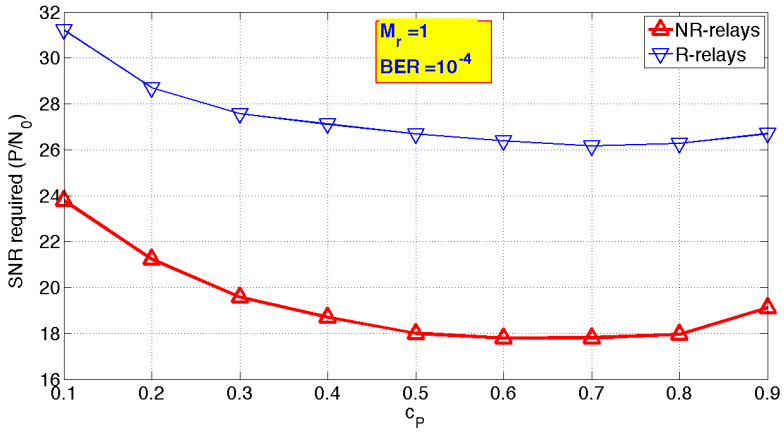

(a) repetition-based

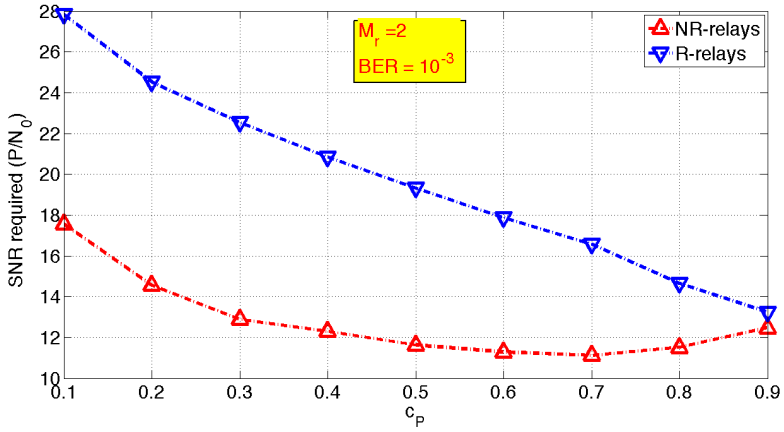

(b) DSTC-based

FIGURE 1.13: BER performance of cooperative relay system with power allocation technique

1.6 Conclusion

In this chapter, a survey of cooperative relay systems (i.e. repetition-based and DSTC-based) with advanced techniques (i.e. relay selection, power allocation and two-way relay) is proposed. Their performances in terms of error probability are considered and generalized for multiple relays (i.e. M_r) in case of NR-relays and R-relays. It is shown that in repetition-based cooperative relays systems, maximum diversity order is proportionally increased with the number of NR-relays. However, in case of R-relays, the maximum diversity order of the systems is always one no matter how many R-relays are used. Similarly, for DSTC-based cooperative relay systems, the maximum diversity order can not be achieved for both NR-relays (using AGC at relays) and R-relays.

Relay selection technique and power allocation are shown to be able to increase the performance in terms of BER for DSTC-based and repetition-based cooperative relay systems. Especially, the relay selection technique can help repetition-based cooperative relay systems to achieve maximum diversity order in case of R-relays.

DSTC-based cooperative relay systems clearly get better bandwidth efficiency than repetition-based cooperative relay systems due to using less time slots for a whole communication. However, the comparison in terms of BER performance shows that, repetition-based cooperative relay systems have significant gain as compared to DSTC-based ones thanks to their higher diversity orders. Although power allocation techniques are shown to have capacity to increase the BER performance of the DSTC-based cooperative relay systems, the maximum diversity order of the systems is unchanged. In this thesis, another technique, based on inter-communication betweens relays, is investigated in Chapter 2. It is proved via mathematical analytic and numerical simulations to be able to increase the maximum diversity order of DSTC-based cooperative relay systems, thus leading to a significant improvement of performances of in terms of not only BER, but also spectral efficiency as well as energy efficiency.

Chapter 2

Fully Distributed Space-Time Codes

2.1 Introduction

Cooperative MIMO (Multi-Input Multi-Output) has recently emerged as an advanced technique to replace traditional MIMO when terminals can only support one antenna due to their limited sizes. In [6] and [7] cooperation among users is considered to achieve spatial diversity and therefore to reduce the required transmit power at the same data rate or to get higher data rate at the same power level as compared to SISO systems.

Nowadays, besides cooperative MIMO, cooperative relay has also been identified as a core technique to overcome challenges in wireless environments. Although the relay technique is firstly considered in 1979 by T. Cover and A. Gama in terms of capacity [52], the advantages of using relay to combat shadowing effects and to get diversity gain have just been proposed in the last decade [12, 53–57]. In [12], energy-efficient transmission protocols, called antenna sharing transmission protocols, are shown to be able to overcome noisy channel between distributed antennas and to outperform single-hop and multi-hop transmissions. Diversity of a system equipped with one and two amplify-and-forward (AF) relays is illustrated through analytical results and numerical simulations in [54]. In [55], effects of multiple antennas at source on outage probability for AF relaying system are considered. Moreover, relaying has been lately investigated in the 3GPP (3rd Generation Partnership Project) LTE-Advanced (Long Term Evolution-Advanced) and agreed to be standardized to fulfill coverage and capacity requirements in a cost-efficient way [56, 57].

2.1.1 Related work

Initial work on using distributed space-time coded (DSTC) protocols over relay channel is considered in [8, 9, 17, 58]. We denote them as conventional distributed space-time coded (cDSTC) protocols, in which the whole communication only consists of two phases. Firstly, source transmits its signal to relays (with or without direct transmission to destination). Secondly, non-regenerative or regenerative relays (NR-relays or R-relays) use the DSTC protocols to forward signals to destination.

Error probability of the cDSTC protocols is derived for NR-relays in [17, 22, 24, 31, 59]. An approximate formula of average symbol error probability (ASEP) for a DSTC system based on multi-user cooperation is found in [17]. On the other hand, performance of the cDSTC protocol in regenerative relay networks is derived in [28, 30, 41, 58, 60, 61]. In [58], a regenerative cDSTC protocol is applied for source and relay with optimal allocation of transmit power in order to minimize the average Bit Error Rate (BER) at final destination. In [61], Anghel et al. propose two Error-Aware Distributed Space-Time (EADST) protocols to overcome worse BER performance of R-relays induced by decoding errors at the relays. However, these two protocols require feedback from destination. Recently, an extension of the cDSTC protocols for more than two hops is considered in [27].

Besides BER performance consideration, in [8] the cDSTC protocol is shown to be effectively used for higher spectral efficiency and to achieve full spatial diversity in some specific cases. In [9], the performance of cooperative protocols is considered in terms of outage probability. The authors show that, except for fixed decode-and-forward (DF) protocol, all of their cooperative protocols are efficient in the sense of achievement of full diversity. In [22], the cDSTC system is shown to have the same diversity as a multiple-antenna system when the coherence interval is greater than the number of relays. With NR-relays, the diversity of the cDSTC system is shown to depend on the scaling factor of the relays [24]. In [62], a diversity-multiplexing trade-off (DMT) analysis is considered in multi-hop MIMO relay networks. A DMT analysis is also considered recently for an AF two path half-duplex relaying scheme in [63]. Wicaksana et al. showed that DMT is achievable for finite codeword lengths with a careful choice of coding strategy.

Cooperative techniques are recently potential candidates to reduce energy consumption in wireless networks. In [64], using cooperative MIMO systems, a tremendous energy saving

is shown for long transmission distances in comparison with SISO systems. Besides, the energy efficiency of different cooperative relaying techniques has been investigated. In LTE-Advanced networks, using relay nodes, it has been shown that energy saving up to 15.6% is possible in the two hop schemes, and up to 8.5% are possible with the multicast cooperative scheme [65]. In [66], a transparent relay with cooperative strategy is shown to save about 60% power consumption as compared to the transparent relay in IEEE 802.16j under given simulation configurations. In [67], cooperative transmission, especially when a feedback channel is available and line-of-sight (LOS) is present between nodes, is shown to be more energy-efficient than non-cooperative transmission even in small transmission ranges.

2.1.2 Contributions

The main contributions of the chapter can be summarized as follows:

1. A new cooperative DSTC protocol, called the fully distributed space-time coded (fDSTC) protocol, in which there is an added inter-relay communication phase, is proposed to improve performances of DSTC-based cooperative relay systems. It is thoroughly considered with both NR-relays and R-relays.

2. A closed-form average symbol error probability (ASEP) for NR-relays and a closed-form expression of error probability for R-relays are derived to verify good performance of the fDSTC protocol.

3. Considering positions of the relays, the effects of the relative distance of relays and the distance between the relays on BER performance are figured out.

4. In addition, the best power allocation between the transmitters is also considered to further increase the BER performance of the fDSTC protocol.

5. For a fair comparison on the data rate, considerations on the outage probability of the fDSTC and cDSTC protocols are given. In addition, the diversity-multiplexing tradeoff (DMT) is also derived.

6. Total energy consumption of the two protocols is estimated using typical and real energy models for a fair consideration on power consumption.

The rest of this chapter is organized as follows. System model is thoroughly described in Section 2.2 to exploit the fDSTC protocol. In Section 2.3, error performance of the fDSTC protocol with NR-relays and R-relays is analyzed through mathematical expressions and followed by numerical results. The outage probability and DMT are considered in Section 2.4 to evaluate the protocol performance in terms of spectral efficiency. Section 2.5 presents two energy models used to evaluate the total energy consumption of the systems and shows energy efficiency of the protocols. Finally, conclusion is given in Section 2.6.

2.2 System Model

In this chapter, a cooperative relay system including one source, one destination and two relays which have only one antenna (Fig. 2.1) is considered to exploit the fully distributed space-time code (fDSTC) protocol. In the system, the relays only play a role to enhance the quality of the source-destination link. They do not have their own data to transmit. In order to avoid self-interference, the relays are used in half-duplex mode, which means they can not transmit and receive data simultaneously. The ideal channel state information (CSI) is known at the receiver, but not at the transmitters. A BPSK modulation is considered for all the analysis and simulations. We assume that all communications are performed over a flat Rayleigh fading channel. Channel coefficients remain the same for two consecutive time intervals. Statistically, we model the channel coefficient $h_{ij}[n]$ with $i \in \{s, r_1, r_2\}$, $j \in \{r_1, r_2, d\}$ and $i \neq j$ as zero mean, independent, complex Gaussian random variables with variances Ω_{ij}^2. Similarly, we model AWGN (Additive White Gaussian Noise) $z_{ij}[n]$ as zero mean mutually independent complex Gaussian random variable with variance N_{ij}. For the clarity of the following expressions, the symbols $h_{ij}[n]$, $G_{ij}[n]$, $\gamma_{ij}[n]$ will be rewritten in brief form of h_{ij}, G_{ij}, γ_{ij}.

The fDSTC protocol can be mathematically described as below. In the first phase, the source transmits signals $\boldsymbol{x} = \begin{bmatrix} x[2k] & x[2k+1] \end{bmatrix}^T$ ($E[x[n]] = 0$, and $E[x^2[n]] = 1$) with the transmit power $\epsilon_s = \epsilon_{sd} = \epsilon_{sr_1} = \epsilon_{sr_2}$ to the relays and the destination at the same time. The received signals at the relays and the destination (Fig. 2.1) can be represented as $\boldsymbol{y_{sr1}}$, $\boldsymbol{y_{sr2}}$ and $\boldsymbol{y_{sd}}$ respectively

$$\boldsymbol{y_{sj}} = \sqrt{\epsilon_{sj}} h_{sj} \boldsymbol{x} + \boldsymbol{z_{sj}}, \quad j \in \{r_1, r_2, d\}, \tag{2.1}$$

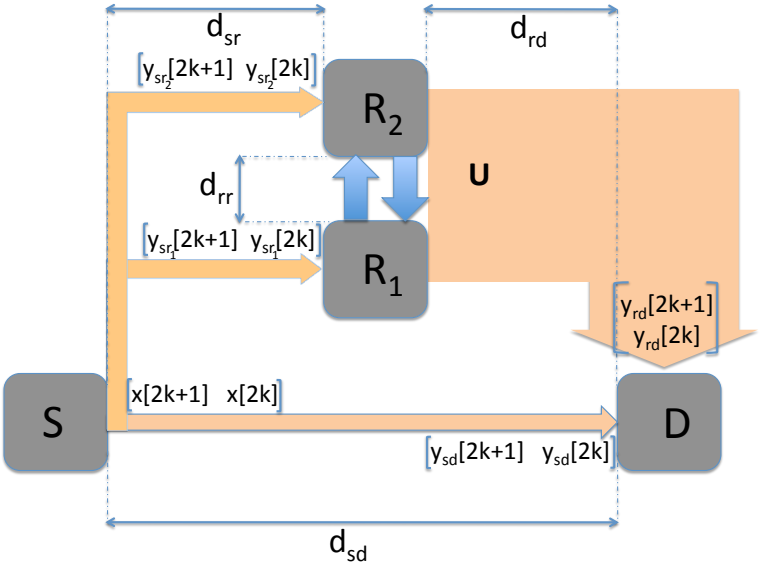

FIGURE 2.1: fDSTC protocol for a system including one source (S), two relays (R1, R2) and one destination (D). Source-relay distance, source-destination distance, relay-destination distance and relay-relay distance are respectively denoted as d_{sr}, d_{sd}, d_{rd} and d_{rr}.

where $\boldsymbol{y_{sj}} = \begin{bmatrix} y_{sj}[2k] & y_{sj}[2k+1] \end{bmatrix}^T$ and $\boldsymbol{z_{ij}} = \begin{bmatrix} z_{ij}[2k] & z_{ij}[2k+1] \end{bmatrix}^T$.

In the second phase, the two relays exchange their data with each other. The received signals at relay R_1 from relay R_2 and vice versa, respectively symbolized as $\boldsymbol{y_{r_2r_1}}$ and $\boldsymbol{y_{r_1r_2}}$, are given by

$$\boldsymbol{y_{ij}} = h_{ij} G_{si} \boldsymbol{y_{si}} + \boldsymbol{z_{ij}}, \quad i, j \in \{r_1, r_2\}, i \neq j, \tag{2.2}$$

where G_{si} is the automatic gain control (AGC) which prevents saturating the relay i [12] and can be chosen as $G_{si} = \sqrt{\frac{\epsilon_{ij}}{\epsilon_s |h_{si}|^2 + N_{si}}}$, $i, j \in \{r_1, r_2\}$, $i \neq j$, with $\epsilon_{rr} = \epsilon_{r_1 r_2} = \epsilon_{r_2 r_1}$ the transmit power between the relays. Traditionally, distance between the two relays is very small in comparison with transmission distance. Therefore, to economize energy, the transmit power between the relays can be chosen as one tenth of the transmit power from the relays to the destination. As a result, the destination can not overhear the inter-communication between the relays.

Then, each relay uses the Maximum Ratio Combining (MRC) technique to combine the signals received from the source and from the other relay

$$\boldsymbol{u_j} = \frac{h_{sj}^* \sqrt{\epsilon_{sj}}}{N_{sj}} \boldsymbol{y_{sj}} + \frac{\sqrt{\epsilon_{sj}} h_{ij}^* G_{si}^* h_{si}^*}{|h_{ij}|^2 |G_{si}|^2 N_{si} + N_{ij}} \boldsymbol{y_{ij}}, \tag{2.3}$$

where $i, j \in \{r_1, r_2\}$, $i \neq j$, $\boldsymbol{y_{ij}} = \begin{bmatrix} y_{ij}[2k] & y_{ij}[2k+1] \end{bmatrix}^T$ and $\boldsymbol{u_j} = \begin{bmatrix} u_j[2k] & u_j[2k+1] \end{bmatrix}^T$.

In the last phase, the two relays use distributed space-time codes to simultaneously transmit the Alamouti re-encoded signals $\boldsymbol{U}$ to the destination (see Section 2.3.1 for more details). The components of the matrix $\boldsymbol{U}$ depend on the protocol that the relays use to forward the signals to the destination: non-regenerative or regenerative. The signals received at the destination from the relays, $\boldsymbol{y_{rd}} = \begin{bmatrix} y_{rd}[2k] & y_{rd}[2k+1] \end{bmatrix}^T$, are expressed as

$$\boldsymbol{y_{rd}} = \boldsymbol{U} \boldsymbol{h_{rd}} + \boldsymbol{z_{rd}}, \tag{2.4}$$

where $\boldsymbol{h_{rd}} = \begin{bmatrix} h_{r_1 d}[2k] & h_{r_2 d}[2k] \end{bmatrix}^T$ is the Rayleigh channel coefficient vector and $\boldsymbol{z_{rd}} = \begin{bmatrix} z_{rd}[2k] & z_{rd}[2k+1] \end{bmatrix}^T$ is the AWGN noise vector.

At the destination, the Alamouti receiver is used to process the signals received from R_1 and R_2. Then, the output of the Alamouti receiver is combined with $\begin{bmatrix} y_{sd}[2k] & y_{sd}[2k+1] \end{bmatrix}^T$ using the MRC technique.

The protocol of the cDSTC is the same as that of the fDSTC except that there is no data exchange between the two relays. In the first phase, the source transmits its signals to the two relays and the destination. In the second phase, the relays encode their received signals into a "distributed" Alamouti code with (NR-relays) or without decoding the received signals (R-relays). Then, they transmit the coded signals to the destination.

2.3 BER performance

2.3.1 fDSTC protocol with NR-relays

In this section, the bounds and closed-form ASEP of non-regenerative fDSTC (NR-fDSTC) protocol is derived. The SNR at terminal j after receiving signals from terminal i is found as $\gamma_{ij} = \frac{\epsilon_{ij} |h_{ij}|^2}{N_{ij}}$ which has an exponential distribution with the mean $\overline{\gamma_{ij}} = \frac{\epsilon_{ij} \Omega_{ij}^2}{N_{ij}}$.

From (2.3), the post-detection SNR at the relay j can be referred as

$$\gamma_j = \gamma_{sj} + \frac{\gamma_{si}\gamma_{ij}}{\gamma_{si} + \gamma_{ij} + 1} \quad i, j \in \{r_1, r_2\}, i \neq j. \tag{2.5}$$

In the NR-fDSTC protocol, after receiving signals from both the source and the other relay, each relay re-encodes the combined signals $\boldsymbol{u_j}$ (2.3) with Alamouti space-time code to form the Alamouti re-encoded signals $\boldsymbol{U} = \begin{bmatrix} G_{r_1 d} u_{r_1}[2k] & G_{r_2 d} u_{r_2}[2k+1] \\ -G^*_{r_1 d} u^*_{r_1}[2k+1] & G^*_{r_2 d} u^*_{r_2}[2k] \end{bmatrix}$.

The combined signals at the relays (2.3) can be remodeled as

$$\boldsymbol{u_j} = \sqrt{\gamma_j}\boldsymbol{x} + \boldsymbol{z_{u_j}}, \quad j \in \{r_1, r_2\}, \tag{2.6}$$

where γ_j is found in (2.5) and $\boldsymbol{z_{u_j}} = \begin{bmatrix} z_{u_j}[2k] & z_{u_j}[2k+1] \end{bmatrix}^T$ is AWGN with zero mean and variance $N_{u_j} = 1$. To prevent the saturation at the relay j, the AGC G_{jd} is chosen as $G_{jd} = \sqrt{\frac{\epsilon_{jd}}{\gamma_j + 1}}$, $j \in \{r_1, r_2\}$ with ϵ_{jd} the transmit power of relay j to the destination ($\epsilon_r = \epsilon_{r_1 d} = \epsilon_{r_2 d}$).

The output signal from Alamouti receiver is

$$\boldsymbol{y_r} = \left[\left| h_{r_1 d} G_{r_1 d} \sqrt{\gamma_{r_1}} \right|^2 + \left| h_{r_2 d} G_{r_2 d} \sqrt{\gamma_{r_2}} \right|^2 \right] \boldsymbol{x} + \boldsymbol{z_{y_r}}, \tag{2.7}$$

where $\boldsymbol{y_r} = \begin{bmatrix} y_r[2k] & y_r[2k+1] \end{bmatrix}^T$ and $\boldsymbol{z_{y_r}} = \begin{bmatrix} z_{y_r}[2k] & z_{y_r}[2k+1] \end{bmatrix}^T$ is AWGN with variance $N_{z_{y_r}} = \left[\left| h_{r_1 d} G_{r_1 d} \sqrt{\gamma_{r_1}} \right|^2 + \left| h_{r_2 d} G_{r_2 d} \sqrt{\gamma_{r_2}} \right|^2 \right] \left[\left| h_{r_1 d} G_{r_1 d} \right|^2 + \left| h_{r_2 d} G_{r_2 d} \right|^2 + 1 \right]$.

Combining the output signals from Alamouti receiver (2.7) and the received signals from the source (2.1) using MRC technique, the signal at the destination is

$$\boldsymbol{y_d} = \frac{h^*_{sd}\sqrt{\epsilon_{sd}}}{N_{sd}} \boldsymbol{y_{sd}} + \frac{1}{\left| h_{r_1 d} G_{r_1 d} \right|^2 + \left| h_{r_2 d} G_{r_2 d} \right|^2 + 1} \boldsymbol{y_r}, \tag{2.8}$$

with $\boldsymbol{y_d} = \begin{bmatrix} y_d[2k] & y_d[2k+1] \end{bmatrix}^T$.

Based on (2.8), the post-detection SNR at the destination can be derived as

$$\gamma_d = \gamma_{sd} + \frac{\sum_{j \in \{r_1, r_2\}} \frac{\gamma_{jd}\gamma_j}{\gamma_j + 1}}{\sum_{j \in \{r_1, r_2\}} \frac{\gamma_{jd}}{\gamma_j + 1} + 1}. \tag{2.9}$$

2.3.1.1 Lower and upper bounds on ASEP of the NR-fDSTC protocol

We have

$$\gamma^L < \gamma_d < \gamma^U, \tag{2.10}$$

where γ^L is the lower bound of γ_d ($\gamma_{ij} \gg \gamma_{sj}$, $i, j \in \{r_1, r_2\}, i \neq j$)

$$\begin{aligned} \gamma^L &= \gamma_{sd} + \frac{\gamma_{sr_1}\gamma_{r_1 d}}{\gamma_{sr_1} + \gamma_{r_1 d} + 1} + \frac{\gamma_{sr_2}\gamma_{r_2 d}}{\gamma_{sr_2} + \gamma_{r_2 d} + 1} \\ &= \gamma_{sd} + \gamma^L_{sr_1 d} + \gamma^L_{sr_2 d}, \end{aligned} \tag{2.11}$$

and γ^U is the upper bound of γ_d

$$\begin{aligned} \gamma^U &= \gamma_{sd} + \frac{(\gamma_{sr_1} + \gamma_{sr_2})\gamma_{r_1 d}}{\gamma_{sr_1} + \gamma_{r_1 d} + \gamma_{sr_2} + 1} + \frac{(\gamma_{sr_2} + \gamma_{sr_1})\gamma_{r_2 d}}{\gamma_{sr_1} + \gamma_{sr_2} + \gamma_{r_2 d} + 1} \\ &= \gamma_{sd} + \gamma^U_{sr_1 d} + \gamma^U_{sr_2 d}. \end{aligned} \tag{2.12}$$

From (2.10), let the lower and upper bounds on ASEP of the fDSTC system be $P^L_{\gamma_d}$ and $P^U_{\gamma_d}$ respectively. Since the ASEP is inversely proportional to the SNR, we have $P^L_{\gamma_d} = P_{\gamma^U}$ and $P^U_{\gamma_d} = P_{\gamma^L}$. That means

$$P^L_{\gamma_d} = P_{\gamma^U} < P_{\gamma_d} < P_{\gamma^L} = P^U_{\gamma_d}. \tag{2.13}$$

In order to find the lower bound on ASEP of the fDSTC system, we first derive the moment generating function (MGF) of γ^U_{sid}, $i \in \{r_1, r_2\}$ which is proved in Appendix A.

$$\begin{aligned} M_{\gamma^U_{sid}}(s) =& e^{\alpha_i/2}\Big[\frac{2}{p_i\sqrt{p_i}}\Big(\big(\frac{p_i}{\overline{\gamma_{id}}} - \sigma_i + \frac{\sigma_i}{2\overline{\gamma_{id}}}\big)\frac{\delta J_0}{\delta\beta_i} + \big(\frac{\sigma_i}{\overline{\gamma_{id}}} + 2\big)\frac{\delta^2 J_0}{\delta\alpha_i\delta\beta_i}\Big) \\ &+ \frac{2}{p_i^2}\Big(\big(\frac{2p_i}{\overline{\gamma_{id}}} + \sigma_i\big)\frac{\delta^2 J_0}{\delta\alpha_i^2} + \frac{p_i}{\overline{\gamma_{id}}}\frac{\delta J_0}{\delta\alpha_i} - \frac{\sigma_i}{4}J_0\Big)\Big], \end{aligned} \tag{2.14}$$

where $t_0 = \overline{\gamma_{id}}$, $\sigma_i = \overline{\gamma_{id}} + \overline{\gamma_{si}}$, $p_i = \overline{\gamma_{id}\gamma_{si}}$, $\beta_i = 2/\sqrt{p_i}$ and $\alpha_i = (\sigma_i - p_i s)/p_i$. The formula of J_0, $\frac{\delta J_0}{\delta\alpha_i}$, $\frac{\delta J_0}{\delta\beta_i}$, $\frac{\delta^2 J_0}{\delta\alpha_i^2}$ and $\frac{\delta^2 J_0}{\delta\alpha_i\delta\beta_i}$ can be found in Appendix A. Note that with the assumption $\overline{\gamma_{sr}} = \overline{\gamma_{sr_1}} = \overline{\gamma_{sr_2}}$, the random variable $\gamma_{sr} = \gamma_{sr_1} + \gamma_{sr_2}$ will have the probability density function $f_{\gamma_{sr}}(\gamma) = \frac{1}{\overline{\gamma_{sr}}^2}\gamma e^{-\frac{\gamma}{\overline{\gamma_{sr}}}}$.

Then, the lower bound on ASEP of the fDSTC system, $P^L_{\gamma_d}$, for BPSK modulation can be derived based on MGF-based approach of [16, Eq. 9.12]

$$P^L_{\gamma_d} = \frac{1}{\pi}\int_0^{\pi/2} \frac{\prod_{i\in\{r_1,r_2\}} M_{\gamma^U_{sid}}(-\frac{g_{BPSK}}{sin^2\theta})}{1+\frac{g_{BPSK}\overline{\gamma_{sd}}}{sin^2\theta}} d\theta, \tag{2.15}$$

where $g_{BPSK} = 1$ [16] and $M_{\gamma_{sd}} = \left(1+\frac{g_{BPSK}\overline{\gamma_{sd}}}{sin^2\theta}\right)^{-1}$ [16, Tab 9.1].

Similarly, the upper bound on ASEP of the fDSTC system, $P^U_{\gamma_d}$, can be written as

$$P^U_{\gamma_d} = \frac{1}{\pi}\int_0^{\pi/2} \frac{\prod_{i\in\{r_1,r_2\}} M_{\gamma^L_{sid}}(-\frac{g_{BPSK}}{sin^2\theta})}{1+\frac{g_{BPSK}\overline{\gamma_{sd}}}{sin^2\theta}} d\theta. \tag{2.16}$$

Fortunately, the moment generating function of γ^L_{sid}, $i \in \{r_1, r_2\}$ is already found in [17, Eq. 13]

$$M_{\gamma^L_{sid}}(s) = \frac{2}{p_i} e^{\alpha_i/2}\Big[-2\frac{\delta J_0}{\delta\alpha_i} - \frac{\sigma_i}{p_i}\frac{\delta J_0}{\delta\beta_i}\Big], \tag{2.17}$$

where $\sigma_i = \overline{\gamma_{id}} + \overline{\gamma_{si}}$, $p_i = \overline{\gamma_{id}\gamma_{si}}$, $\beta_i = 2/\sqrt{p_i}$ and $\alpha_i = (\sigma_i - p_i s)/p_i$. The formula of $\frac{\delta J_0}{\delta\alpha_i}$ and $\frac{\delta J_0}{\delta\beta_i}$ is given in Appendix A.

On the other hand, for the NR-DSTC protocol where there is no data exchange between the two relays, the post-detection SNR at destination is found as

$$\gamma^{'}_d = \gamma_{sd} + \epsilon_{sd}\frac{\sum_{j\in\{r_1,r_2\}} |h_{jd}G^{'}_{jd}a^{'}_j|^2}{\sum_{j\in\{r_1,r_2\}} |h_{jd}G^{\prime}{}_{jd}|^2 + 1}, \tag{2.18}$$

where $a^{'}_j = h_{sj}$ and $G^{'}_{jd} = \frac{h^*_{sj}}{|h_{sj}|}\sqrt{\frac{\epsilon_j}{\epsilon_s|h_{sj}|^2+1}}$.

We find that $\gamma^{'}_d < \gamma^L$ so $P^U_{\gamma_d} = P_{\gamma^L}$ is also the lower bound on ASEP of the NR-DSTC system.

2.3.1.2 Closed-form ASEP of the NR-fDSTC protocol

In this part, a closed-form ASEP of the NR-fDSTC protocol is derived when the relay-relay SNR is much larger than the source-relay SNR ($\gamma_{ij} \gg \gamma_{si}$). (2.5) can be rewritten as $\gamma_j \approx \gamma_{sj} + \gamma_{si} \quad i,j \in \{r_1, r_2\}, i \neq j$. One should note that the equality happens ($\gamma_j = \gamma_{sj} + \gamma_{si}$) when there is no error in the data exchange between the two relays.

Since $\gamma_{r_1} = \gamma_{r_2} = \gamma_r \approx \gamma_{sr_1} + \gamma_{sr_2}$, (2.9) can be approximated by

$$\gamma_d \approx \gamma_{sd} + \frac{(\gamma_{r_1 d} + \gamma_{r_2 d})\gamma_r}{\gamma_{r_1 d} + \gamma_{r_2 d} + \gamma_r + 1} = \gamma_{sd} + \frac{\gamma_{rd}\gamma_r}{\gamma_{rd} + \gamma_r + 1} = \gamma_{sd} + \gamma_{srd}, \tag{2.19}$$

with $\gamma_{rd} = \gamma_{r_1 d} + \gamma_{r_2 d}$ and $\gamma_{srd} = \frac{\gamma_{rd}\gamma_r}{\gamma_{rd}+\gamma_r+1}$.

Once again using the MGF-based approach, the closed form ASEP of the NR-fDSTC protocol can be derived by evaluating the MGF of γ_{sd} and γ_{srd}. The MGF of γ_{sd} is already shown in (2.15).

The MGF of γ_{srd} proved in Appendix B is given by

$$\begin{aligned} M_{\gamma_{srd}}(s) =& e^{\alpha/2}\Big[\frac{2}{p\sqrt{p}}\Big(-\big(1-\frac{\sigma^2}{p}\big)\frac{\delta J_0}{\delta\beta} + \big(\frac{\sigma^2}{p} - \frac{2\sigma}{p} - 2\big)\frac{\delta^2 J_0}{\delta\alpha\delta\beta} - \frac{4\sigma}{p}\frac{\delta^3 J_0}{\delta\beta\delta\alpha^2}\Big) \\ &+ \frac{2}{p^2}\Big(-\big(\frac{\sigma^2}{p}+4\big)\frac{\delta^3 J_0}{\delta\alpha^3} - \frac{1}{2}\big(\frac{\sigma^2}{p}+4\big)\frac{\delta^2 J_0}{\delta\alpha^2} + \frac{\sigma^2}{p}\frac{\delta J_0}{\delta\alpha} - \frac{\sigma^2}{8p}J_0\Big)\Big], \end{aligned} \tag{2.20}$$

where $\sigma = \overline{\gamma_{rd}} + \overline{\gamma_r}$, $p = \overline{\gamma_{rd}\gamma_r}$, and $\alpha = (\sigma - ps)/p$. The formulas of J_0, $\frac{\delta J_0}{\delta\alpha}$, $\frac{\delta J_0}{\delta\beta}$, $\frac{\delta^2 J_0}{\delta\alpha^2}$, $\frac{\delta^2 J_0}{\delta\alpha\delta\beta}$, $\frac{\delta^3 J_0}{\delta\beta\delta\alpha^2}$ and $\frac{\delta^3 J_0}{\delta\alpha^3}$ can be found in Appendix B. Note that the random variable $\gamma_{rd} = \gamma_{r_1 d} + \gamma_{r_2 d}$ will have a probability density function $f_{\gamma_{rd}}(\gamma) = \frac{1}{\overline{\gamma_{rd}}^2}\gamma e^{-\frac{\gamma}{\overline{\gamma_{rd}}}}$. Similarly, the probability density function of random variable $\gamma_r = \gamma_{sr_1} + \gamma_{sr_2}$ is $f_{\gamma_r}(\gamma) = \frac{1}{\overline{\gamma_r}^2}\gamma e^{-\frac{\gamma}{\overline{\gamma_r}}}$.

The ASEP of the NR-fDSTC protocol, with BPSK modulation, can be derived as

$$P_{\gamma_d} = \frac{1}{\pi}\int_0^{\pi/2} \frac{M_{\gamma_{srd}}(-\frac{g_{BPSK}}{sin^2\theta})}{1 + \frac{g_{BPSK}\overline{\gamma_{sd}}}{sin^2\theta}} d\theta, \tag{2.21}$$

where $g_{BPSK} = 1$ [16].

2.3.2 fDSTC protocol with R-relays

In this work, the destination is not aware of the error probabilities at the relays, making the use of the ML decoder at the destination impossible. Therefore taking the decoding errors at the two relays into account, the error probability of regenerative fDSTC (R-fDSTC) protocol, conditioned to the channel, is derived via a sub-optimal decoder at the destination. The Alamouti re-encoded signals $\boldsymbol{U}$ of the R-fDSTC protocol have the form of

$$\boldsymbol{U} = \begin{bmatrix} \sqrt{\epsilon_{r_1}}\hat{x}_{r_1}[2k] & \sqrt{\epsilon_{r_2}}\hat{x}_{r_2}[2k+1] \\ -\sqrt{\epsilon_{r_1}}\hat{x}^*_{r_1}[2k+1] & \sqrt{\epsilon_{r_2}}\hat{x}^*_{r_2}[2k] \end{bmatrix}, \tag{2.22}$$

where $\hat{x}_j[n]$ is obtained by decoding the combined signal $u_j[n]$ (2.3) at the relay $j \in \{r_1, r_2\}$ using ML decoder.

Using the MRC technique, the combined signal at the destination is

$$\begin{aligned} y_d[2k] = &\frac{\epsilon_s \left|h_{sd}\right|^2}{N_{sd}} x[2k] + \frac{\epsilon_{r_1} \left|h_{r_1 d}\right|^2}{N_{r_1 d}} \hat{x}_{r_1}[2k] + \frac{\epsilon_{r_2} \left|h_{r_2 d}\right|^2}{N_{r_2 d}} \hat{x}_{r_2}[2k] \\ &- \frac{\sqrt{\epsilon_{r_1}\epsilon_{r_2}} h^*_{r_1 d} h_{r_2 d}}{N_{r_2 d}} \hat{x}_{r_1}[2k+1] + \frac{\sqrt{\epsilon_{r_1}\epsilon_{r_2}} h^*_{r_1 d} h_{r_2 d}}{N_{r_1 d}} \hat{x}_{r_2}[2k+1] + z_{y_d}[2k], \end{aligned} \tag{2.23}$$

where z_{y_d} is AWGN with zero mean and variance $N_{z_{y_d}} = \frac{\epsilon_{r_1} \left|h_{r_1 d}\right|^2}{N_{r_1 d}} + \frac{\epsilon_{r_2} \left|h_{r_2 d}\right|^2}{N_{r_2 d}} + \frac{\epsilon_s \left|h_{sd}\right|^2}{N_{sd}}$.

The sub-optimal scalar decoder [30] is used instead of the ML decoder to decode the combined signal $y_d[2k]$. The decision on the transmitted symbol $x[2k]$ can be specifically obtained as

$$\hat{x}[2k] = sign\{Re\{y_d[2k]\}\}. \tag{2.24}$$

Then, in the presence of the decision errors at the relays, the closed-form expression of the error probability, conditioned to the channel, for the R-fDSTC protocol can be derived as (see Appendix C for more details)

$$\begin{aligned} P_{2k} = &\frac{1}{2}\left(1-p^{r_1}_{2k}\right)\left(1-p^{r_2}_{2k}\right)\left[\left(1-p^{r_1}_{2k+1}\right)\left(1-p^{r_2}_{2k+1}\right)+p^{r_1}_{2k+1}p^{r_2}_{2k+1}\right]\operatorname{erfc}(\beta_{2k}) \\ &+ \frac{1}{2}\left(1-p^{r_1}_{2k}\right)p^{r_2}_{2k}\left[\left(1-p^{r_1}_{2k+1}\right)\left(1-p^{r_2}_{2k+1}\right)+p^{r_1}_{2k+1}p^{r_2}_{2k+1}\right]\operatorname{erfc}(\delta_{2k}) \\ &+ \frac{1}{2}p^{r_1}_{2k}\left(1-p^{r_2}_{2k}\right)\left[\left(1-p^{r_1}_{2k+1}\right)\left(1-p^{r_2}_{2k+1}\right)+p^{r_1}_{2k+1}p^{r_2}_{2k+1}\right]\operatorname{erfc}(\lambda_{2k}) \\ &+ \frac{1}{2}p^{r_1}_{2k}p^{r_2}_{2k}\left[\left(1-p^{r_1}_{2k+1}\right)\left(1-p^{r_2}_{2k+1}\right)+p^{r_1}_{2k+1}p^{r_2}_{2k+1}\right]\operatorname{erfc}(\phi_{2k}) \\ &+ \frac{1}{4}\left(1-p^{r_1}_{2k}\right)\left(1-p^{r_2}_{2k}\right)\left[p^{r_1}_{2k+1}\left(1-p^{r_2}_{2k+1}\right)+\left(1-p^{r_1}_{2k+1}\right)p^{r_2}_{2k+1}\right]\left[\operatorname{erfc}(\beta_{2k}+\theta_{2k})+\operatorname{erfc}(\beta_{2k}-\theta_{2k})\right] \\ &+ \frac{1}{4}\left(1-p^{r_1}_{2k}\right)p^{r_2}_{2k}\left[p^{r_1}_{2k+1}\left(1-p^{r_2}_{2k+1}\right)+\left(1-p^{r_1}_{2k+1}\right)p^{r_2}_{2k+1}\right]\left[\operatorname{erfc}(\delta_{2k}+\theta_{2k})+\operatorname{erfc}(\delta_{2k}-\theta_{2k})\right] \\ &+ \frac{1}{4}p^{r_1}_{2k}\left(1-p^{r_2}_{2k}\right)\left[p^{r_1}_{2k+1}\left(1-p^{r_2}_{2k+1}\right)+\left(1-p^{r_1}_{2k+1}\right)p^{r_2}_{2k+1}\right]\left[\operatorname{erfc}(\lambda_{2k}+\theta_{2k})+\operatorname{erfc}(\lambda_{2k}-\theta_{2k})\right] \\ &+ \frac{1}{4}p^{r_1}_{2k}p^{r_2}_{2k}\left[p^{r_1}_{2k+1}\left(1-p^{r_2}_{2k+1}\right)+\left(1-p^{r_1}_{2k+1}\right)p^{r_2}_{2k+1}\right]\left[\operatorname{erfc}(\phi_{2k}+\theta_{2k})+\operatorname{erfc}(\phi_{2k}-\theta_{2k})\right], \end{aligned} \tag{2.25}$$

where

$$\beta_{2k} = \sqrt{\gamma_{r_1 d} + \gamma_{r_2 d} + \gamma_{sd}}; \quad \delta_{2k} = \frac{\gamma_{r_1 d} - \gamma_{r_2 d} + \gamma_{sd}}{\sqrt{\gamma_{r_1 d} + \gamma_{r_2 d} + \gamma_{sd}}}$$

$$\lambda_{2k} = \frac{-\gamma_{r_1 d} + \gamma_{r_2 d} + \gamma_{sd}}{\sqrt{\gamma_{r_1 d} + \gamma_{r_2 d} + \gamma_{sd}}}; \quad \phi_{2k} = \frac{-\gamma_{r_1 d} - \gamma_{r_2 d} + \gamma_{sd}}{\sqrt{\gamma_{r_1 d} + \gamma_{r_2 d} + \gamma_{sd}}}$$

$$\theta_{2k} = \frac{\sqrt{\epsilon_{r_1}\epsilon_{r_2}}Re\{h^*_{r_1d}h_{r_2d}\}}{\sqrt{\gamma_{r_1d}+\gamma_{r_2d}+\gamma_{sd}}}\Big(\frac{1}{N_{r_1d}}+\frac{1}{N_{r_2d}}\Big); \quad \text{erfc}(z) = \int_z^\infty \frac{exp(-x^2/2)}{\sqrt{2\pi}}dx$$

and p^j_{2k}, p^j_{2k+1} ($j \in \{r_1, r_2\}$) are the conditional error probabilities at relay j on $x[2k]$ and $x[2k+1]$ respectively. When considering the R-cDSTC protocol, the R-fDSTC protocol without transmission errors between relays (ideal case) and the R-fDSTC protocol with transmission errors between relays, p^j_{2k} can be found as

$$p^j_{2k} = \begin{cases} \frac{1}{2}\,\text{erfc}(\sqrt{\gamma_{sj}}), & \text{R-cDSTC protocol} \\ \frac{1}{2}\,\text{erfc}(\sqrt{\gamma_{sr_1}+\gamma_{sr_2}}), & \text{R-fDSTC protocol without transmission errors between relays} \\ \frac{1}{2}\,\text{erfc}(\sqrt{\gamma_{sj}+\frac{\gamma_{si}\gamma_{ij}}{\gamma_{si}+\gamma_{ij}+1}}), & \text{R-fDSTC protocol with transmission errors between relays} \end{cases} \tag{2.26}$$

2.3.3 Simulation results

Assuming that both relays have the same distance from source $d_{sr} = d_{sr_1} = d_{sr_2}$, let denote $r = \frac{d_{sr}}{d_{sd}}$ the relative distance of relays defined by the ratio of the source-relay distance d_{sr} and the source-destination distance d_{sd} and $rr = \frac{d_{rr}}{d_{sd}}$ the relative inter-distance of relays defined by the ratio of the relay-relay distance d_{rr} and the source-destination distance. In this section, the BER performance of the fDSTC protocol is evaluated for NR-relays and R-relays. Using a common transmission model, we set the path-loss $\Omega_{ij} \propto d_{ij}^{-pl}$ where d_{ij} is the distance between terminal i and terminal j, and pl is the path-loss exponent. In our simulations, $pl = 2$ is used and BPSK modulation is considered. For a fair comparison, the total transmit power of the protocol is kept as the same (i.e. P). For the cDSTC protocol $\epsilon_s + 2\epsilon_r = P$. In the other hand, for the fDSTC protocol, we have $\epsilon_s + 2\epsilon_r + 2\epsilon_{rr} = P$ ($\epsilon_{rr} = \frac{1}{10}\epsilon_r$). Unless other stated, we assume that $\epsilon_s = \epsilon_r$.

2.3.3.1 Bounds on ASEP of the NR-fDSTC protocol

To evaluate the bounds on ASEP of the NR-fDSTC protocol, we first consider the special case of a symmetric network in which the fading variances are identical, e.g, $\Omega_{ij} = 1\ \forall i, j$. In this simulation, the condition that $\gamma_{ij} \gg \gamma_{sj}$, $i, j \in \{r_1, r_2\}, i \neq j$ is satisfied. From Fig. 2.2, the BER performance of the NR-fDSTC protocol is exactly in the middle of the upper and lower bounds on ASEP, $P^U_{\gamma_d}$ and $P^L_{\gamma_d}$ respectively. Moreover, from the

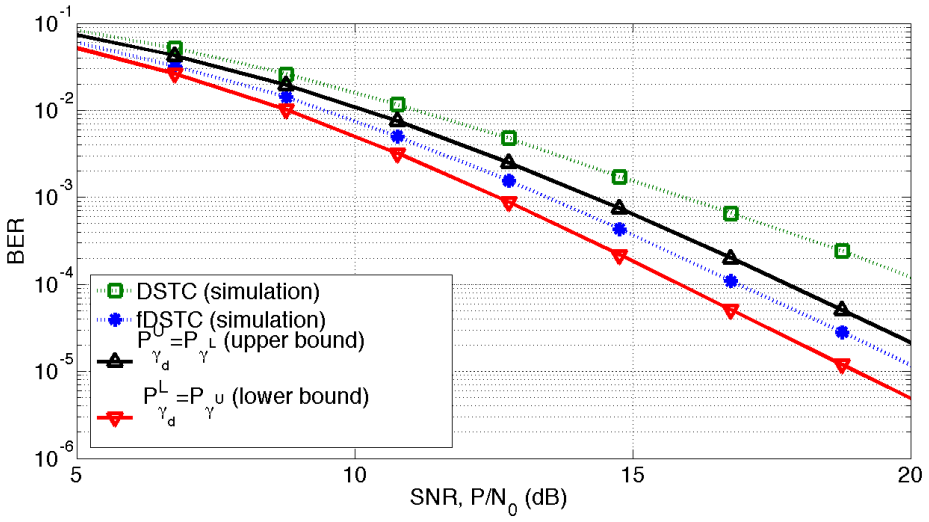

FIGURE 2.2: Upper bound and lower bound of the fDSTC system

simulation results, $P_{\gamma_d}^U$ is shown to be exactly the lower bound on ASEP of the NR-cDSTC protocol as mentioned in the end of Section 2.3.1.1.

2.3.3.2 fDSTC protocol vs cDSTC protocol

Fig. 2.3 shows the BER comparison between the fDSTC and cDSTC protocols as a function of the SNR (P/N_0) under some cases of the relative inter-distance between relays, rr. Fig. 2.3(a) shows the simulations for NR-relays while the simulations for R-relays are shown in Fig. 2.3(b). In these simulations, the relays are in the middle of the source and the destination ($r = 0.5$). The performance of the fDSTC protocol in terms of BER is shown to be much better than that of the cDSTC protocol thanks to the data exchange between the relays. When the relative inter-distance of relays is small ($rr < 0.2$), the performance of the fDSTC protocol is still comparable in comparison with the ideal case ($\Omega_{rr}^2 \gg \Omega_{sr}^2$) where there is no errors in the data exchange between the two relays. However, when the quality of the relay-relay link is too bad ($\Omega_{rr}^2 \ll \Omega_{sr}^2$), the BER performance of the fDSTC protocol logically tends to that of the cDSTC protocol since the inter-relay transmission does not bring any gain as compared to the cDSTC protocol. Mathematically, when $\frac{\Omega_{rr}^2}{\Omega_{sr}^2} \to 0$, the post-destination SNR at relays γ_j (2.5) tends to the source-relay SNR γ_{sj} ($\gamma_j \approx \gamma_{sj} + \gamma_{ij} \approx \gamma_{sj}$) as a result of $\gamma_{sj}, \gamma_{si} \gg \gamma_{ij}$. That leads to equal BER performance between the cDSTC and fDSTC protocols.

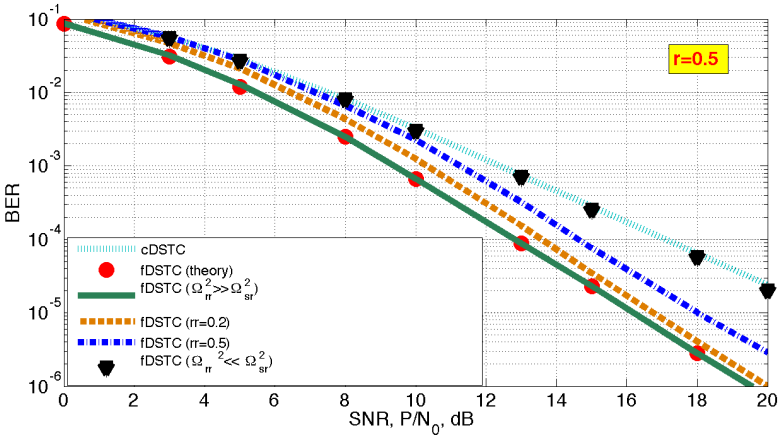

(a) non-regenerative fDSTC (NR-fDSTC)

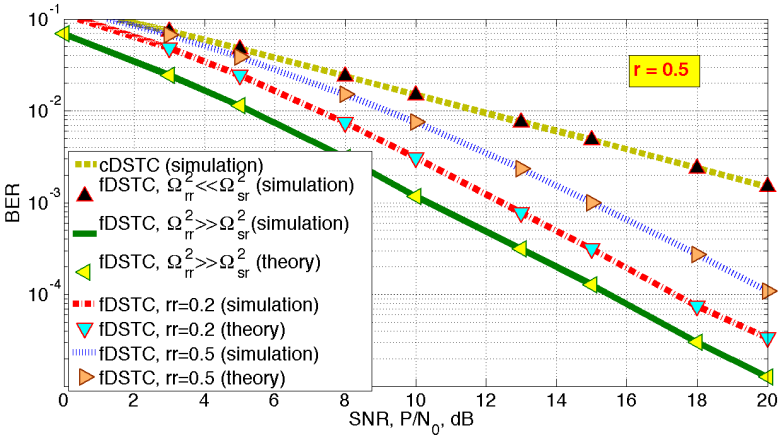

(b) regenerative fDSTC (R-fDSTC)

FIGURE 2.3: Effect of the inter-distance between relays when the relays are in the middle of the source and the destination ($r = 0.5$) for: a) NR-fDSTC protocol, b) R-fDSTC protocol.

2.3.3.3 Effect of the relative distance of relays

The effect of the relative distance of relays on the BER performance of the fDSTC and cDSTC protocols is shown in Fig. 2.4. At a desired $BER = 10^{-5}$, the required SNR is shown as a function of the relative distance of relays. Obviously, there will be a difference in the required SNR of each protocol when the relative distance of relays, r changes from 0.1 to 0.9. For the NR-cDSTC protocol, the difference is $6.3dB$. However, for the NR-fDSTC protocol, this difference is decreased to $1.6dB$, which means that the effect of the relative distance of relays is reduced by up to 75%. For R-relays, we still get up to a 64% reduction of the effect of the relative distance of relays. The difference of required SNR changes from $20.5dB$ in case of the R-cDSTC protocol down to $7.4dB$ in case of the

R-fDSTC protocol. This is a very impressive result especially for the mobile relays since for the fDSTC protocol, the required SNR has almost no change (NR-relays) or a little change (R-relays) when the relays are moving between the source and the destination.

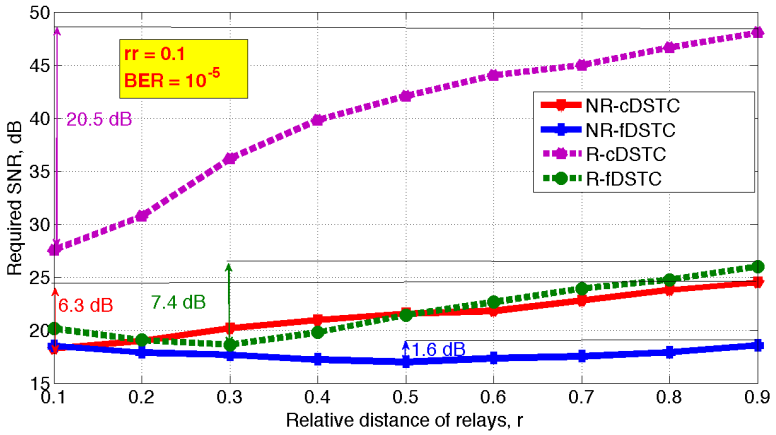

FIGURE 2.4: Required SNR versus relative distance of relays for a desired $BER = 10^{-5}$ and when the relative inter-distance of relays is equal to 0.1 ($rr = 0.1$).

The SNR gain of the fDSTC protocol over the cDSTC protocol versus the relative distance of relays at a desired $BER = 10^{-5}$ is shown in Fig. 2.5. The average SNR gain of the NR-fDSTC protocol over the NR-cDSTC protocol is $3.7dB$ as shown in [68]. However, the average SNR gain of the R-fDSTC protocol over the R-cDSTC protocol is even much more impressive. By using the simple data exchange between the two relays, we can get the average SNR gain up to $18.1dB$.

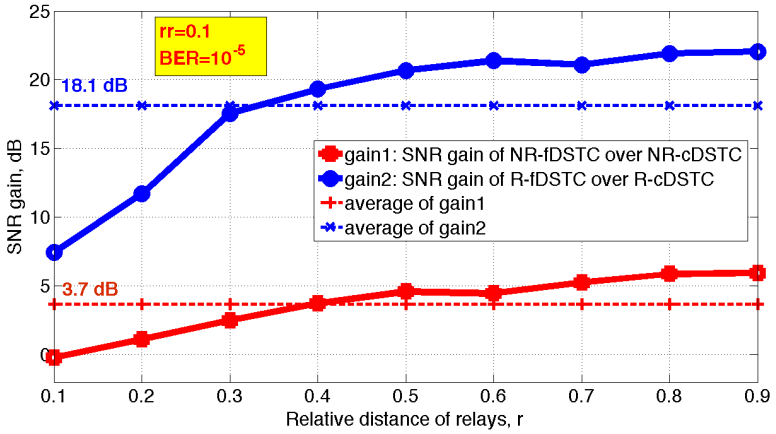

FIGURE 2.5: SNR gain of the fDSTC protocol over the cDSTC protocol as a function of the relative distance of relays ($BER = 10^{-5}$ and $rr = 0.1$).

2.3.4 Power allocation

Let $\epsilon_s = c_P P$ $(0 < c_P < 1)$ and $\epsilon_r = \frac{10}{22}(1 - c_P)P$. Using the exhaustive search by simulation, we can find the best value of c_P (i.e. c_P^{opt}) to further increase the BER performance of the fDSTC protocol as shown in Fig. 2.6. The best power allocation points of the fDSTC protocol for NR-relays and R-relays are respectively $c_P^{opt} = 0.4$ and $c_P^{opt} = 0.6$ when considered in the case $BER = 10^{-5}$, $r = 0.5$ and $rr = 0.1$. In addition, as compared to the case of equal power allocation (i.e. $c_P = 10/32$), the SNR gains of $0.5dB$ (NR-relays) and $1.5dB$ (R-relays) are obtained.

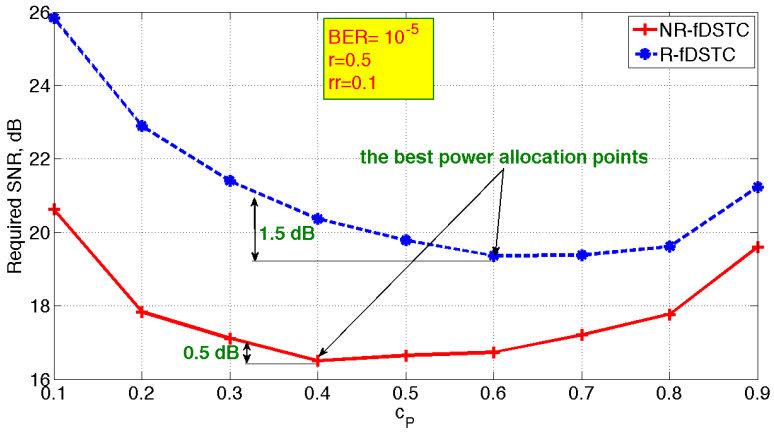

FIGURE 2.6: Optimal power allocation of the fDSTC protocols ($rr = 0.1$ and $r = 0.5$).

2.4 Spectral efficiency

In this section, the cDSTC and fDSTC protocols are considered in terms of outage probability while having the same spectral efficiency R(bits/s/Hz). Using the methodology in [9] to find the approximations of the outage probability of the protocols, it is shown that the NR-fDSTC protocol can achieve the maximum diversity order despite using AGC at the relays. Besides, the R-fDSTC protocol also brings us a higher diversity oder in comparison with the R-cDSTC protocol.

2.4.1 Outage probability analysis

Outage probability is defined as $P_{out} = Pr\{I < R\}$ where I is the maximum average mutual information between source and destination and R is the spectral efficiency. In this work, without loss of generality we note $\Omega_{sr}^2 = \Omega_{sr_1}^2 = \Omega_{sr_2}^2$ and $\Omega_{rd}^2 = \Omega_{r_1d}^2 = \Omega_{r_2d}^2$. The function $f(x,y) = \frac{xy}{x+y+1}$ used for the fading coefficients in the following expressions is defined in [9].

For a fair comparison, once again the total transmit power is the same for the protocols, i.e. $\epsilon_s + 2\epsilon_r = P$ (cDSTC) and $\epsilon_s + 2\epsilon_r + 2\epsilon_{rr} = P$ (fDSTC with $\epsilon_{rr} = \frac{1}{10}\epsilon_r$). Let the transmit power be equally allocated among source and the relays ($\epsilon_s = \epsilon_r = \epsilon$, $N_{ij} = N_0$ $(\forall i,j)$ and $SNR = \epsilon/N_0$. The outage probability of the protocols is determined based on the SNR parameter for different types of relays. For shortening the following expressions, we note $|h_{sr}|^2 = \min\{|h_{sr_1}|^2, |h_{sr_2}|^2\}$, $||\boldsymbol{a_{sr}}||^2 = |h_{sr_1}|^2 + |h_{sr_2}|^2$ and $||\boldsymbol{a_{rd}}||^2 = |h_{r_1d}|^2 + |h_{r_2d}|^2$.

2.4.1.1 NR-relays

a/ cDSTC protocol

The maximum average mutual information can be expressed as

$$I_{cDSTC}^{NR} = \frac{1}{2}\log\Big(1 + SNR.|h_{sd}|^2 + f\big(SNR.|h_{sr}|^2, SNR.||\boldsymbol{a_{rd}}||^2\big)\Big). \tag{2.27}$$

In the high SNR region, the outage probability of the cDSTC protocol can be approximated as

$$\begin{aligned} Pr\{I_{cDSTC}^{NR} < R\} &= Pr\Big\{|h_{sd}|^2 + \frac{1}{SNR} f\big(SNR.|h_{sr}|^2, SNR.||\boldsymbol{a_{rd}}||^2\big) < \frac{2^{2R}-1}{SNR}\Big\} \\ &\sim \frac{1}{2}\frac{1}{\Omega_{sr}^2}\frac{1}{\Omega_{sd}^2}\Big(\frac{2^{2R}-1}{SNR}\Big)^2 \text{ when } SNR \to \infty. \end{aligned} \tag{2.28}$$

Using AGC at the relays, it is claimed in [24] that the NR-fDSTC protocol can not achieve full diversity. Here, the maximum diversity order is only two. This result is totally suitable to the simulation results in [24].

b/ fDSTC protocol

The maximum average mutual information can be derived as

$$I_{fDSTC}^{NR} = \frac{1}{4}\log\Big(1 + SNR.|h_{sd}|^2 + f\big(SNR.||\boldsymbol{a_{sr}}||^2, SNR.||\boldsymbol{a_{rd}}||^2\big)\Big). \tag{2.29}$$

The approximation of the outage probability in the high SNR region is

$$\begin{aligned} Pr\{I_{fDSTC}^{NR} < R\} &= Pr\Big\{|h_{sd}|^2 + \frac{1}{SNR} f\big(SNR.||\boldsymbol{a_{sr}}||^2, SNR.||\boldsymbol{a_{rd}}||^2\big) < \frac{2^{4R}-1}{SNR}\Big\} \\ &\sim \frac{1}{3!}\frac{\Omega_{sr}^4 + \Omega_{rd}^4}{\Omega_{sr}^4\Omega_{rd}^4}\frac{1}{\Omega_{sd}^2}\Big(\frac{2^{4R}-1}{SNR}\Big)^3 \text{ when } SNR \to \infty. \end{aligned} \tag{2.30}$$

With NR-relays, the fDSTC protocol can achieve full diversity order.

2.4.1.2 R-relays

a/ cDSTC protocol

The maximum average mutual information can be expressed as

$$I_{cDSTC}^{R} = \frac{1}{2}\min\Big\{\log(1 + SNR.|h_{sr}|^2), \log\big(1 + SNR.(|h_{sd}|^2 + ||\boldsymbol{a_{rd}}||^2)\big)\Big\}. \tag{2.31}$$

The outage probability in high SNR regions can be approximated as

$$\begin{aligned} Pr\{I_{cDSTC}^{R} < R\} &= Pr\Big\{\min\big\{|h_{sr}|^2, |h_{sd}|^2 + ||\boldsymbol{a_{rd}}||^2\big\} < \frac{2^{2R}-1}{SNR}\Big\} \\ &\sim \frac{1}{\Omega_{sr}^2}\Big(\frac{2^{2R}-1}{SNR}\Big) \text{ when } SNR \to \infty. \end{aligned} \tag{2.32}$$

The diversity order of the R-cDSTC system is only 1.

b/ fDSTC protocol

The maximum average mutual information can be derived as

$$I_{fDSTC}^{R} = \frac{1}{4}\min\Big\{\log\big(1 + SNR.||\boldsymbol{a_{sr}}||^2\big), \log\big(1 + SNR.(|h_{sd}|^2 + ||\boldsymbol{a_{rd}}||^2)\big)\Big\}. \tag{2.33}$$

In high SNR regions, the outage probability becomes

$$\begin{aligned} Pr\{I^R_{fDSTC} < R\} &= Pr\Big\{\min\big\{||\boldsymbol{a_{sr}}||^2, |h_{sd}|^2 + ||\boldsymbol{a_{rd}}||^2\big\} < \frac{2^{4R}-1}{SNR}\Big\} \\ &\sim \frac{1}{2}\frac{1}{\Omega^4_{sr}}\Big(\frac{2^{4R}-1}{SNR}\Big)^2 \text{ when } SNR \to \infty. \end{aligned} \tag{2.34}$$

The R-fDSTC protocol can not achieve the full diversity. However, it can help us increase the system diversity order from 1 to 2 in comparison with the R-cDSTC protocol.

2.4.2 Diversity-multiplexing tradeoff (DMT)

The diversity-multiplexing tradeoff illuminates the relationship between the reliability of data transmissions in terms of diversity gain, and the spectral efficiency in terms of multiplexing gain. The multiplexing gain which illustrates how fast the source data rate varies with respect to SNR is defined as [69]

$$g = \lim_{SNR\to\infty} \frac{R}{\log SNR}. \tag{2.35}$$

The diversity gain $d(g)$ can be characterized as a function of g [69]

$$d(g) = \lim_{SNR\to\infty} -\frac{\log P_{out}}{\log SNR}. \tag{2.36}$$

Based on the approximations of outage probability for the protocols in the above parts, the DMT of the cDSTC and fDSTC protocols for NR-relays and R-relays can be expressed respectively as

$$d^{NR}_{cDSTC}(g) = 2(1-2g), \tag{2.37}$$

$$d^{NR}_{fDSTC}(g) = 3(1-4g), \tag{2.38}$$

$$d^{R}_{cDSTC}(g) = 1(1-2g), \tag{2.39}$$

$$d^{R}_{fDSTC}(g) = 2(1-4g). \tag{2.40}$$

2.4.3 Numerical results

In this subsection, numerical results of the outage probability for the protocols are considered in statistically symmetric networks, e.g. $\Omega_{ij}^2 = 1$ and in small fixed R regime, e.g. $R = 1$. Fig. 2.7 shows the outage probability of the cDSTC and fDSTC protocols for NR-relays and R-relays as a function of SNR_{norm} which is defined by $SNR_{norm} = \frac{P}{N_0}\frac{1}{[2^R-1]}$ [9]. The analytic expressions perfectly match with the simulation results in high SNR region. The R-fDSTC protocol has better performance than the R-cDSTC protocol when SNR_{norm} is greater than $21dB$. Similarly, in the case of NR-relays, the fDSTC protocol provides better performance than the cDSTC protocol when SNR_{norm} is greater than $30.5dB$. This result is quite interesting since, despite using more time slots for the transmission protocol (due to the data exchange between relays), the fDSTC protocol still reaches a better outage probability than the cDSTC protocol in the high SNR region, no matter what type of relays is used as a result of higher diversity order of the fDSTC system as compared to the cDSTC system.

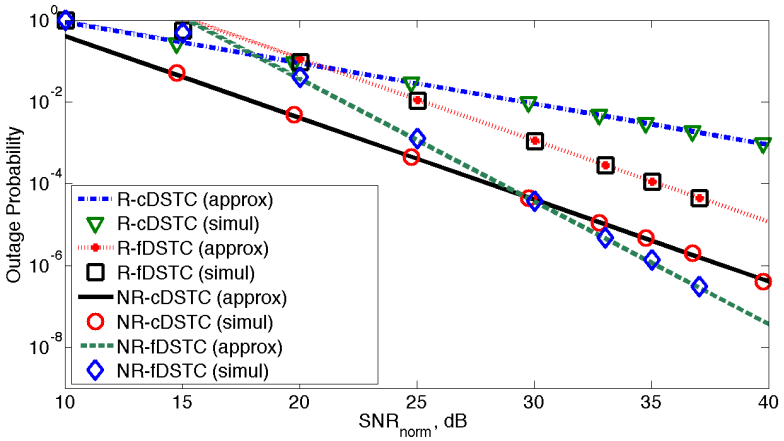

FIGURE 2.7: Outage probability versus SNR_{norm}, small, fixed R regime (R=1) and for statistically symmetric networks, i.e. $\Omega_{ij}^2 = 1$.

The tradeoff between the diversity order and the multiplexing gain of the systems is shown in Fig. 2.8. The NR-fDSTC system can achieve a maximum diversity order ($d(g) = 3$ for a system with one source, two relays and one destination). On the other hand, the diversity order of the NR-cDSTC system is only two. For R-relays, while the cDSTC system only gets the first diversity order, the fDSTC system can achieve the second diversity order. This means, in all cases (i.e. NR-relays or R-relays), using the fDSTC system can help to get higher diversity order. Moreover, there are some interesting sharp transitions in Fig. 2.8. We will use the fDSTC protocol for R-relays

when $g < 1/6$, otherwise when $g \geqslant 1/6$ the cDSTC protocol is used; similarly for NR-relays, the fDSTC will be preferred for $g < 1/8$.

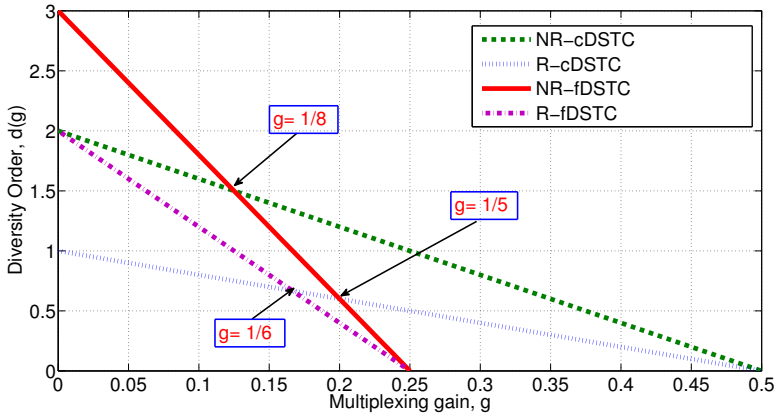

FIGURE 2.8: Diversity order $d(g)$ versus multiplexing gain g.

2.5 Energy efficiency

Energy consumption in wireless communications becomes a crucial design in future wireless generation, i.e green communications. Therefore, many energy-efficient communication protocols are proposed. However, they only consider on transmission energy, but forget circuit energy consumption. That leads to inaccurate evaluation of total energy consumption of the protocols. Consequently, for a precise comparison in terms of energy efficiency, the total energy consumption of the communication techniques including both the transmission energy and the circuit energy should be considered.

In the literature, many energy models (i.e. artificial or real models) have been addressed to evaluate the total energy consumption in recent years. Some famous artificial energy models based on theoretical calculations are derived in [70–72]. In [73], the parameters of the low power FSK radio transceiver developed at CSEM within the WiseNET project [70] is used to evaluate the energy performance of the WiseMAC protocol. In [11, 74], the authors used an On-Off-Keying transceiver designed by the PicoRadio RF group BWRC [71]. On the other hand, in [64], an energy model of a sensor node is given based on [72] by Shuguang Cui et al. Thanks to the accuracy and simplicity, Cui energy model are widely used to evaluate the total energy consumption of the protocols in [10, 67, 75–79].

Besides the artificial energy models, realistic energy models of a sensor node which are based on a real platform are also interesting to evaluate the total energy consumption

since the estimation of energy consumption is more precise. In [80], Rene Motes using the Atmel AT90LS8535 micro-controller [81] and the TR1000 radio transceiver of RF Monolithics [82] is considered to show the energy efficiency of the S-MAC protocol. The Mica2 mote and the CC1000 transceiver are considered in [83, 84] to evaluate the energy performance of the B-MAC and CL-MAC protocols respectively. Recently, a pragmatic and precise hybrid model is proposed based on the PowWow platform [85]. Besides, a realistic power consumption model for a sensor node based on two widely used transceivers, CC1000 and CC2420 is also presented by Qin Wang and his colleagues in [86].

Energy modeling is also an important issue for designing low power sensor networks. However, it is out of bounds of this thesis where we only use some existent energy models to evaluate the energy efficiency of our protocols. To compare our results with the previous works, we will consider the widely used artificial energy model (i.e. Cui energy model) and to have a more precise energy evaluation, a realistic energy model based on PowWow platform is chosen. For the rest of the thesis, unless otherwise stated, all the statements about typical energy model and realistic energy model are respectively referring to Cui model and the PowWow platform.

2.5.1 Energy models

2.5.1.1 Typical energy model

In this section, a typical energy model is presented for a general communication link connecting two wireless nodes. In order to have a precise estimation, the total energy consumption consists of the transmission and circuit energy. Here, the circuit energy consumption is the sum of all the energy consumed by all the circuit blocks at the transmitter and the receiver (i.e. Analog to Digital Converter (ADC), Digital to Analog Converter (DAC), Intermediate Frequency Amplifier (IFA), Frequency Synthesizer, Mixer, Low Noise Amplifier (LNA), Power Amplifier (PA), and base band Digital Signal Processing (DSP)). However, in order to keep the energy model from being over-complicated, baseband DSP blocks (e.g. source coding, pulse-shaping, and digital modulation) are intentionally omitted. The energy model is also assumed to include no Error Correction Code (ECC) blocks.

The typical radio frequency (RF) system blocks of transmitter and receiver are respectively shown in Fig. 2.9 and Fig. 2.10 where M_t and M_r are the number of transmitter and receiver antennas respectively.

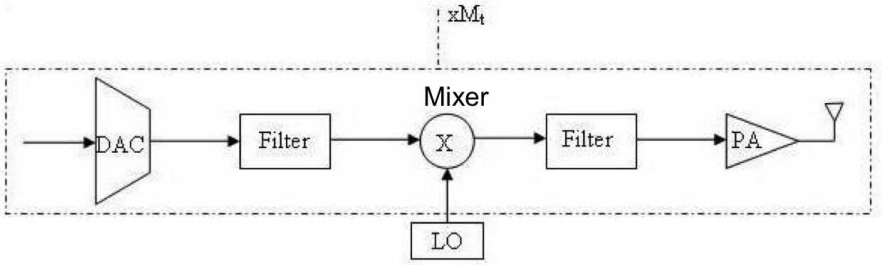

FIGURE 2.9: Transmitter Circuit Blocks

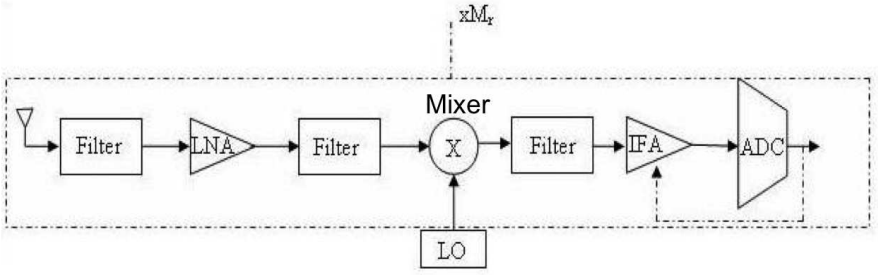

FIGURE 2.10: Receiver Circuit Blocks

As mentioned above, the total average power consumption along the signal path can be divided into two main components: the transmission power consumption consisting of the power consumption of all the power amplifiers P_{PA} and the circuit power consumption referred as the power consumption of all other circuit blocks P_c. P_{PA} depends on the needed transmission power P_{Tx}^{needed}. In this thesis, the channel is square law path loss (i.e. power loss factor $pl = 2$). Consequently, the needed transmission power P_{Tx}^{needed} can be calculated as a function of transmission distance d_{sd}

$$P_{Tx}^{needed}(d_{sd}) = \bar{E}_b R_b \times \frac{(4\pi d_{sd})^2}{G_t G_r \lambda_c^2} M_l N_f, \tag{2.41}$$

where $\bar{E}_b$ is the mean required energy per bit for ensuring a given error rate requirement, R_b is the bit rate, d_{sd} is the transmission distance, G_t and G_r are the transmitter and receiver antenna gains, λ is the carrier wave length, M_l is the link margin, N_f is the receiver noise figure defined as $N_f = N_r/N_0$ with $N_0 = -174dBm/Hz$ single-side thermal noise Power Spectral Density (PSD) and N_r is the PSD of the total effective noise at receiver input.

The power consumption P_{PA} of the power amplifiers can be approximated as

$$P_{PA} = (1 + c_o)P_{out}, \tag{2.42}$$

where $c_o = \frac{\xi}{\eta} - 1$ with η the drain efficiency of the RF power amplifier and ξ the Peak-to-Average Ratio (PAR) which depends on the modulation scheme and the associated constellation size.

$f_c = 2.5GHz$	$\xi = 0.35$
$G_t G_r = 5dBi$	$\eta = 1$
$B = 10KHz$	$\sigma^2 = \frac{N_0}{2} = -174dBm/Hz$
$P_{mix} = 30.3mW$	$P_{syn} = 50.0mW$
$P_b = 10^{-5}$	$P_{LNA} = 20mW$
$P_{filt} = P_{filr} = 2.5mW$	$P_{IFA} = 3mW$
$P_{ADC} = 6.69mW$	$P_{DAC} = 15.4mW$
$N_f = 10dB$	$M_l = 40dB$

TABLE 2.1: The system parameters

The total circuit power consumption P_c of the general communication link is the sum of the circuit power consumption of the transmitter and receiver and is given by

$$P_c \approx M_{tx}P_c^{tx} + M_{rx}P_c^{rx}, \tag{2.43}$$

where M_{tx} and M_rx are the number of transmit and receive antennas respectively, $P_c^{tx} = P_{DAC} + P_{mix} + P_{filt} + P_{syn}$ is the circuit power consumption of the transmitter, $P_c^{rx} = P_{LNA}+P_{mix}+P_{IFA}+P_{filr}+P_{ADC}+P_{syn}$ is the circuit power consumption of the receiver, P_{DAC}, P_{mix}, P_{LNA}, P_{IFA}, P_{filt}, P_{filr}, P_{ADC} and P_{syn} are the power consumption values for the DAC, the mixer, the LNA, the IFA, the active filters at the transmitter side, the active filters at the receiver side, the ADC, and the frequency synthesizer, respectively. To estimate the values of P_{DAC}, P_{mix}, P_{LNA}, P_{IFA}, P_{filt}, P_{filr}, P_{ADC} and P_{syn}, the artificial transceiver model introduced in [72] is used. Its parameters are shown in Tab. 2.1.

Finally, the total energy consumption per bit for a fixed rate system can be obtained as

$$E^b = (P_{PA} + P_c)/R_b. \tag{2.44}$$

2.5.1.2 Realistic energy model

2.5.1.2.a PowWow platform

The energy consumption of the systems can also be evaluated based on the parameters of PowWow platform (Fig. 3), developed by INRIA/CAIRN project-team [87] in 2008. PowWow is a hardware platform for wireless sensor networks and its associated software infrastructure. As the main constraint in WSN is energy consumption, both are specifically designed to be very energy efficient:

FIGURE 2.11: PowWow platform

- To reduce the radio activity, the MAC layer is based on an asynchronous rendezvous scheme initiated by the receiver
- Architectural and circuit level optimizations were performed to design the platorm, which offers the possibility to add efficient FPGA co-processing
- The software is derived from the Protothread library of Contiki and offers the flexibility and the compactness of event-driven programming

As a consequence, PowWow requires a lighter hardware system than ZigBee to be processed (memory usage is less than 10kb), the lifetime of WSN is increased, and the

price per node is decreased. Currently some demo applications are provided (a temperature monitoring and a motion tracking for mobile node) and PowWow is already used in several research projects (CAPTIV, SVP, GEODES) [88]. In order to optimize the network regarding a particular application, PowWow offers the following extra features: over-the-air re-programmation (and soon reconfiguration), analytical power estimation based on software profiling and power measurements, a network analyzer to probe and fix transmission errors in the network.

PowWow platform is composed of:

- The motherboard, designed to reduce power consumption of sensors node, embeds an MSP430 microcontroller and all needed components to process PowWow protocol except radio chip. JTAG, RS232, and I2C interfaces are available on this board.
- The radio chip daughter board is currently based on a TI CC2420.
- The coprocessing daughter board includes a low-power FPGA which allows for hardware acceleration for some PowWow features and also includes dynamic voltage scaling features to increase power efficiency. The current version of PowWow integrates an Actel IGLOO AGL250 FPGA and a programmable DC-DC converter.

2.5.1.2.b Energy Analysis

The real experiments on PowWow claimed that for a RF transmission, the energy consumption of mother board is much less significant in comparison with radio chip daughter board. Therefore, in this thesis the energy consumption of mother board is considered as negligible. The component consuming the most significant energy is the TI CC2420 transceiver. The RF structure of CC2420 transceiver chip can be modeled in Fig. 2.12

The total power consumption for transmitting and for receiving, denoted by P_T and P_R are calculated by:

$$P_T(d_{sd}) = P_{TB} + P_c^{tx} + P_{PA}(d_{sd}) = P_{T0} + P_{PA}(d_{sd}), \tag{2.45}$$

$$P_R = P_{RB} + P_c^{rx} + P_{LNA} = P_{R0}, \tag{2.46}$$

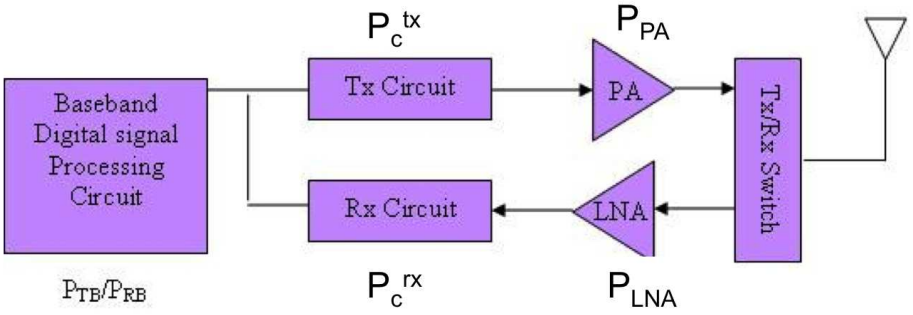

FIGURE 2.12: RF components of CC2420 chip

where P_{TB}/P_{RB} is the power consumption (mW) in baseband digital signal processing circuit for transmitting or receiving, P_c^{tx}/P_c^{rx} is the power consumption (mW) in front-end circuit for transmitting or receiving (including ADC, DAC, IFA, etc.). P_{PA} is the power consumption (mW) of the power amplifier, P_{LNA} is the power consumption (mW) of the low noise amplifier. Since P_{TB} and P_c^{tx} do not depend on the transmission distance d_{sd}, the two components can be modeled as a constant, P_{T0}. Similarly, since P_{RB}, P_c^{rx} and P_{LNA} do not depend on the transmission distance, the power consumption of the receiving circuit can also be considered as a constant, P_{R0}. Unlike the above typical artificial energy model, here, the energy consumption for baseband DSP is taken into account.

In general, the power consumption of the power amplifier, for reliable transmission $P_{PA}(d_{sd})$ depends on the needed transmit power $P_{Tx}^{needed}(d_{sd})$ and is given by

$$P_{PA}(d_{sd}) = \frac{P_{Tx}^{needed}(d_{sd})}{\eta}, \tag{2.47}$$

with η the drain efficiency.

From (2.45) and (2.47) the total transmitting power consumption is expressed as

$$P_T(d_{sd}) = P_{T0} + \frac{P_{Tx}^{needed}(d_{sd})}{\eta}. \tag{2.48}$$

From [89], we can draw the function of P_T depending on P_{Tx}^{needed}, as illustrated by Fig. 2.13. Moreover, as mentioned in [86], the P_{R0} and P_{T0} values of TI CC2420 transceiver is measured to be equal to $59.1mW$ and $26.5mW$ respectively.

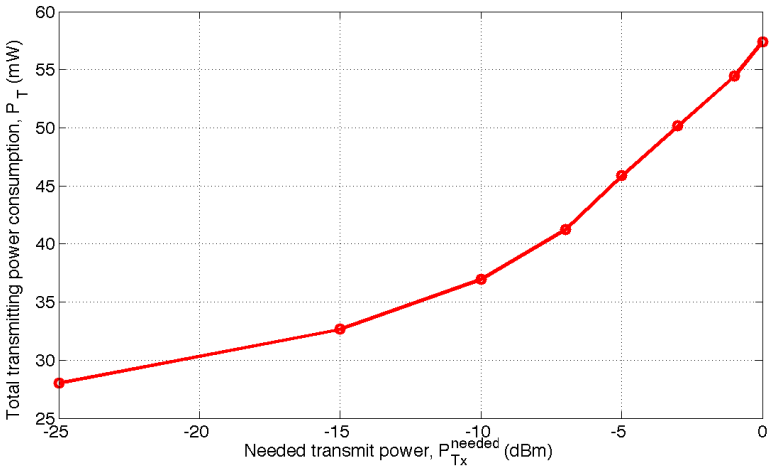

FIGURE 2.13: The total transmitting power consumption at the needed transmit power ($V_{dd} = 3.3V$)

On the other hand, in free space propagation, the needed transmit power can be derived as a function of the desired receive power at the receiver [90].

$$P_{Tx}^{needed}(d_{sd}) = P_{Rx}^{desired} \times \frac{(4\pi d_{sd})^2 L}{G_t G_r \lambda_c^2}, \tag{2.49}$$

where G_t and G_r are the transmitter and receiver antenna gains, L is the system loss factor not related to propagation, λ is the carrier wavelength and $P_{Rx}^{desired}$ is the desired receive power at destination. (2.49) is very close to (2.45) except that $P_{Rx}^{desired}$ is precisely calculated (2.50) instead of a rough estimation like (2.45).

$P_{Rx}^{desired}$ can be referred as [91]

$$P_{Rx}^{desired} = N_0 \rho^{(P_e,r)} (1 + c_f) N_f R_b, \tag{2.50}$$

with c_f the roll-off factor, N_f the noise figure, $\rho^{(P_e,r)}$ the needed SNR at the receiver which is a function of the desired error probability P_e and the relative distance of relay r, N_0 the single-sided thermal noise Power Spectral Density and R_b the transmit bit rate.

Replacing (2.50) into (2.49), $P_{Tx}^{needed}(d_{sd})$ can be derived as

$$P_{Tx}^{needed} = \frac{N_0 \rho^{(P_e,r)} (1 + c_f) N_f (4\pi d_{sd})^2 L R_b}{G_t G_r \lambda^2}. \tag{2.51}$$

In a CC2420 transceiver, the maximum transmit power, P_{Tx}^{max}, is $0dBm$ and the sensitivity of the receiver low noise amplifier P_{Rx}^{min} is $-95dBm$. Therefore, in a real communication, the following conditions must be satisfied

$$P_{Tx}^{needed} \leq P_{Tx}^{max}(0dBm), \tag{2.52}$$

$$P_{Rx}^{desired} \geq P_{Rx}^{min}(-95dBm). \tag{2.53}$$

Finally, the total energy consumption per bit of a fixed rate system using the PowWow platform is derived as

$$E^b = (P_T(d_{sd}) + P_R)/R_b. \tag{2.54}$$

For the energy consumption estimation of systems using the PowWow platform, the real parameters of TI CC2420 transceiver (Tab. 2.2) are used in this thesis

$f_c = 2.4GHz$	$c_f = 0.25$
$G_t G_r = 1$	$R_b = 250kbit/s$
$P_{R0} = 59.1mW$	$P_{T0} = 26.5mW$
$N_f = 10dB$	$L = 1$
$\frac{N_0}{2} = -174dBm/Hz$	$P_e = 10^{-5}$

TABLE 2.2: Parameters of CC2420 transceiver

2.5.2 Simulation results

To have a fair comparison in the total power consumption of the two protocols, the total energy consumption for both protocols (fDSTC and cDSTC) is considered. Obviously, the fDSTC protocol consumes supplement transmit and circuit energy due to the inter-relay communication. However, by simulations, the fDSTC protocol is shown to be an energy-efficient protocol for long-range transmissions.

The total energy consumption per bit of the fDSTC protocol E_{fDSTC}^b can be calculated by the sum of the total energy consumption per bit of the broadcast phase of the source E_s^b, the data exchange phase between the two relays E_{rr}^b, the transmission phase from the relays to the destination E_{rd}^b. The total energy consumption per bit of the cDSTC protocol E_{cDSTC}^b is the same except that there is no energy consumption for the data

exchange phase between the relays.

$$E^b_{fDSTC} = E^b_s + E^b_{rr} + E^b_{rd}, \tag{2.55}$$

$$E^b_{cDSTC} = E^b_s + E^b_{rd}. \tag{2.56}$$

Note that E^b_s, E^b_{rr}, and E^b_{rd} are calculated based on the energy models in previous parts based on the typical or realistic energy models.

On the one hand, Fig. 2.14 shows the total energy consumption per bit of the cDSTC and fDSTC protocols with NR-relays and R-relays based on parameters of typical energy model as shown in Tab. 2.1 in two cases: (a) when the transmission distance $d_{sd} < 30m$ and (b) when $d_{sd} > 100m$. The case when $30m < d_{sd} < 100m$ is not illustrated since there is no cross-over point. At short-range transmissions, the fDSTC protocol consumes more energy than the cDSTC protocol due to the data exchange between the relays. However, for long-range transmissions, the lower transmission energy of the fDSTC protocol makes it become energy-efficient. With R-relays, at $d_{sd} = 25m$, the fDSTC protocol can save up to 50% of the total energy consumption. Otherwise, with NR-relays, the fDSTC protocol consumes less energy than the cDSTC only when $d_{sd} > 200m$ and at $d_{sd} = 270m$, the fDSTC protocol can save 20% of the total energy consumption.

On the other hand, the parameters extracted from TI CC2420 (Tab. 2.2) are used to illustrate the total energy consumption per bit of the cDSTC and fDSTC protocols. Unlike some typical energy models used to evaluate the energy consumption, the real transceiver has its own maximum transmit power, P^{max}_{Tx}, and sensitivity of receiver low noise amplifier is P^{min}_{Rx}. These constraints must be considered in the real transmission (i.e. the total transmit power of the protocols must be lower than P^{max}_{Tx}). For TI CC2420, $P^{max}_{Tx} = 0dBm$ and $P^{min}_{Rx} = -95dBm$. The fDSTC protocol consumes more circuit energy than the cDSTC protocol due to the data exchange between the relays. However, the lower transmission energy of the fDSTC protocol makes it able to increase the transmission range, d_{sd} (Fig. 2.15). With R-relays, d_{sd} is increased from $15m$ to $190m$. Otherwise, with NR-relays, the fDSTC protocol can widen d_{sd} from $165m$ to $290m$.

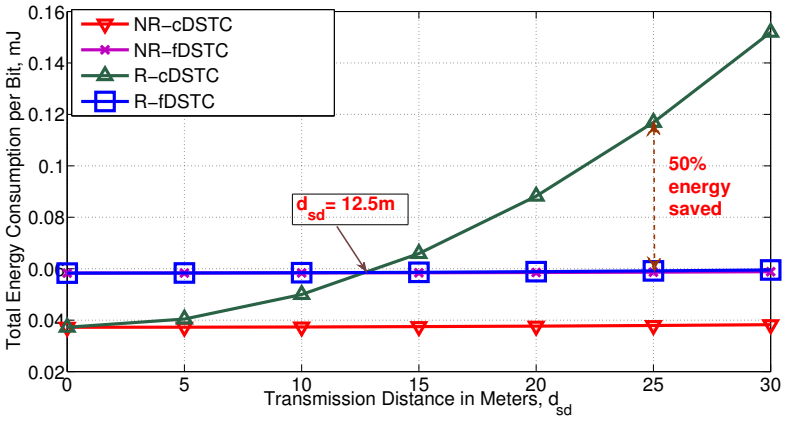

(a) $d_{sd} < 30m$

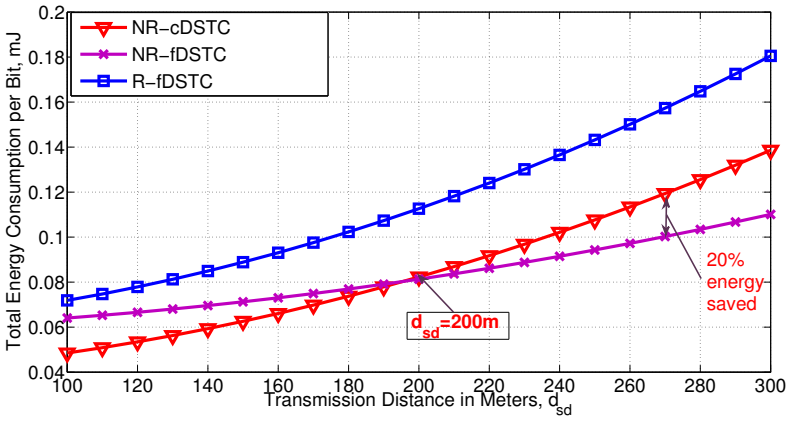

(b) $d_{sd} > 100m$

FIGURE 2.14: Total energy consumption per bit of the fDSTC and cDSTC protocol with NR-relays and R-relays for two cases: a) the transmission distance $d_{sd} < 30m$, b) the transmission distance $d_{sd} > 100m$).

2.6 Conclusion

The main contribution of this chapter is to propose and evaluate the fDSTC protocol with NR-relays and R-relays. A thorough analysis on error performance of the fDSTC protocol, followed by simulation results, is given to show its good performance. With two simple SISO transmissions added between the two relays, a significant SNR gain is obtained ($3.7dB$ for NR-relays and $18.1dB$ for R-relays). The relative distance of relays is shown to have a large impact on the BER performance of the cDSTC protocol. However, thanks to the fDSTC protocol, this impact can be significantly reduced by up to 75%. Besides, the suitable power allocation among the source and the relays is shown to be able to further increase the BER performance of the fDSTC protocol. In terms of outage

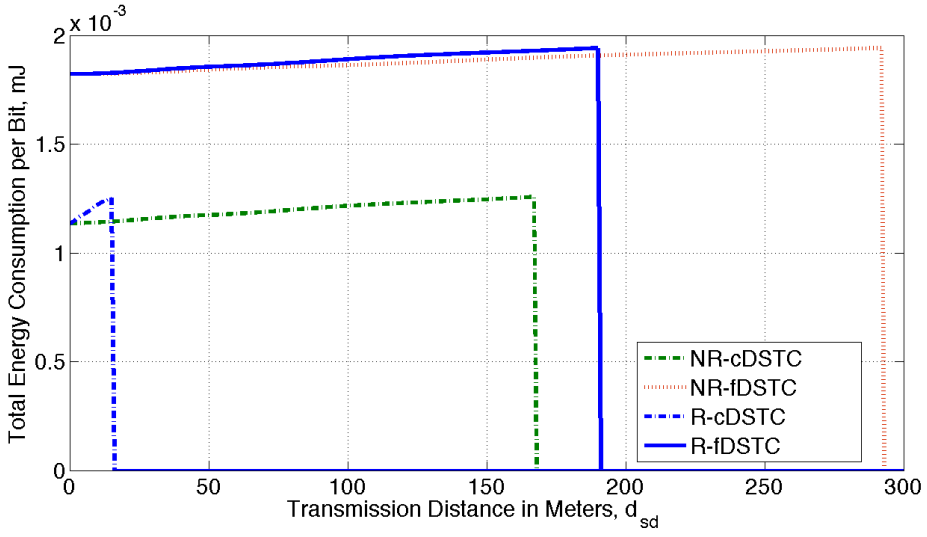

FIGURE 2.15: Total energy consumption per bit of the fDSTC and cDSTC protocol with NR and R-relays

probability, at the same spectral efficiency, the fDSTC protocol turns out to outperform the cDSTC protocol in high SNR regions. This is due to the fact that the fDSTC protocol helps to get higher system diversity order (full diversity in case of NR-relays) as compared to the cDSTC protocol. In terms of energy consumption, the fDSTC protocol is still more energy efficient than the cDSTC protocol for long-range transmissions or gets longer maximum transmission distance. Although the fDSTC protocol is not shown to be the best cooperative protocol in any case, with its many advantages in comparison with the cDSTC protocol, it could be one of the promising cooperative protocols.

The good performance of the fDSTC protocol is clearly demonstrated in this chapter by using simple NR-relays and R-relays in single-antenna system. The deployment of the fDSTC protocol in multi-antenna systems and its performance will be considered in next chapter.

Chapter 3

MIMO Cooperative Relay Systems

3.1 Introduction

It is well known that cooperative techniques such as cooperative MIMO and cooperative relay are among the best candidates to form virtual MIMO networks in case that the deployment of multi-antenna system is impossible due to the limited size and cost of devices. However, in some networks such as cellular networks, base stations are normally designed with many antennas. In addition, with the quick development of nanotechnology and material sciences, it is expected that one day not far the deployment of multi-antenna on a small device (e.g. sensor nodes, mobile phones, etc.) will be passed through without difficulty. Therefore, besides having a role of forming virtual MIMO systems, the cooperative techniques can be associated with MIMO systems to further improve performances of the systems. While in [8, 92], the cooperative techniques are considered as a function of virtual MIMO systems the use of cooperative relay techniques in MIMO systems is considered in [93, 94]. In [93], the BER performance analysis of a multi-antenna cooperative relay system is derived. In [94], using beam forming technique and Amplify and Forward (AF) relaying, a system having a two-antenna source, two one-antenna relays and one-antenna destination is proposed. However, the proposed model does not include a direct transmission from source to destination and use repetition-based cooperative relay protocols to forward signals from relays to destination. In [95], the distributed space-time coding (DSTC) between source and relay is considered to exploit diversity and rate gain. Furthermore, a DSTC-based cooperative system with two relays stations is proposed and its average symbol error probability is also derived in [17].

In the previous chapter, the fDSTC protocol in which the relays cooperate with the source to form a virtual MIMO is shown to be able to improve the performance of the DSTC-based cooperative system in terms of error probability, outage probability, diversity order, spectral efficiency and energy efficiency. However, it is only considered in a single-antenna system. The present chapter will exploit the fDSTC protocol in a multiple-antenna system which have a two-antenna source, two one-antenna relays and one-antenna destination. This system can be referred as the downlink in the cellular networks where the source is the base station and the relays and the destination are mobile users. Depending on the cooperative relay protocols (i.e. fDSTC or cDSTC) it is classified into two models: MIMO full cooperative relay (MFCR) exploiting the fDSTC protocol and MIMO simple cooperative relay (MSCR) exploiting the cDSTC protocol. Once again, the performance of the models will be evaluated via BER, spectral efficiency and energy efficiency.

Contributions

The contributions of the chapter are:

1. Two models, MSCR and MFCR, are proposed to associate the DSTC-based cooperative relay techniques with multi-antenna system and compared with the model in [94] (including a direct transmission from source to destination), called MIMO normal cooperative relay model (MNCR), exploiting repetition-based cooperative relay protocol.

2. The analytic results in terms of error probability are derived in the models using non-regenerative relays (NR-relays). However, in the simulation section, the performances of the models with regenerative relays (R-relays) are figured out. Like Chapter 2, the effects of the relative distance of relays (r) on the bit-error-rate (BER) performance are also considered.

3. The outage probability and diversity order of the systems using NR-relays are derived.

4. Unlike Chapter 2, in this chapter the total energy consumption is thoroughly considered through mathematical analysis and numerical simulations to illustrate the

best cooperative strategy for multi-antenna systems. In addition, the error synchronization effect on the BER performance is also carefully discussed.

The remainder of this chapter is organized as follows. In Section 3.2, the transmission protocols of the MFCR, MSCR and MNCR models are thoroughly described. Then the analysis of error probability followed by the simulations for MSCR and MFCR are considered in Section 3.3. The outage probability and the diversity order of the models are derived in Section 3.5. In addition, in Section 3.6 the energy consumption of these models is thoroughly analyzed. Section 3.7 illustrates the effect of the synchronization error of the DSTC transmission from the relays to the destination on the system performance. Finally, conclusion is given in Section 3.8.

3.2 System Model

In this chapter, we consider a system consisting of a two-antenna source, a one-antenna destination and two one-antenna relays (Fig. 3.1). From this system, we distinguish three models. That is MNCR, MSCR and MFCR. While MNCR uses repetition-based cooperative relay protocols, MSCR and MNCR take advantage of the DSTC-based cooperative relay protocols (i.e using the fDSTC protocol in case of MFCR and the cDSTC protocol in case of MSCR). The transmission process of these communication models can be divided into the following steps:

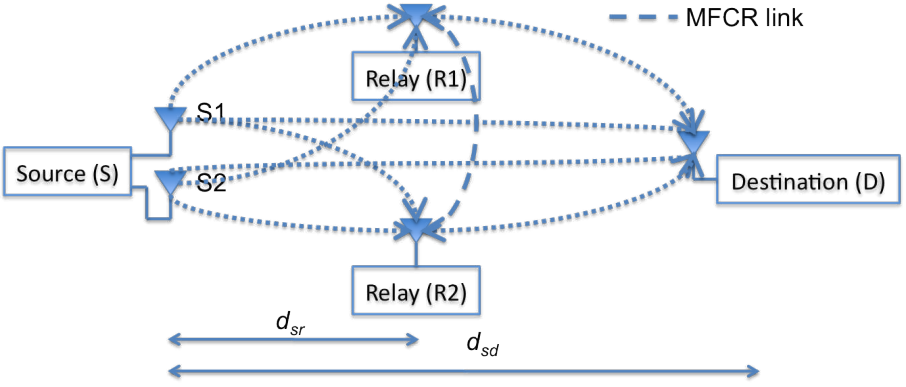

FIGURE 3.1: Cooperative Model

Step 1:

The two-antenna source ($S1$, $S2$) transmits simultaneously the Alamouti coded signal $\boldsymbol{X} = \begin{bmatrix} x[2k] & x[2k+1] \\ -x^*[2k+1] & x^*[2k] \end{bmatrix}$ to the two relays ($R1$, $R2$) and to the destination (D) (where $x[2k]$ and $x[2k+1]$ are two consecutive signals at the source). The received signals at the two relays and at the destination are $\boldsymbol{y_{sr_1}}$, $\boldsymbol{y_{sr_2}}$, $\boldsymbol{y_{sd}}$ respectively:

$$\boldsymbol{y_{ij}} = \sqrt{\epsilon_{ij}}\boldsymbol{X}\boldsymbol{h_{ij}} + \boldsymbol{z_{ij}} \quad i \in \{s\}, j \in \{r_1, r_2, d\}, \tag{3.1}$$

where $\boldsymbol{h_{ij}} = \begin{bmatrix} h_{ij}[2k] & h_{ij}[2k+1] \end{bmatrix}^T$ is the Rayleigh channel coefficient vector, $\boldsymbol{y_{ij}} = \begin{bmatrix} y_{ij}[2k] & y_{ij}[2k+1] \end{bmatrix}^T$, $\boldsymbol{z_{ij}} = \begin{bmatrix} z_{ij}[2k] & z_{ij}[2k+1] \end{bmatrix}^T$ is the AWGN noise vector and $\epsilon_s = \epsilon_{sd} = \epsilon_{sr_1} = \epsilon_{sr_2}$ is the source transmit power.

Step 2:

- For MNCR, the two relays use repetition-based protocols to forward the signals consecutively to the destination. The received data at the destination from the relays is given by

$$y_{jd}[m] = \begin{cases} \sqrt{\epsilon_{jd}} h_{jd}[m] G_{jd} u_j[m] + z_{jd}[m], & j \in \{r_1, r_2\}, m \in \{2k, 2k+1\}, \quad \text{NR-relays} \\ \sqrt{\epsilon_{jd}} h_{jd}[m] \hat{x}_{sj}[m] + z_{jd}[m], & j \in \{r_1, r_2\}, m \in \{2k, 2k+1\}, \quad \text{R-relays} \end{cases} \tag{3.2}$$

  where $\epsilon_r = \epsilon_{r_1 d} = \epsilon_{r_2 d}$ is the transmit power of the relays, $\hat{\boldsymbol{x}}_{\boldsymbol{sj}}$ is obtained by decoding the signal $\boldsymbol{y_{sj}}$ at the relay $j \in \{r_1, r_2\}$, and G_{jd} is the amplying factor of the NR-relay j. The forwarded signal at the relays, $u_j[m]$, can be expressed as

$$\boldsymbol{u_j} = (\boldsymbol{H_{sj}^H} \tilde{\boldsymbol{y}}_{\boldsymbol{sj}}) / \sqrt{\epsilon_s} (\boldsymbol{H_{sj}^H} \boldsymbol{H_{sj}}), \quad j \in \{r_1, r_2\}, \tag{3.3}$$

  where $\tilde{\boldsymbol{y}}_{\boldsymbol{sj}} = \begin{bmatrix} y_{sj}[2k] & y_{sj}^*[2k+1] \end{bmatrix}^T$, $\boldsymbol{u_j} = \begin{bmatrix} u_j[2k] & u_j[2k+1] \end{bmatrix}^T$ and $\boldsymbol{H_{sj}} = \begin{bmatrix} h_{sj}[2k] & h_{sj}[2k+1] \\ h_{sj}^*[2k+1] & -h_{sj}^*[2k] \end{bmatrix}$.

- For MSCR, the two relays use the cDSTC protocol to transmit simultaneously the Alamouti re-encoded signals $\boldsymbol{U}$ to the destination, where

$$\boldsymbol{U} = \begin{cases} \begin{bmatrix} G_{r_1d}u_{r_1}[2k] & G_{r_2d}u_{r_2}[2k+1] \\ -G^*_{r_1d}u^*_{r_1}[2k+1] & G^*_{r_2d}u^*_{r_2}[2k] \end{bmatrix}, & \text{NR-relays} \\ \begin{bmatrix} \hat{x}_{sr_1}[2k] & \hat{x}_{sr_2}[2k+1] \\ -\hat{x}^*_{sr_1}[2k+1] & \hat{x}^*_{sr_2}[2k] \end{bmatrix}, & \text{R-relays} \end{cases}$$

with $u_j[m], j \in \{r_1, r_2\}$ are found by (3.3) and G_{jd} the amplying factor [12]. Similar to MNCR, here $\hat{x}_{sj}[2k]$ and $\hat{x}_{sj}[2k+1]$ are obtained by decoding the signals $y_{sj}[2k]$ and $y_{sj}[2k+1]$ at the relay $j \in \{r_1, r_2\}$ respectively. The received signal at the destination is

$$\boldsymbol{y_{rd}} = \sqrt{\epsilon_r}\boldsymbol{U}\boldsymbol{h_{rd}} + \boldsymbol{z_{rd}}, \tag{3.4}$$

where $\boldsymbol{h_{rd}} = \begin{bmatrix} h_{rd}[2k] & h_{rd}[2k+1] \end{bmatrix}^T$ and $\boldsymbol{z_{rd}} = \begin{bmatrix} z_{rd}[2k] & z_{rd}[2k+1] \end{bmatrix}^T$ are the Rayleigh channel coefficient and AWGN noise vectors of the relay-destination link respectively and $\boldsymbol{y_{rd}} = \begin{bmatrix} y_{rd}[2k] & y_{rd}[2k+1] \end{bmatrix}^T$.

- For MFCR, before forwarding the signals to the destination, the two relays exchange their data ($\boldsymbol{y_{sr_1}}$ and $\boldsymbol{y_{sr_2}}$) with each other to get the reception diversity. From the previous chapter, it is claimed that when the distance between the relays is small enough, the system performance still remains. Therefore, in this work, we assume that there is no error in the inter-communication between the two relays. As a result, the forwarded signals at two relays are the same, $\boldsymbol{u_{r1}} = \boldsymbol{u_{r2}}$ and can be represented by

$$\boldsymbol{u_{r1}} = \boldsymbol{u_{r2}} = \boldsymbol{u_r} = \frac{(\boldsymbol{H^H_{sr_1}}\tilde{\boldsymbol{y}}_{\boldsymbol{sr_1}} + \boldsymbol{H^H_{sr_2}}\tilde{\boldsymbol{y}}_{\boldsymbol{sr_2}})}{\sqrt{\epsilon_s}(\boldsymbol{H^H_{sr_1}}\boldsymbol{H_{sr_1}} + \boldsymbol{H^H_{sr_2}}\boldsymbol{H_{sr_2}})}, \tag{3.5}$$

where $\boldsymbol{H_{sj}} = \begin{bmatrix} h_{sj}[2k] & h_{sj}[2k+1] \\ h^*_{sj}[2k+1] & -h^*_{sj}[2k] \end{bmatrix}$, $\boldsymbol{u_r} = \begin{bmatrix} u_r[2k] & u_r[2k+1] \end{bmatrix}^T$, $\boldsymbol{u_j} = \begin{bmatrix} u_j[2k] & u_j[2k+1] \end{bmatrix}^T$, and $\tilde{\boldsymbol{y}}_{\boldsymbol{sj}} = \begin{bmatrix} y_{sj}[2k] & y^*_{sj}[2k+1] \end{bmatrix}^T$ with $j \in \{r_1, r_2\}$. The received signal at the destination is represented by (3.4) with the Alamouti

re-encoded signals

$$\boldsymbol{U} = \begin{cases} \begin{bmatrix} G_{rd}u_r[2k] & G_{rd}u_r[2k+1] \\ -G^*_{rd}u^*_r[2k+1] & G^*_{rd}u^*_r[2k] \end{bmatrix}, & \text{NR-relays} \\ \begin{bmatrix} \hat{x}_{sr}[2k] & \hat{x}_{sr}[2k+1] \\ -\hat{x}^*_{sr}[2k+1] & \hat{x}^*_{sr}[2k] \end{bmatrix}, & \text{R-relays} \end{cases}$$

where $\hat{x}_{sr}[2k]$ and $\hat{x}_{sr}[2k+1]$ are obtained by decoding the signals $u_r[2k]$ and $u_r[2k+1]$ and G_{rd} is the amplying factor at the relays.

Step 3:

At the destination, all the received signals are combined together to take advantage of spatial diversity and the maximal ratio combining (MRC) technique is used to decode the signals.

We assume that the communications are performed over flat Rayleigh fading channel. The channel coefficients remain the same for two consecutive time intervals. Statistically, we model $h_{ij}[m]$ with $i \in \{s, r_1, r_2\}$ and $j \in \{r_1, r_2, d\}$ as zero mean, independent, complex Gaussian random variables with variances Ω^2_{ij}. Similarly, we model $z_{ij}[m]$ as zero mean mutually independent complex Gaussian random variable with variance N_0. The protocols of these models with NR-relays are summarized in the following tables, Tab. 3.1 for MNCR, Tab. 3.2 for MSCR and Tab. 3.3 for MFCR. One should note that, the white cells represent the transmission phases, the light gray cells represent the reception phases and the bold gray cells represent the sleep phases of the terminals.

Time Slot	**S1**	**S2**	**R1**	**R2**	**D**
$2k$	$x[2k]$	$x[2k+1]$	$y_{sr_1}[2k]$	$y_{sr_2}[2k]$	$y_{sd}[2k]$
$2k+1$	$-x^*[2k+1]$	$x^*[2k]$	$y_{sr_1}[2k+1]$	$y_{sr_2}[2k+1]$	$y_{sd}[2k+1]$
$2k+2$			$G_{r_1d}u_{r_1}[2k]$		$y_{r_1d}[2k]$
$2k+3$			$G_{r_1d}u_{r_1}[2k+1]$		$y_{r_1d}[2k+1]$
$2k+4$				$G_{r_2d}u_{r_2}[2k]$	$y_{r_2d}[2k]$
$2k+5$				$G_{r_2d}u_{r_2}[2k+1]$	$y_{r_2d}[2k+1]$

TABLE 3.1: Protocol of the MIMO normal cooperative relay model (NR-relays)

Time slot	S1	S2	R1	R2	D
$2k$	$x[2k]$	$x[2k+1]$	$y_{sr_1}[2k]$	$y_{sr_2}[2k]$	$y_{sd}[2k]$
$2k+1$	$-x^*[2k+1]$	$x^*[2k]$	$y_{sr_1}[2k+1]$	$y_{sr_2}[2k+1]$	$y_{sd}[2k+1]$
$2k+2$			$G_{r_1d}u_{r_1}[2k]$	$G_{r_2d}u_{r_2}[2k+1]$	$y_{rd}[2k]$
$2k+3$			$-G^*_{r_1d}u^*_{r_1}[2k+1]$	$G^*_{r_2d}u^*_{r_2}[2k]$	$y_{rd}[2k+1]$

TABLE 3.2: Protocol of the MIMO simple cooperative relay model (NR-relays)

Time Slot	S1	S2	R1	R2	D
$2k$	$x[2k]$	$x[2k+1]$	$y_{sr_1}[2k]$	$y_{sr_2}[2k]$	$y_{sd}[2k]$
$2k+1$	$-x^*[2k+1]$	$x^*[2k]$	$y_{sr_1}[2k+1]$	$y_{sr_2}[2k+1]$	$y_{sd}[2k+1]$
$2k+2$			$y_{sr_1}[2k]$	$y_{sr_1}[2k]$	
$2k+3$			$y_{sr_1}[2k+1]$	$y_{sr_1}[2k+1]$	
$2k+4$			$y_{sr_2}[2k]$	$y_{sr_2}[2k]$	
$2k+5$			$y_{sr_2}[2k+1]$	$y_{sr_2}[2k+1]$	
$2k+6$			$G_{rd}u_r[2k]$	$G_{rd}u_r[2k+1]$	$y_{rd}[2k]$
$2k+7$			$-G^*_{rd}u^*_r[2k+1]$	$G^*_{rd}u^*_r[2k]$	$y_{rd}[2k+1]$

TABLE 3.3: Protocol of the MIMO full cooperative relay model (NR-relays)

3.3 Error Probability Analysis

In this section, the error probability of MFCR and MSCR is considered in the case of NR-relays. The error probability (for BPSK modulation) is

$$P_{\gamma_d} = Q(\sqrt{2\gamma_d}), \tag{3.6}$$

with $Q(x) = \frac{1}{2\pi}\int_x^\infty e^{\frac{-z^2}{2}}dz$ the error function and γ_d the received SNR at the destination.

3.3.1 MIMO full cooperative relay model (MFCR)

In this model, after receiving the signal transmitted from the source and exchanging data with each other, each relay needs to combine and normalize the signals before forwarding to the destination. The relays will forward the signals $\boldsymbol{u_r}$ (3.5) using the fDSTC protocol to the destination.

In our work, $G_{rd} = 1$ is chosen. So, the forwarded signals at the relays can be expressed as

$$\boldsymbol{u_r} = \boldsymbol{x} + (\boldsymbol{H^H_{sr_1}}\tilde{\boldsymbol{z}}_{\boldsymbol{sr_1}} + \boldsymbol{H^H_{sr_2}}\tilde{\boldsymbol{z}}_{\boldsymbol{sr_2}})/\sqrt{\epsilon_s}(||\boldsymbol{h_{sr_1}}||^2 + ||\boldsymbol{h_{sr_2}}||^2), \tag{3.7}$$

with $\tilde{\boldsymbol{z}}_{\boldsymbol{sj}} = \begin{bmatrix} z_{sj}[2k] & z_{sj}^*[2k+1] \end{bmatrix}^T$, $j \in \{r_1, r_2\}$.

The power of the forwarded signals at the relays is guaranteed to be normalized to one:

$$E(u_r[m]^* u_r[m]) = E(x[m]^* x[m]) + \frac{1}{\epsilon_s(||\boldsymbol{h}_{\boldsymbol{sr_1}}||^2 + ||\boldsymbol{h}_{\boldsymbol{sr_2}}||^2)}.$$

So, when $\epsilon_s \gg 1$, we have $E(u_r[m]^* u_r[m]) \approx E(x[m]^* x[m]) = 1$.

Then the two NR-relays will use two time slots to forward the re-encoded signals $\boldsymbol{U} = \begin{bmatrix} u_r[2k] & u_r[2k+1] \\ -u_r^*[2k+1] & u_r^*[2k] \end{bmatrix}$ to the destination. The combined signal can be derived as

$$\begin{aligned} \boldsymbol{y_d} = \boldsymbol{x} &+ \frac{\epsilon_r ||\boldsymbol{h}_{\boldsymbol{rd}}||^2 (\boldsymbol{H}_{\boldsymbol{sr_1}}^{\boldsymbol{H}} \tilde{\boldsymbol{z}}_{\boldsymbol{sr_1}} + \boldsymbol{H}_{\boldsymbol{sr_2}}^{\boldsymbol{H}} \tilde{\boldsymbol{z}}_{\boldsymbol{sr_2}})}{\sqrt{\epsilon_s}(||\boldsymbol{h}_{\boldsymbol{sr_1}}||^2 + ||\boldsymbol{h}_{\boldsymbol{sr_2}}||^2)(\epsilon_s ||\boldsymbol{h}_{\boldsymbol{sd}}||^2 + \epsilon_r ||\boldsymbol{h}_{\boldsymbol{rd}}||^2)} \\ &+ \frac{\sqrt{\epsilon_s} \boldsymbol{H}_{\boldsymbol{sd}}^{\boldsymbol{H}} \tilde{\boldsymbol{z}}_{\boldsymbol{sd}} + \sqrt{\epsilon_r} \boldsymbol{H}_{\boldsymbol{rd}}^{\boldsymbol{H}} \tilde{\boldsymbol{z}}_{\boldsymbol{rd}}}{(\epsilon_s ||\boldsymbol{h}_{\boldsymbol{sd}}||^2 + \epsilon_r ||\boldsymbol{h}_{\boldsymbol{rd}}||^2)}, \end{aligned} \tag{3.8}$$

with $\boldsymbol{y_d} = \begin{bmatrix} y_d[2k] & y_d[2k+1] \end{bmatrix}^T$.

If all noises are mutually independent, the probability distribution of $y_d[2k]$ and $y_d[2k+1]$ is also a normal one with the mean and the variance:

$$y_d[2k] \sim \boldsymbol{N}(x[2k], \Omega_F^2),$$
$$y_d[2k+1] \sim \boldsymbol{N}(x[2k+1], \Omega_F^2),$$

where $\Omega_F^2 = \frac{\epsilon_r^2 ||\boldsymbol{h}_{\boldsymbol{rd}}||^4}{\epsilon_s(||\boldsymbol{h}_{\boldsymbol{sr_1}}||^2 + ||\boldsymbol{h}_{\boldsymbol{sr_2}}||)(||\epsilon_s \boldsymbol{h}_{\boldsymbol{sd}}||^2 + \epsilon_r ||\boldsymbol{h}_{\boldsymbol{rd}}||^2)^2} + \frac{1}{(\epsilon_s ||\boldsymbol{h}_{\boldsymbol{sd}}||^2 + \epsilon_r ||\boldsymbol{h}_{\boldsymbol{rd}}||^2)})$.

Finally, the SNR at the destination can be derived as

$$\gamma_d = \frac{E(|x|^2)}{4} \frac{\epsilon_s(||\boldsymbol{h}_{\boldsymbol{sr_1}}||^2 + ||\boldsymbol{h}_{\boldsymbol{sr_2}}||^2)(\epsilon_s ||\boldsymbol{h}_{\boldsymbol{sd}}||^2 + \epsilon_r ||\boldsymbol{h}_{\boldsymbol{rd}}||^2)^2}{\epsilon_r^2 ||\boldsymbol{h}_{\boldsymbol{rd}}||^4 + \epsilon_s(||\boldsymbol{h}_{\boldsymbol{sr_1}}||^2 + ||\boldsymbol{h}_{\boldsymbol{sr_2}}||^2)(\epsilon_s ||\boldsymbol{h}_{\boldsymbol{sd}}||^2 + \epsilon_r ||\boldsymbol{h}_{\boldsymbol{rd}}||^2)}. \tag{3.9}$$

Here, we normalize the power of each signal constellation to be $1/4$, thus the total received power at the destination is unity.

3.3.2 MIMO simple cooperative relay model (MSCR)

Since no data is exchanged between the two relays, after receiving signal from the source, the relays will forward the signals $\boldsymbol{u_j}$ (3.3) using the cDSTC protocol to the destination.

If we choose the amplifying factor $G_{r_1d} = G_{r_2d} = 1$, the forwarded signals of the relays are $\boldsymbol{U} = \begin{bmatrix} u_{r_1}[2k] & u_{r_2}[2k+1] \\ -u^*_{r_1}[2k+1] & u^*_{r_2}[2k] \end{bmatrix}$ with

$$\boldsymbol{u_j} = \boldsymbol{x} + \boldsymbol{H^H_{sj}}\tilde{\boldsymbol{z}}_{\boldsymbol{sj}}/\sqrt{\epsilon_s}||\boldsymbol{h_{sj}}||^2, \quad j \in \{r_1, r_2\}. \tag{3.10}$$

Let note $\acute{\boldsymbol{z}}_{\boldsymbol{sj}} = \boldsymbol{H^H_{sj}}\tilde{\boldsymbol{z}}_{\boldsymbol{sj}}/\sqrt{\epsilon_s}||\boldsymbol{h_{sj}}||^2$ where $\acute{\boldsymbol{z}}_{\boldsymbol{sj}} = \begin{bmatrix} \acute{z}_{sj}[2k] & \acute{z}_{sj}[2k+1] \end{bmatrix}^T$ is the received noise at the relay $j \in \{r_1, r_2\}$ respectively. Then, the forwarded signals of the relays $\boldsymbol{U}$ can be rewritten as

$$\boldsymbol{U} = \boldsymbol{X} + \acute{\boldsymbol{Z}}_{\boldsymbol{sr}}, \tag{3.11}$$

where $\boldsymbol{X} = \begin{bmatrix} x[2k] & x[2k+1] \\ -x^*[2k+1] & x^*[2k] \end{bmatrix}$ is the original transmitted signals and $\acute{\boldsymbol{Z}}_{\boldsymbol{sr}} = \begin{bmatrix} \acute{z}_{sr_1}[2k] & \acute{z}_{sr_2}[2k+1] \\ -\acute{z}^*_{sr_1}[2k+1] & \acute{z}^*_{sr_2}[2k] \end{bmatrix}$ is the received noise at the relays.

So, the signal received at the destination from the relays is

$$\begin{aligned} \boldsymbol{y_{rd}} &= \sqrt{\epsilon_r}\boldsymbol{X}\boldsymbol{h_{rd}} + \sqrt{\epsilon_r}\acute{\boldsymbol{Z}}_{\boldsymbol{sr}}\boldsymbol{h_{rd}} + \boldsymbol{z_{rd}} \\ &= \sqrt{\epsilon_r}\boldsymbol{X}\boldsymbol{h_{rd}} + \bar{\boldsymbol{z}}_{\boldsymbol{rd}}, \end{aligned} \tag{3.12}$$

where $\bar{\boldsymbol{z}}_{\boldsymbol{rd}} = \begin{bmatrix} \bar{z}_{rd}[2k] \\ \bar{z}_{rd}[2k+1] \end{bmatrix} = \begin{bmatrix} \sqrt{\epsilon_r}h_{rd}[2k]\acute{z}_{sr_1}[2k] + \sqrt{\epsilon_r}h_{rd}[2k+1]\acute{z}_{sr_2}[2k+1] + z_{rd}[2k] \\ -\sqrt{\epsilon_r}h_{rd}[2k]\acute{z}^*_{sr_1}[2k+1] + \sqrt{\epsilon_r}h_{rd}[2k+1]\acute{z}^*_{sr_2}[2k] + z_{rd}[2k+1] \end{bmatrix}$ is the total noise at destination.

(3.12) can be rewritten as

$$\tilde{\boldsymbol{y}}_{\boldsymbol{rd}} = \sqrt{\epsilon_r}\boldsymbol{H_{rd}}\boldsymbol{x} + \tilde{\boldsymbol{z}}_{\boldsymbol{rd}}, \tag{3.13}$$

with $\tilde{\boldsymbol{z}}_{\boldsymbol{rd}} = \begin{bmatrix} \bar{z}_{rd}[2k] \\ \bar{z}^*_{rd}[2k+1] \end{bmatrix}$ and $\tilde{\boldsymbol{y}}_{\boldsymbol{rd}} = \begin{bmatrix} y_{rd}[2k] \\ y^*_{rd}[2k+1] \end{bmatrix}$.

Then, the combined signal at the destination is given by

$$\boldsymbol{y_d} = \boldsymbol{x} + (\sqrt{\epsilon_s}\boldsymbol{H^H_{sd}}\tilde{\boldsymbol{z}}_{\boldsymbol{sd}} + \sqrt{\epsilon_r}\boldsymbol{H^H_{rd}}\tilde{\boldsymbol{z}}_{\boldsymbol{rd}})/(\epsilon_s||\boldsymbol{h_{sd}}||^2 + \epsilon_r||\boldsymbol{h_{rd}}||^2). \tag{3.14}$$

The probability distribution of $\boldsymbol{y_d}$ is

$$y_d[2k] \sim \boldsymbol{N}(x[2k], \Omega_S^2), \tag{3.15}$$

$$y_d[2k+1] \sim \boldsymbol{N}(x[2k+1], \Omega_S^2), \tag{3.16}$$

where $\Omega_S^2 = \frac{\epsilon_s||\boldsymbol{h_{sd}}||^2+\epsilon_r||\boldsymbol{h_{rd}}||^2(\frac{\epsilon_r}{\epsilon_s||\boldsymbol{h_{sr_1}}||^2}+\frac{\epsilon_r}{\epsilon_s||\boldsymbol{h_{sr_2}}||^2}+1)}{(\epsilon_s||\boldsymbol{h_{sd}}||^2+\epsilon_r||\boldsymbol{h_{rd}}||^2)^2}$.

Finally, the SNR at the destination of the MSCR model can be derived as

$$\gamma_d = \frac{E(|x|^2)}{4}\left(\frac{(\epsilon_s||\boldsymbol{h_{sd}}||^2 + \epsilon_r||\boldsymbol{h_{rd}}||^2)^2}{\epsilon_s||\boldsymbol{h_{sd}}||^2 + \epsilon_r||\boldsymbol{h_{rd}}||^2(\frac{\epsilon_r}{\epsilon_s||\boldsymbol{h_{sr_1}}||^2} + \frac{\epsilon_r}{\epsilon_s||\boldsymbol{h_{sr_2}}||^2} + 1)}\right). \tag{3.17}$$

3.4 Simulation Results

In this section, the performances of MNCR, MSCR and MFCR using NR-relays and R-relays are simulated in terms of BER. With a common model for path-loss, $\Omega_{ij}^2 \propto d_{ij}^{-pl}$ where d_{ij} is the distance between terminal i and j, and $pl = 2$ is the path-loss exponent. Taking the effects of relays' positions into account, the performance of the models is simulated depending on the relative distance of relays $r = \frac{d_{sr}}{d_{sd}}$ defined by the ratio of the source-relay distance d_{sr} and the source-destination distance d_{sd}. In this chapter, the performance of the models will be evaluated and compared with that of Alamouti models since Alamouti model represents traditional MIMO system without cooperative techniques. In addition, to have a fair comparison between the models, the total transmit power of the models is kept the same (i.e. P).

3.4.1 MNCR vs MSCR (NR-relays)

The BER performances of MNCR and MSCR using NR-relays with different values of r in case of NR-relays are shown in Fig. 3.2. The performance of MNCR is lightly better than that of MSCR. In MSCR, the re-encoded signals at the relays are not orthogonal. Therefore, the performance of the DSTC transmission from the relays to the destination is degraded. The closer the relays get to the destination, the less orthogonal the forwarded signals at the relays is. That leads to worse performance of MSCR in comparison with Alamouti 2-1 model (having a two-antenna source and a one-antenna destination) when r is high.

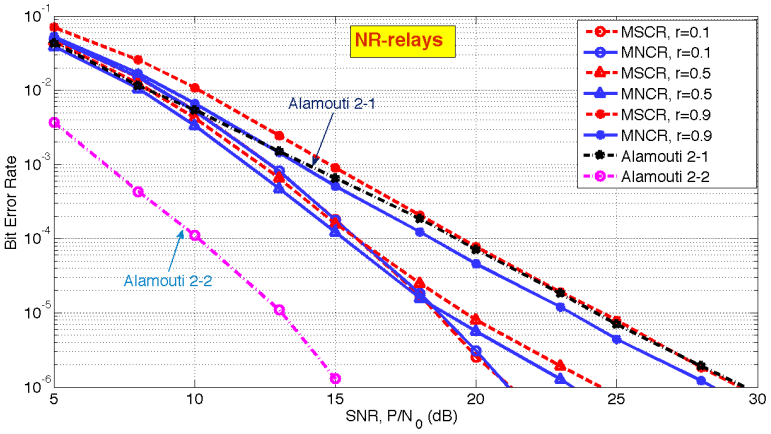

FIGURE 3.2: BER of MNCR and MSCR (NR-relays)

3.4.2 MSCR vs MFCR

Fig. 3.3 shows the performances of MFCR and MSCR in case of NR-relays at r equal to 0.1, 0.5 and 0.9. On the one hand, the performance of the MFCR is always better than that of the MSCR. Moreover, the larger r is, the better the performance of MFCR is. However, when r is small ($r = 0.1$) the performances of MSCR and MFCR are the same. On the other hand, in Fig. 3.3, the $3dB$ power reduction of MFCR ($r = 0.9$) in comparison with Alamouti 2-2 scheme is due to the fact that the power of each constellation in MFCR is normalized to be 1/4 while in Alamouti 2-2 scheme the power of each constellation is only halved. The performance of the models in case of R-relays is shown in Fig. 3.4. Similar to NR-relays, the performance of MFCR in case of R-relays is always better than that of MSCR.

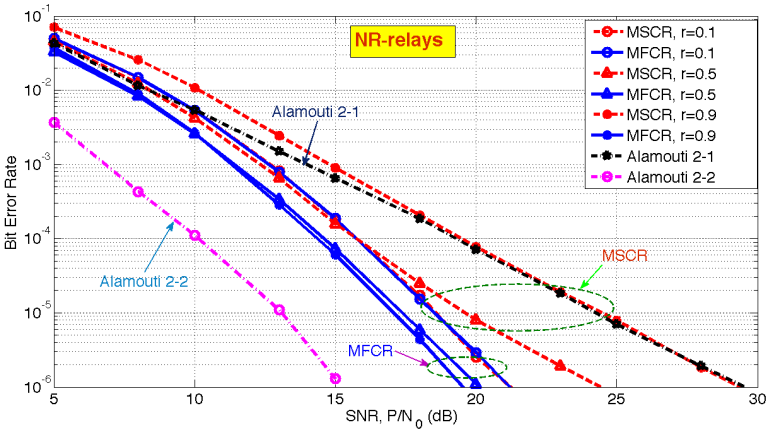

FIGURE 3.3: BER of MFCR and MSCR (NR-relays)

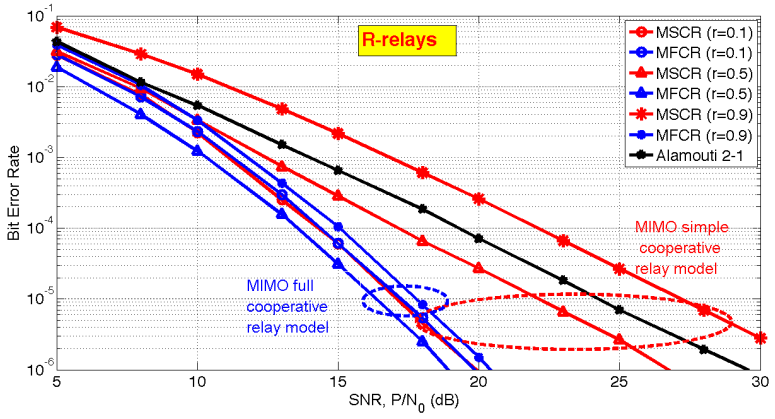

FIGURE 3.4: BER of MFCR and MSCR (R-relays)

3.4.3 Performance comparison between NR-relays and R-relays

To compare the performance of the models in case of using NR-relays or R-relays, the needed SNR for MFCR and MSCR at the desired BER equal to 10^{-5} is derived. The results in Fig. 3.5 show that, for MSCR, R-relays bring a better performance than NR-relays when r is larger than 0.3. On the other hand, in the MFCR, R-relays can obtain better performance than NR-relays until when r is smaller than 0.8. These results are important to choose the suitable relays depending on the relay position and the model. Besides, we can also see that in the MSCR the needed SNR increases quickly when r increases. However, in MFCR, the needed SNR is almost no change when r changes. Therefore, in WSNs where the relays are mobile, the MFCR is recommended to ensure the constant BER performance.

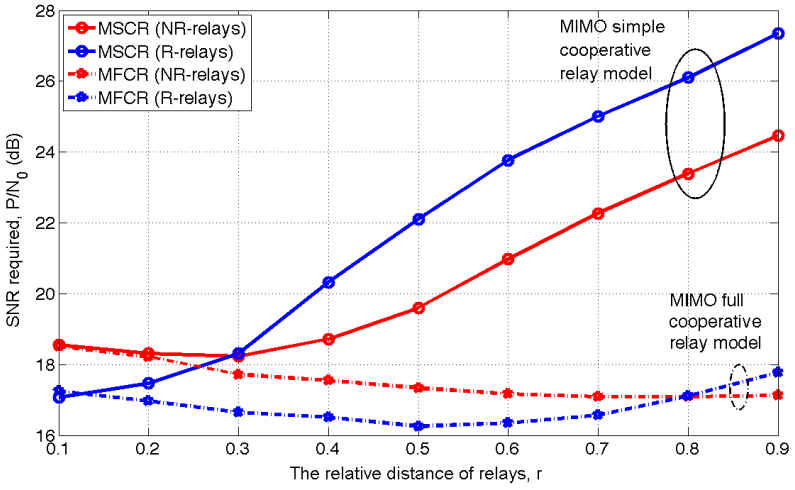

FIGURE 3.5: Performance comparison of NR-relays and R-relays

3.5 Outage Analysis

In this section, we characterize the performance of the models using NR-relays in terms of outage probability in high SNR regions. Let $\epsilon_s = \epsilon_r = \epsilon$ and define the signal to noise ratio $SNR = \epsilon/N_0$, we can determine the outage probability of the models based on SNR. Note that, for Rayleigh fading, $|h_{ij}|^2$ is exponentially distributed with parameter Ω_{ij}^{-2}. Its probability density function is given by

$$p_x(x) = \frac{1}{\Omega_{ij}^2} e^{-\frac{1}{\Omega_{ij}^2}x}, \quad i \in \{s, r_1, r_2\}, j \in \{r_1, r_2, d\}. \tag{3.18}$$

In this work, we assume that the two relays have the same relative distance to source and destination. That means $\Omega_{sr_1}^2 = \Omega_{sr_2}^2 = \Omega_{sr}^2$ and $\Omega_{r_1d}^2 = \Omega_{r_2d}^2 = \Omega_{rd}^2$. In addition, the probability density function of random variable $||\boldsymbol{h_{ij}}||^2 = \big|h_{ij}[2k]\big|^2 + \big|h_{ij}[2k+1]\big|^2$ is given by

$$p_x(x) = \Big(\frac{1}{\Omega_{ij}^2}\Big)^2 x e^{-\frac{1}{\Omega_{ij}^2}x}, \quad i \in \{s, r_1, r_2\}, j \in \{r_1, r_2, d\}. \tag{3.19}$$

3.5.1 MIMO Normal Cooperative Relay model (MNCR)

For MNCR, the maximum average mutual information between the source and the destination for random signals generated i.i.d circularly symmetric, complex Gaussian at the source and two NR-relays can be shown to be

$$\begin{aligned} I_{MNCR} = \frac{1}{3}\log\Big(1 + SNR||\boldsymbol{h_{sd}}||^2 + f(SNR||\boldsymbol{h_{sr_1}}||^2, SNR|h_{r_1d}|^2) \\ + f(SNR||\boldsymbol{h_{sr_2}}||^2, SNR|h_{r_2d}|^2)\Big), \end{aligned} \tag{3.20}$$

with $f(a,b) = \frac{ab}{a+b+1}$ defined in [9]. The outage probability of MNCR for spectral efficiency R is defined as

$$\begin{aligned} Pr[I_{MNCR} < R] = Pr\Big[|\boldsymbol{h_{sd}}||^2 + \frac{1}{SNR} f(SNR||\boldsymbol{h_{sr_1}}||^2, SNR|h_{r_1d}|^2) \\ + \frac{1}{SNR} f(SNR||\boldsymbol{h_{sr_2}}||^2, SNR|h_{r_2d}|^2)\Big) < \frac{2^{3R}-1}{SNR}\Big]. \end{aligned} \tag{3.21}$$

Using the approximation in [6, eq. (16), (17)], the lower and upper bounds of the outage probability of MNCR can be derived as

$$\frac{1}{48}\frac{1}{\Omega_{rd}^4\Omega_{sd}^4}\Big(\frac{2^{3R}-1}{SNR}\Big)^4 \leq Pr[I_{MNCR} < R] \leq \frac{1}{12}\frac{1}{\Omega_{rd}^4\Omega_{sd}^4}\Big(\frac{2^{3R}-1}{SNR}\Big)^4. \tag{3.22}$$

3.5.2 MIMO Simple Cooperative Relay model (MSCR)

The maximum average mutual information between the source and the destination in MSCR for random signals generated i.i.d circularly symmetric, complex Gaussian at the source and two NR-relays can be shown to be

$$I_{MSCR} = \frac{1}{2}\log\Big(1 + SNR||\boldsymbol{h_{sd}}||^2 + f(SNR||\boldsymbol{h_{sr}}||^2, SNR||\boldsymbol{h_{rd}}||^2\Big), \tag{3.23}$$

where $||\boldsymbol{h_{sr}}||^2 = \min(||\boldsymbol{h_{sr1}}||^2, ||\boldsymbol{h_{sr2}}||^2)$. Without the loss of generality, we assume that $||\boldsymbol{h_{sr}}||^2 = ||\boldsymbol{h_{sr1}}||^2$.

So, the outage probability of MSCR for the spectral efficiency R is

$$Pr[I_{MSCR} < R] = Pr\Big[||\boldsymbol{h_{sd}}||^2 + \frac{1}{SNR}f(SNR||\boldsymbol{h_{sr}}||^2, SNR||\boldsymbol{h_{rd}}||^2) < \frac{2^{2R}-1}{SNR}\Big]. \tag{3.24}$$

The outage probability of MSCR can be approximated in high SNR region by (proved in Appendix D)

$$Pr[I_{MSCR} < R] \sim \frac{1}{4!}\frac{\Omega_{sr}^4 + \Omega_{rd}^4}{\Omega_{sr}^4\Omega_{rd}^4}\frac{1}{\Omega_{sd}^4}\Big(\frac{2^{2R}-1}{SNR}\Big)^4. \tag{3.25}$$

3.5.3 MIMO Full Cooperative Relay Model (MFCR)

For MFCR, the maximum average mutual information between the source and the destination for random signals generated i.i.d circularly symmetric, complex Gaussian at the source and two NR-relays can be shown to be

$$I_{MFCR} = \frac{1}{4}\log\Big(1 + SNR||\boldsymbol{h_{sd}}||^2 + f\big(SNR||\boldsymbol{H_{sr}}||^2, SNR||\boldsymbol{h_{rd}}||^2\big)\Big), \tag{3.26}$$

where $||\boldsymbol{H_{sr}}||^2 = ||\boldsymbol{h_{sr1}}||^2 + ||\boldsymbol{h_{sr2}}||^2$ since there is an inter-communication between the two relays in MFCR.

The outage event for spectral efficiency R is given by $I_{MFCR} < R$ and is equivalent to the event

$$SNR||\boldsymbol{h_{sd}}||^2 + f(SNR||\boldsymbol{H_{sr}}||^2, SNR||\boldsymbol{h_{rd}}||^2) < 2^{4R} - 1. \tag{3.27}$$

With the attention that the probability density function of random variable $||\boldsymbol{H_{sr}}||^2$ is $p_x(x) = \left(\frac{1}{\Omega_{sr}^2}\right)^4 x^3 e^{-\frac{1}{\Omega_{sr}^2}x}$, the outage probability of MFCR (proved in Appendix E) can be derived as

$$Pr[I_{MFCR} < R] \sim \frac{1}{4!}\frac{1}{\Omega_{rd}^4\Omega_{sd}^4}\left(\frac{2^{4R}-1}{SNR}\right)^4. \tag{3.28}$$

3.5.4 Simulation of outage probability

Fig. 3.6 shows the outage probability of MNCR, MSCR and MFCR (in case of NR-relays) versus the rate-normalized $SNR_{norm} = \frac{P}{N_0}\frac{1}{[2^R-1]}$ [9] in small, fixed R regime ($R = 1$) for statistically symmetric networks, i.e. $\Omega_{ij}^2 = 1$. Solid curves correspond to high-SNR approximations obtained from the previous subsections. Dashed curves correspond to the simulations obtained via Monte Carlo method. From Fig. 3.6, the obtained outage probability approximations for MSCR and MFCR are well-matched with the simulations at high SNR, while for MNCR the simulation results are exactly in the middle of the lower and upper bound approximations. Furthermore, despite having the same diversity order of 4, MSCR is the model which has the best outage probability. Moreover, in comparison with the system [96] denoted by Karim06 (1-3-1) having 1 one-antenna source, 3 one-antenna relays and 1 one-antenna destination, MNCR, MSCR and MFCR all have better outage probability. The tradeoff between the diversity order, $d(g)$ and the multiplexing gain g at high SNR region is shown in Fig. 3.7. At the same diversity order $d(g)$, the MSCR has larger multiplexing gain than MNCR and MFCR.

3.6 Energy efficiency

In this section, the performance of the models in terms of energy efficiency is considered. Using two energy models discussed in Chapter 2 (i.e. typical and realistic energy models), the total energy consumption per bits of the models is derived.

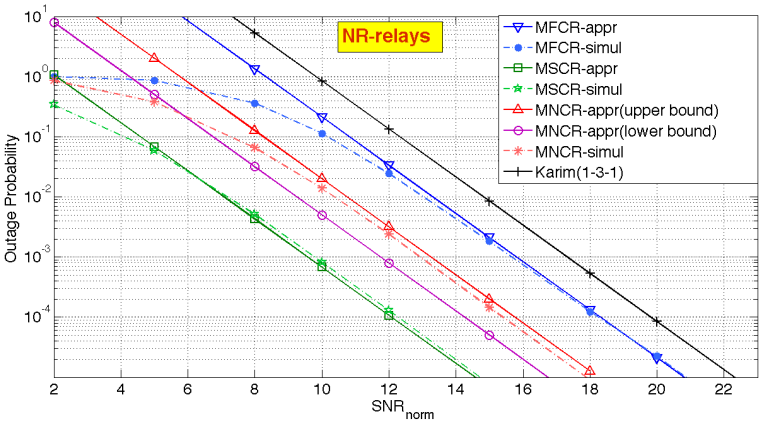

FIGURE 3.6: Outage probability versus SNR_{norm}, small, fixed R regime, for statistically symmetric networks, i.e. $\Omega_{ij}^2 = 1$

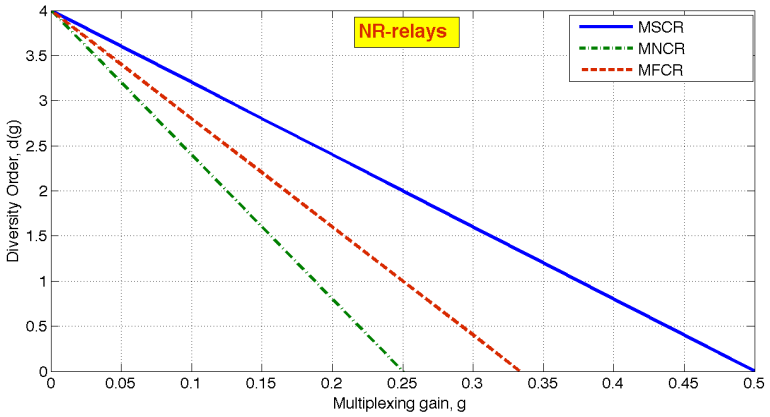

FIGURE 3.7: Diversity order $d(g)$ versus multiplexing gain g.

3.6.1 Typical energy model

We only evaluate the energy consumption of MSCR and MFCR via typical energy model. The energy efficiency of MNCR in comparison with MSCR and MFCR will be thoroughly evaluated via the realistic energy model in Section 3.6.2.

3.6.1.1 Analytic results

The total energy consumption per bits of MFCR E_F^b includes the energy consumption of the three-phase communication. The source firstly broadcasts data to the two relays and the destination. Secondly, the two relays exchange the received data with each other. Finally, they use the DSTC protocol to forward the data to the destination. For MSCR, its total energy consumption per bit E_S^b only consists of two phases since in MSCR there

is no inter-communication between the two relays. Therefore, we get

$$E_F^b = E_{srd}^b + E_{rr}^b + E_{rd}^b, \tag{3.29}$$

$$E_S^b = E_{srd}^b + E_{rd}^b, \tag{3.30}$$

where $E_{srd}^b = (P_{PA} + 2P_c^{tx} + 3P_c^{rx})/R_b$ is the energy consumption of the broadcast phase, $E_{rr}^b = 2E_{SISO}^b$ is the energy consumption of the inter-communication between the two relays and $E_{rd}^b = (P_{PA} + 2P_c^{tx} + P_c^{rx})/R_b$ is the energy consumption of the forward phase. The amplify power P_{PA} and the circuit consumption power for transmitting P_c^{tx} and receiving P_c^{rx} are clearly demonstrated in Chapter 2.

3.6.1.2 Simulation results

MFCR and MSCR have better BER performances than Alamouti model. However, they need more circuit energy consumption. Therefore, considering the typical energy model with system parameters as in Tab. 2.1 the energy efficiency of these models based on r and d_{sd} is evaluated to have a fair comparison on their energy consumption. The total energy consumption per bit of MFCR and MSCR as a function of transmission distance and relative distance of the relays is illustrated on Fig. 3.8. Besides, Fig. 3.9 is the projection of Fig. 3.8 on the z axis to show the best model that minimizes the total energy consumption. For instance, with $r = 0.4$, when $d_{sd} \leq 132m$ we will choose the Alamouti 2-1 model and the MSCR (NR-relays) has the best energy efficiency when $132m < d_{sd} \leq 300m$, otherwise, MFCR (R-relays) is the best choice.

3.6.2 Real energy model

In this section, the total energy consumption per bit of MSCR, MNCR and MFCR is considered via a real energy model with the parameters extracted from the transceiver, CC2420.

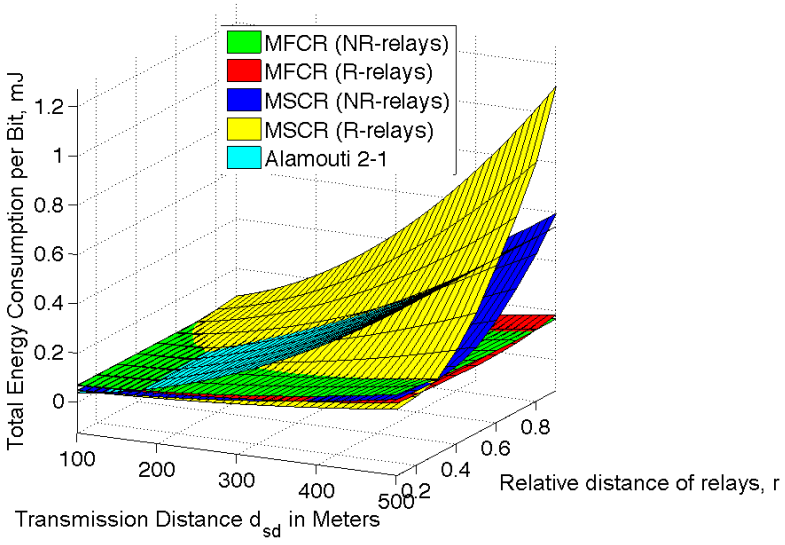

FIGURE 3.8: Total energy consumption per bit at BER = 10^{-5}

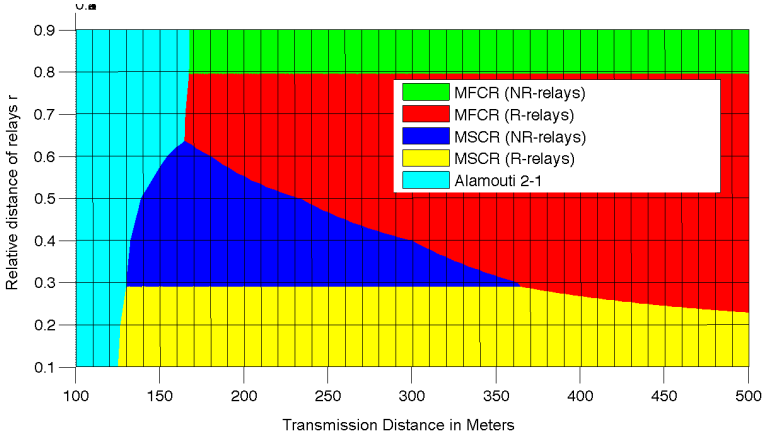

FIGURE 3.9: The optimal energy efficient scheme selection at BER = 10^{-5}

3.6.2.1 Analytic results

From Chapter 2, the total power consumption of MFCR is given by

$$P = P_T(d) + P_R = \frac{N_0 \gamma_F^{(P_e,r)} (1+\alpha) N_f (4\pi d_{sd})^2 L R_b}{\eta G_t G_r \lambda^2} + 6P_{T0} + 6P_{R0}. \tag{3.31}$$

Therefore, the energy consumption per bit of MFCR E_F^b can be derived as

$$E_F^b = \frac{N_0 \gamma_F^{(P_e,r)} (1+\alpha) N_f (4\pi d_{sd})^2 L}{\eta G_t G_r \lambda^2} + \frac{6P_{T0} + 6P_{R0}}{R_b}. \tag{3.32}$$

Similarly, the energy consumption per bit for MSCR E_S^b, MNCR $E_N^b$and Alamouti E_A^b models are given respectively

$$E_S^b = \frac{N_0\gamma_S^{(P_e,r)}(1+\alpha)N_f(4\pi d_{sd})^2 L}{\eta G_t G_r \lambda^2} + \frac{4P_{T0}+4P_{R0}}{R_b}, \tag{3.33}$$

$$E_N^b = \frac{N_0\gamma_N^{(P_e,r)}(1+\alpha)N_f(4\pi d_{sd})^2 L}{\eta G_t G_r \lambda^2} + \frac{4P_{T0}+5P_{R0}}{R_b}, \tag{3.34}$$

$$E_A^b = \frac{N_0\gamma_A^{(P_e)}(1+\alpha)N_f(4\pi d_{sd})^2 L}{\eta G_t G_r \lambda^2} + \frac{2P_{T0}+1P_{R0}}{R_b}. \tag{3.35}$$

Let denote $d_F^{max}(P_e,r)$, $d_S^{max}(P_e,r)$, $d_N^{max}(P_e,r)$ and $d_A^{max}(P_e)$ the maximum transmission distances of MFCR, MSCR, MNCR and Alamouti models at the specific values of P_e and r.

The MFCR is the best choice if $E_F^b < \min(E_S^b, E_N^b, E_A^b)$. From (3.32), (3.33), (3.34) and (3.35) we can derive

$$\max(B,C,D) < d_{sd} < d_F^{max}(P_e,r), \tag{3.36}$$

where $B = \min\Big(\sqrt{\frac{(2P_{T0}+2P_{R0})A}{(\gamma_S^{(P_e,r)}-\gamma_F^{(P_e,r)})}}, d_S^{max}(P_e,r)\Big)$,

$C = \min\Big(\sqrt{\frac{(2P_{T0}+1P_{R0})A}{(\gamma_N^{(P_e,r)}-\gamma_F^{(P_e,r)})}}, d_N^{max}(P_e,r)\Big)$,

$D = \min\Big(\sqrt{\frac{(4P_{T0}+5P_{R0})A}{(\gamma_A^{(P_e)}-\gamma_F^{(P_e,r)})}}, d_A^{max}(P_e)\Big)$

and $A = \frac{\eta G_t G_r \lambda^2}{N_0(1+\alpha)N_f(4\pi)^2 L R_b}$.

Similarly, Alamouti scheme is chosen if

$$0 < d_{sd} < \min(D,E,F), \tag{3.37}$$

where $E = \min\Big(\sqrt{\frac{(2P_{T0}+3P_{R0})A}{(\gamma_A^{(P_e)}-\gamma_S^{(P_e,r)})}}, d_A^{max}(P_e)\Big)$,

and $F = \min\Big(\sqrt{\frac{(2P_{T0}+4P_{R0})A}{(\gamma_A^{(P_e)}-\gamma_N^{(P_e,r)})}}, d_A^{max}(P_e)\Big)$.

The threshold for MSCR and MNCR is denoted by K. So, the MSCR is chosen if

$$d_{sd} < K, \tag{3.38}$$

where $K = \min\Big(\sqrt{\frac{P_{R0}A}{(\gamma_S^{(P_e,r)}-\gamma_N^{(P_e,r)})}}, d_N^{max}(P_e,r)\Big)$.

From (3.36), (3.37) and (3.38), we define the best cooperative strategy, as illustrated by Fig. 3.10.

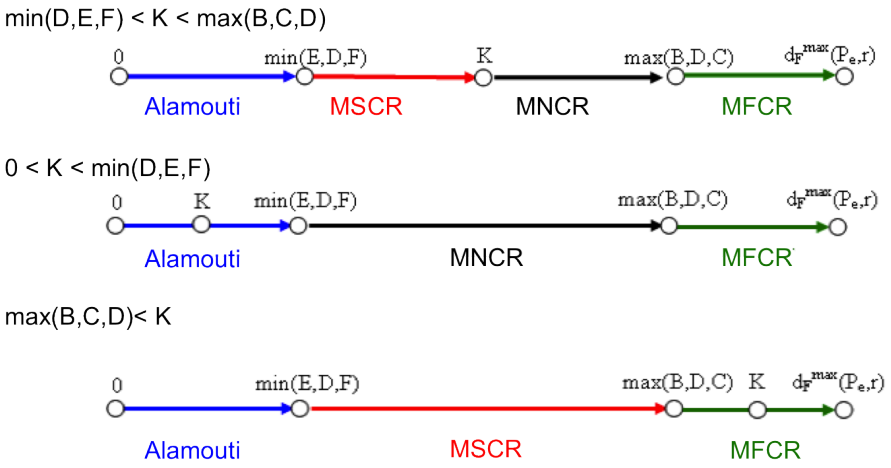

FIGURE 3.10: The best cooperative strategy

It is noteworthy that if $K < \min(D, E, F)$ or $K > \max(B, C, D)$, MSCR or MNCR respectively do not represent an energy efficient solution and hence will not be used.

3.6.2.2 Simulation results

Fig. 3.11 shows the simulation of the needed transmission energy at $P_e = 10^{-5}$ for MNCR, MSCR, MFCR (with NR-relays and R-relays) and Alamouti models. Due to the best performance, MFCR needs less transmission energy than the others. However, it requires the highest circuit energy consumption. So, to find the best energy-efficient model, the total energy consumption must be considered.

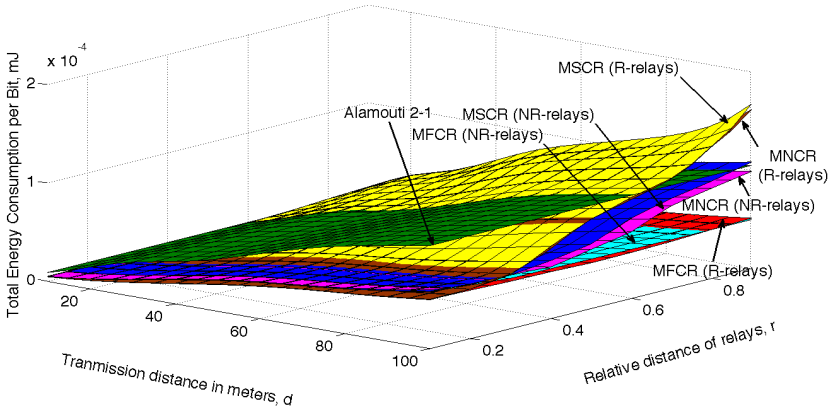

FIGURE 3.11: Transmission energy per bit ($P_e = 10^{-5}$)

Fig. 3.12 shows the best energy-efficient model versus the function of transmission distance and relative distance of relays. Each colored area represents the model which is the best choice for this range. In addition, the white on the right hand side of the figure is the out of range area in which using CC2420, it is impossible to get the desired reliable transmission ($P_e = 10^{-5}$). Despite its highest energy consumption, MFCR is the one which has the longest maximum transmission distance. So it is the best choice for long transmission distance. Alamouti 2-1 model has the most energy efficiency for short transmission distances. For example, when the relative distance of relays r is equal to 0.2, we will choose Alamouti scheme when the transmission distance d_{sd} is less than $135m$. When d_{sd} is between $135m$ and $295m$, the MSCR (R-relays) will bring us the best energy efficiency. The MNCR(NR-relays) is the best energy-efficient model when $295m < d_{sd} < 305m$. Finally, when $305m < d_{sd} < 320m$ the MFCR (R-relays) is the best choice. One should note that the MNCR (R-relays) is not an energy efficient scheme, since it is not present in this figure.

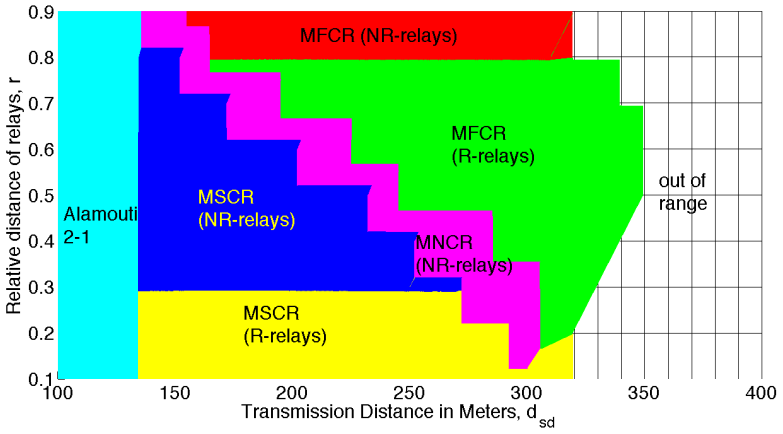

FIGURE 3.12: The optimal energy efficient scheme selection at $P_e = 10^{-5}$

In the other hand, Fig. 3.13 shows the specific case when the relative distance of relay is equal to 0.5. The maximum transmission distance of all models can be clearly determined, e.g. using MFCR (R-relays), reliable transmission can be achieved until d_{sd} equals to $345m$ while Alamouti scheme only has the reliable transmission up to $135m$. The maximum transmission distances of MFCR (NR-relays), MNCR (NR-relays), MSCR (NR-relays), MSCR (R-relays), MNCR (R-relays) are respectively $310m$, $248m$, $235m$, $175m$ and $170m$. From Fig. 3.13, we can derive the lower bound of total energy consumption per bit of the system when the relative distance of relays r is equal to 0.5 as shown in Fig. 3.14.

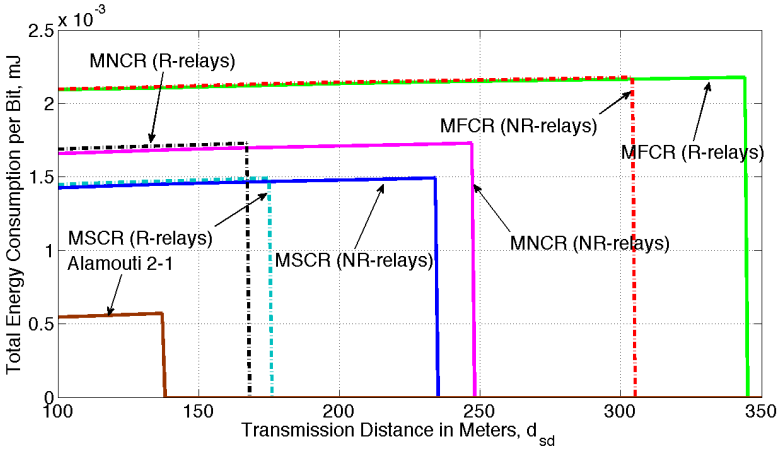

FIGURE 3.13: Total energy consumption per bit with the transmit power lower than 0dBm ($P_e = 10^{-5}$, $r = 0.5$)

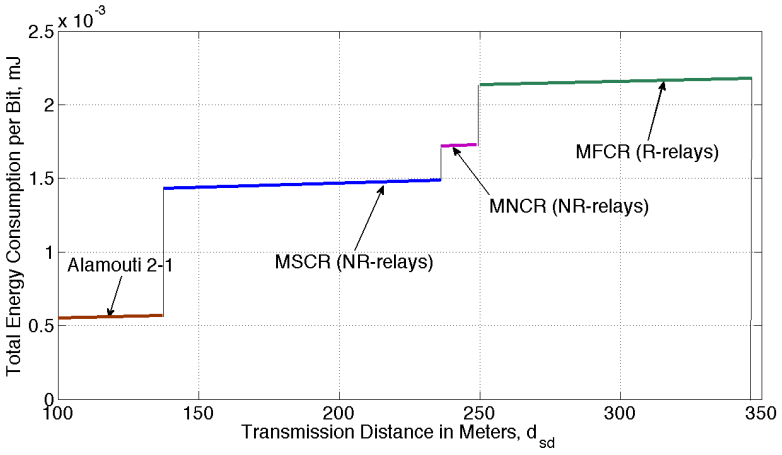

FIGURE 3.14: The lower bound of energy consumption per bit ($P_e = 10^{-5}$, $r = 0.5$)

3.7 Effect of synchronization error

3.7.1 Analysis

For all above parts, we assumed that there is a perfectly synchronized transmission from the two relays to the destination. In fact, this is too difficult to ensure this condition in reality because the two relays are separate and forward data independently to destination. In this section, the effect of the unsynchronized transmission [97] from the relays to the destination is considered. In this case, the DSTC transmission of the two relays seen at destination is no longer orthogonal. After the synchronization process, there will be the inter-symbol interference (ISI) of non-synchronized sequences. Therefore, we can not have the orthogonal space time combination at the destination, thus decreasing the desired signal amplitude and generating more interference.

In case of the synchronization error, the received signal at the destination is expressed as

$$\begin{aligned} y_{rd}[2k] = \sqrt{\epsilon_r}\Big(& \sum_{l=-\infty}^{\infty} h_{rd}[l]u_r[l]p\big((2k-l)T_s\big) \\ & + \sum_{l=-\infty}^{\infty} h_{rd}[l+1]u_r[l+1]p\big((2k-l)T_s-\delta\big)\Big) + n_{rd}[2k], \end{aligned} \tag{3.39}$$

$$\begin{aligned} y_{rd}[2k+1] = \sqrt{\epsilon_r}\Big(& -\sum_{l=-\infty}^{\infty} h_{rd}[l-1]u_r^*[l]p\big((2k+1-l)T_s\big) \\ & + \sum_{l=-\infty}^{\infty} h_{rd}[l]u_r^*[l-1]p\big((2k+1-l)T_s-\delta\big)\Big) + n_{rd}[2k+1], \end{aligned} \tag{3.40}$$

where T_s the symbol period, $p(t)$ the raised cosine pulse shape with roll-off factor of 0.25 and δ is the time offset error between the relay 1 and the relay 2.

For simplicity, we consider the ISI is just created by the four nearest neighbor symbols. So, we have

$$\begin{aligned} y_{rd}[2k] &= \sqrt{\epsilon_r}\Big(h_{rd}[2k]u_r[2k] + h_{rd}[2k+1]u_r[2k+1] + ISI\big(u_r[2k]\big)\Big) + n_{rd}[2k], \\ y_{rd}[2k+1] &= \sqrt{\epsilon_r}\Big(-h_{rd}[2k]u_r^*[2k+1] + h_{rd}[2k+1]u_r^*[2k] + ISI\big(u_r^*[2k+1]\big)\Big) + n_{rd}[2k+1], \end{aligned}$$

where the inter symbol interference terms are:

$$\begin{aligned} ISI(u_r[2k]) = & h_{rd}[2k+1]\Big(u_r[2k+1]\big(p(-\delta)-1\big) + u_r^*[2k-2]p(T_s+\delta) \\ & + u_r[2k-1]p(2T_s+\delta) + u_r^*[2k]p(T_s-\delta) + u_r[2k+3]p(2T_s-\delta)\Big), \end{aligned} \tag{3.41}$$

$$\begin{aligned} ISI(u_r^*[2k+1]) = & h_{rd}[2k+1]\Big(u_r^*[2k](p(-\delta)-1) + u_r[2k+1]p(T_s+\delta) \\ & + u_r^*[2k-2]p(2T_s+\delta) + u_r[2k+3]p(T_s-\delta) + u_r^*[2k+2]p(2T_s-\delta)\Big). \end{aligned} \tag{3.42}$$

In this case, the signal received at destination from relays can be rewritten:

$$\boldsymbol{y_{rd}} = \sqrt{\epsilon_r}\boldsymbol{U}\boldsymbol{h_{rd}} + \boldsymbol{n_{srd}}, \tag{3.43}$$

where $\boldsymbol{n_{srd}} = \begin{bmatrix} n_{srd}[2k] \\ n_{srd}[2k+1] \end{bmatrix} = \begin{bmatrix} n_{rd}[2k] + \sqrt{\epsilon_r} ISI(u_r[2k]) \\ n_{rd}[2k+1] + \sqrt{\epsilon_r} ISI(u_r^*[2k+1]) \end{bmatrix}$ with the distribution $n_{srd}[2k], n_{srd}[2k+1] \sim \boldsymbol{N}(0, 1 + \epsilon_r \Omega_{ISI}^2)$ where Ω_{ISI}^2 is the variance of ISI.

So, for the MIMO full cooperative relay model, the SNR can be inferred:

$$\gamma_d^F = \frac{E(|x|^2)}{4} \Big(\frac{\epsilon_r^2 ||\boldsymbol{h_{rd}}||^4}{\epsilon_s (||\boldsymbol{h_{sr1}}||^2 + ||\boldsymbol{h_{sr2}}||)(||\epsilon_s \boldsymbol{h_{sd}}||^2 + \epsilon_r ||\boldsymbol{h_{rd}}||^2)^2} + \frac{1}{(\epsilon_s ||\boldsymbol{h_{sd}}||^2 + \epsilon_r ||\boldsymbol{h_{rd}}||^2)} + \frac{\epsilon_r \Omega_{ISI}^2}{(\epsilon_s ||\boldsymbol{h_{sd}}||^2 + \epsilon_r ||\boldsymbol{h_{rd}}||^2)^2} \Big)^{-1}. \tag{3.44}$$

Similarly, the SNR of MIMO simple cooperative model is:

$$\gamma_d^S = \Big(\frac{\epsilon_s ||\boldsymbol{h_{sd}}||^2 + \epsilon_r ||\boldsymbol{h_{rd}}||^2 \big(\frac{\epsilon_r}{\epsilon_s ||\boldsymbol{h_{sr1}}||^2} + \frac{\epsilon_r}{\epsilon_s ||\boldsymbol{h_{sr2}}||^2} + 1 \big)}{(\epsilon_s ||\boldsymbol{h_{sd}}||^2 + \epsilon_r ||\boldsymbol{h_{rd}}||^2)^2} + \frac{\epsilon_r \Omega_{ISI}^2}{(\epsilon_s ||\boldsymbol{h_{sd}}||^2 + \epsilon_r ||\boldsymbol{h_{rd}}||^2)^2} \Big)^{-1} \frac{E(|x|^2)}{4}. \tag{3.45}$$

3.7.2 Effect of the synchronization errors on the BER performance of the models

In this work, the time offset error δ has a uniform distribution in $[-\Delta T_{syn}/2, \Delta T_{syn}/2]$ with ΔT_{syn} the synchronization error range. From Fig. 3.15, Fig. 3.16, Fig. 3.17 and Fig. 3.18, the performance of MFCR and MSCR using NR-relays and R-relays with different synchronization error ranges is shown. As we see the BER performance of the models is still considerable with the perfect synchronization case when $\Delta T_{syn} \leq 0.2$, otherwise if $\Delta T_{syn} > 0.2$, the BER performance of the models is degraded very quickly.

3.8 Conclusion

In this chapter, the MFCR and MSCR models representing the association between MIMO and cooperative relaying techniques are considered and compared with each other. It is shown that besides having a role as forming virtual MIMO in single-antenna system, the cooperative relay techniques can also be applied in MIMO systems to significantly improve the system performance.

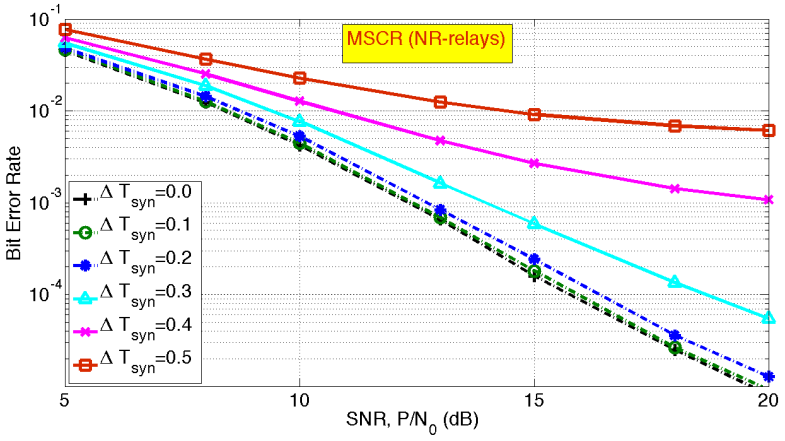

FIGURE 3.15: MSCR (NR-relays) with desynchronization (r=0.5)

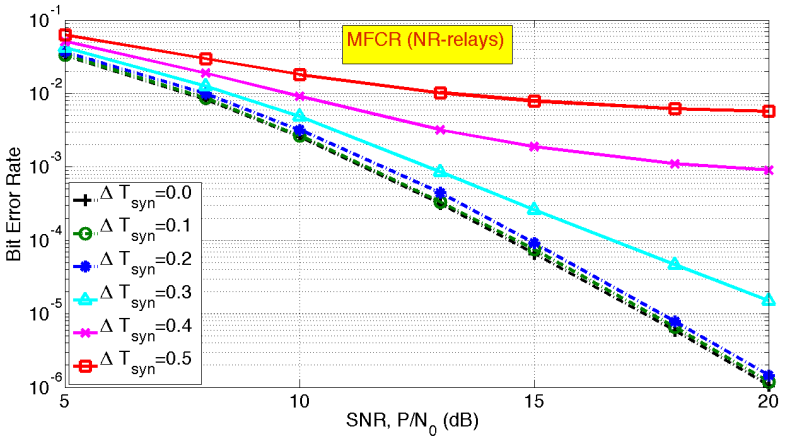

FIGURE 3.16: MFCR (NR-relays) with desynchronization (r=0.5)

In Chapter 2, it is claimed that single-antenna systems exploiting the fDSTC protocol outperform that exploiting the cDSTC protocol in terms of BER, spectral efficiency and energy efficiency. However, as illustrated in this chapter, multi-antenna systems exploiting the fDSTC protocol (i.e. MFCR) are shown to have better performances than that exploiting the cDSTC protocol (i.e. MSCR) except the spectral efficiency. Since MSCR can achieve the full diversity order, the inter-communication between the relays in MFCR can not help to get higher system diversity order. Therefore, that MFCR needs more time slots for its communication make it less spectral efficiency than MSCR.

In WSNs, where the constraint of throughput and data rate is loosen, MFCR is one of the best models to minimize the total energy consumption in long range transmissions. The effect of r on the BER performance of these models is also figured out. The comparison on BER of the models with NR-relays and R-relays shows that BER of MSCR is very sensitive to the change of r, while that of MFCR changes slowly when r changes. The

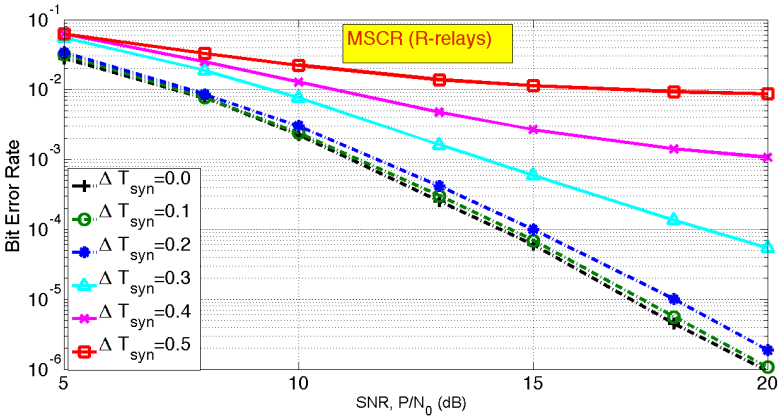

FIGURE 3.17: MSCR (R-relays) with desynchronization (r=0.5)

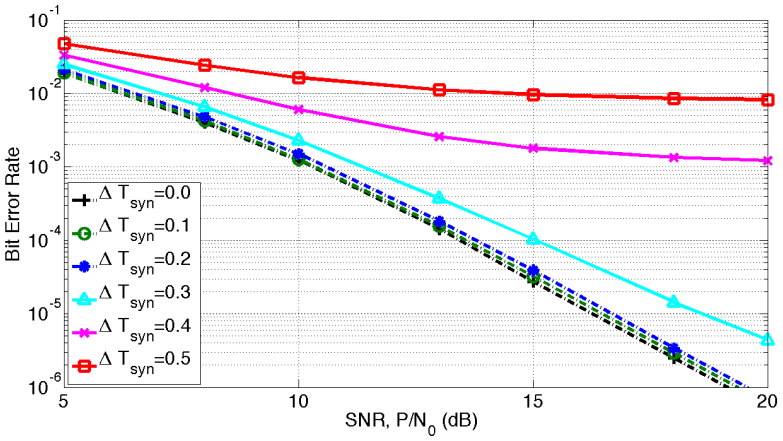

FIGURE 3.18: MFCR (R-relays) with desynchronization (r=0.5)

outage probability and the diversity order of the models are also derived. In addition, simulations on energy consumption shows the optimal application range of these models to get the best energy efficiency. Finally, the synchronization error of the models at the relays is considered. It is shown that, BER of the models is still considerable if the synchronization error range is lower than 0.2.

Obviously, through Chapter 2 and this chapter, the advantages of cooperative relays techniques are shown to be able to significantly improve the system performances, especially energy efficiency which is the most interested concern in resource-constrained networks, such as WSNs. The good performances of cooperative relay techniques come from their complicated protocols as a trade-off. In the previous results, the energy efficiency of the cooperative relay systems is approximated and evaluated without concerning about MAC protocols (i.e. ideal MAC protocols). However, the complicated transmission protocols of the cooperative relay systems bring many problems in designing energy-efficient

cooperative MAC protocols and that can reduce their energy efficiency gain. As a result, the following chapter will thoroughly and precisely evaluate the energy performance of the cooperative relay systems by considering real energy-efficient MAC protocols for cooperative WSNs.

Chapter 4

MAC Protocols for Low-Power Cooperative Wireless Sensor Networks

4.1 Introduction

In last decade, cooperative techniques such as cooperative relay and cooperative MIMO have been shown to play an important role in the evolution of wireless networks. They are shown to be able to enhance system capacity, improve the BER performance and reduce the energy consumption. There is obviously an enormous interest in cooperative techniques in the research community. However, most of the performance analysis for cooperative communication is widely studied at physical layer [6–10, 12, 19, 30, 31, 55, 56, 61, 68]. In order to make cooperative techniques be able to be utilized in the next generation of wireless networks, the higher layer protocols such as medium access control (MAC) layer, routing layer, ... must be thoroughly considered. Among the higher layers, MAC layer is responsible for regulating the shared wireless medium access of the networks, therefore, it has great influences on the network performance. In addition, MAC layer is also expected to improve throughput or energy efficiency, reduce delay while keeping minimum collisions.

Recently, different MAC protocols for repetition-based and DSTC-based cooperative diversity algorithms were proposed in [98–109]. In repetition-based cooperative techniques,

spatial diversity gain is obtained thanks to the help of relays which will forward another fading version of signals to destination [12, 19, 56], while for DSTC-based cooperative techniques, the relays themselves with or without the combination of the source will utilize DSTC transmission to forward signals to destination [6–10, 30, 31, 55, 61, 68]. MAC protocols for repetition-based cooperative algorithms [98–104] represent relatively simple protocols by utilizing the broadcasting nature of the wireless medium, while MAC protocols for DSTC-based cooperative approach [105–109] tend to be more complicated and may require hardware modifications.

4.1.1 Related work

Study on wireless sensor networks (WSNs) has impressively attracted many researchers due to advances in integrated circuit technology. WSNs are expected to be low-cost, reliable and easy to deploy. Each node in a WSN is powered by a small battery that may not be rechargeable or renewable for a long time. Therefore, energy consumption is the most critical constraint in WSNs. To preserve energy, many efforts are proposed in literature for energy-efficient MAC protocols. Among them, low power listening (LPL) or preamble sampling techniques, in which regular sleep periods are scheduled for each node, are among the best strategies to satisfy the energy constraint of WSNs [11, 73, 74, 83, 110].

In repetition-based cooperative relay networks, the destination receives signals from different nodes through independent fading channels. Therefore, the performance of the networks is increased, which leads to a reduction in the transmission energy. This is the reason why cooperative relay is identified as a core technique to minimize total energy consumption in WSNs. Considering the parameters of RF circuit with ideal MAC protocol, the comparison between cooperative and non-cooperative transmission schemes in terms of energy efficiency has been explored a lot in the literature [67, 77, 111, 112]. In [111], the effects of cell radius, relay position, number of relays and target data rate on energy consumption are investigated for cooperative systems using low-cost fixed relays. A thorough comparison on energy efficiency of single-hop, multi-hop and cooperative transmission in WSNs is derived when the receiver is constrained by packet loss and end-to-end throughput [67]. In [112], an energy efficient cooperative multicast transmission scheme with power control is proposed to obtain a balance between system throughput

and energy consumption. The application of energy-efficient cooperative techniques for intelligent transport system networks is illustrated in [77].

The aforementioned articles [67, 77, 111, 112], however, always considered ideal MAC protocols. Energy-efficiency evaluation of some MAC protocols in the case of cooperative systems are considered in [79, 113–116]. In [113], a cooperative MAC protocol combined with physical layer power/rate control is proposed to reduce energy consumption. Non-cooperative Hybrid-Automatic-Repeat-ReQuest (HARQ) and cooperative HARQ are considered in [79]. Results show that, selection of the transmission energy is not only dictated by the outage constraint, but also affected by the need to reduce the number of retransmissions. In [114], the HARQ protocol is analyzed in conjunction with hybrid relaying schemes from an energy efficiency perspective. CoopMAC is improved by facilitating cooperative signal combining at the destination and employing two relays in the context of a successive relaying technique in [115]. The evaluation of the energy consumption of Persistent Relay Carrier Sensing Multiple Access (PRCSMA) [116], an 802.11-based MAC protocol, is proposed to coordinate the retransmissions from the relays of wireless networks.

Previous works proposed MAC protocols supporting cooperative relay techniques. However, most of them extend the IEEE 802.11 standard for cooperative relay networks. Unlike other networks, WSNs are low power and lossy. Therefore, it exists a need to design low-power cooperative MAC protocols for WSN applications. The initial work on this problem has been considered in [84]. A cooperative low-power MAC (CL-MAC) protocol for WSNs is proposed in [84]. However, on the one hand CL-MAC protocol is initiated by the transmitter which may lead in the worst performance under strong fading conditions [11]. On the other hand, CL-MAC needs a perfect synchronization between source, relay and destination which is somehow very difficult to be satisfied in reality. Moreover, the energy consumption of CL-MAC is only derived as a function of number potential of relays, but latency and traffic load are not thoroughly considered though they also have considerable impacts on the energy consumption. The protocol proposed in the present chapter takes advantage of receiver initiated protocols, such as RICER [11, 74], to design a low power cooperative MAC protocol, RIC-MAC, which is simultaneously considered with the latency and traffic load impacts.

4.1.2 Contributions

The contributions of the chapter are:

1. RIC-MAC and adaptive RIC-MAC (associating with relay selection technique) protocols are proposed for cooperative WSNs.
2. Unlike some existent relay selection techniques presented in Chapter 1, here a new relay selection technique based on the wakeup period of nodes is proposed.
3. Energy consumption is precisely evaluated through parameters extracted from realistic and typical energy models presented in Chapter 2.
4. A comparison of energy consumption between single-hop Single-Input Single-Output (SISO), multi-hop SISO and cooperative relay systems is given for an ideal and a real MAC protocol to show the significant impact of the MAC layer on the total energy consumption.
5. The latency is considered, since energy consumption in WSNs is usually minimized subjected to some latency constraints. Moreover, the traffic load is also shown to have considerable impact on energy and latency.

The rest of this chapter is organized as follows. Section 4.2 presents the system model. The RIC-MAC and adaptive RIC-MAC protocols are thoroughly detailed in Section 4.3 while the energy analysis is derived in Section 4.4. Results are presented in Section 4.5 to compare with existing non-cooperative approaches and, finally, conclusion is given in Section 4.6.

4.2 System Model

In this chapter, a typical cooperative relay model (Fig. 4.1) which has one source (S), one relay (R1) and one destination (D) is considered. All terminals are only equipped with one antenna. Regenerative relays are used in the multi-hop SISO and cooperative relay models. After receiving signals from the source, the relays will decode the signals and then forward the decoded signals to the destination. The relays are uniformly distributed between S and D and the distance between S and D is denoted as d_{sd}. We assume that all

communications are performed over flat Rayleigh fading channel and that the transmit power is equally allocated among the transmitters (e.g. source and relays). Ideal channel state information (CSI) is known at the receiver, but not at the transmitters. Using a common transmission model, the signal to noise ratio (SNR) of the link from node i to node j is $\gamma_{ij} \propto d_{ij}^{-\alpha}$ where d_{ij} is the distance between i and j and $\alpha = 2$ is the path-loss exponent. BPSK modulation is considered. With these assumptions, the average SNRs of other links can be derived based on the SNR of the S-D link, e.g. for the cooperative relay system (similarly for multi-hop SISO systems), we can derive $\bar{\gamma}_{sr1} = \bar{\gamma}_{r1d} = \bar{\gamma}_{sd} + 3(dB)$ where $\bar{\gamma}_{sr1}$, $\bar{\gamma}_{r1d}$ and $\bar{\gamma}_{sd}$ are average SNRs corresponding to S-R1, R1-D and S-D links.

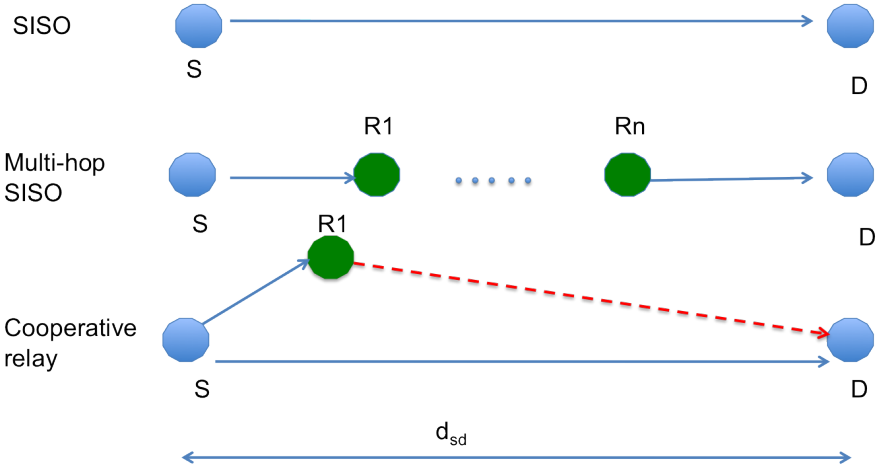

FIGURE 4.1: SISO, multi-hop SISO and cooperative relay models

4.3 RIC-MAC and adaptive RIC-MAC protocols

4.3.1 Communication protocol

In receiver-initiated MAC protocols, packet exchanges are initiated by the targeted node. Each receiver node X periodically wakes up. If the channel is free, it transmits a tagged wakeup beacon (WB) and then monitors the channel in M slots to receive a request-to-send (RTS) packet. When a source node S needs to transmit some packets to X, it first needs to listen to the channel and to wait for the WB of X. Then, S sends a buzz signal (BZ) right after the WB to initiate the communication with X. After sending BZ, S randomly chooses one of the M slots to transmit its RTS and waits for a clear-to-send (CTS) from X. If X does not receive BZ, it returns to sleep to reduce energy waste of monitoring the M slots.

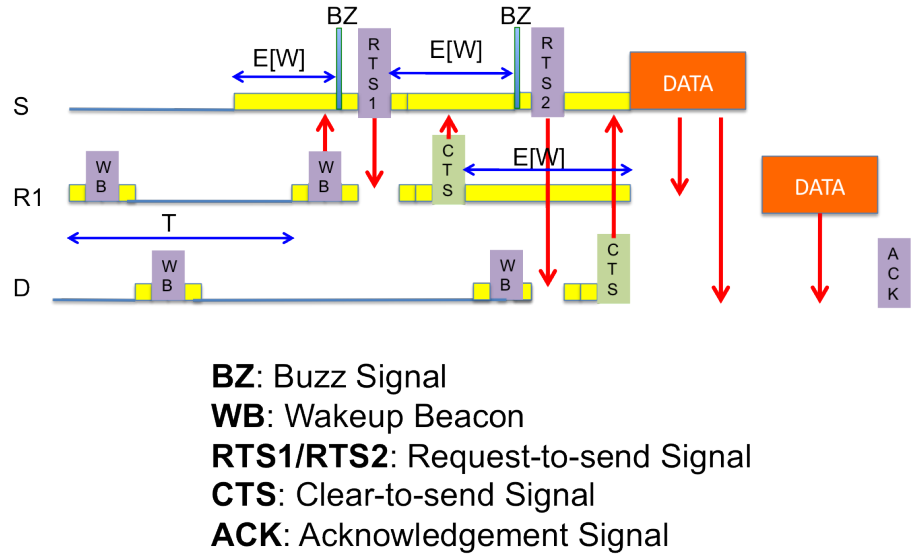

(a) relay wakes up before destination

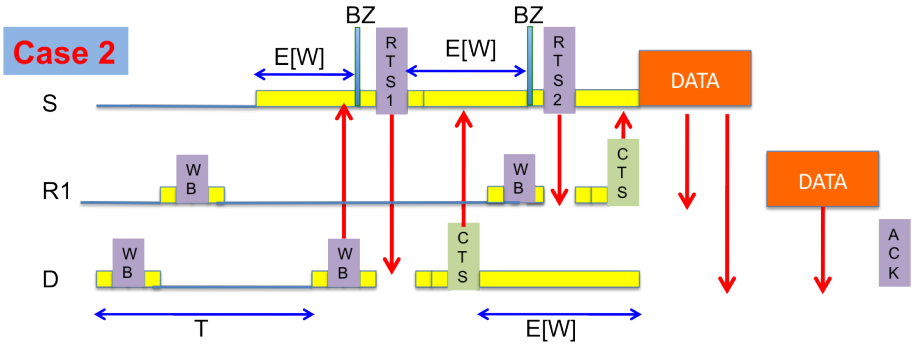

(b) destination wakes up before relay

FIGURE 4.2: RIC-MAC protocol for cooperative relay system when the relay wakes up before the destination (a) and vice versa (b)

The principle of the RIC-MAC protocol is shown in Fig. 4.2. Each S-D transmission takes advantage of a fixed relay node R1 to enhance communication performance. When S wakes up, it senses the channel to know whether R1 or D are awake.

- Case 1: R1 wakes up before D

  1. R1 transmits WB and waits for RTS packets from S if it receives BZ; otherwise it returns to sleep.
  2. After receiving RTS1, R1 sends CTS to S and waits for S-D connection.
  3. S sends BZ then RTS2 to D when it receives WB from D.

4. If S and R1 receive CTS from D, S starts to transmit data to D and R1. Then R1 decodes data, forwards them to D then goes to sleep. Otherwise, S and R1 return to sleep.
5. When D gets data from R1, it sends ACK to S to end the communication. If ACK is not received by S, S returns to sleep and waits for another period to resend data to D.

- Case 2: R1 wakes up after D. The communication protocol is nearly the same as case 1, but with D receiving RTS1 from S and R1 receiving RTS2 from S.

In our scheme, there are three types of RTS packet (i.e. RTS0, RTS1 and RTS2).

- RTS0 is for SISO, multi-hop SISO communications.
- RTS1 and RTS2 are reserved for the cooperative relay communication.

The role of a terminal acting as a relay or a destination is included in the address field of RTS0, RTS1 and RTS2 packets. X may receive RTS0, RTS1 and RTS2 in the same wakeup period from different sources. To minimize the power consumption of monitoring, X will choose the source depending on the priority order of RTS packets (RTS2 > RTS1 > RTS0). If X receives the same type of RTS packets (e.g. RTS0 or RTS1 or RTS2), it will randomly choose a source to make a connection by sending CTS packet. The other sources will go to sleep and wait for another period to communicate with X.

4.3.2 Models for transceiver and channel

4.3.2.1 MAC and Physical Layer Model

In order to evaluate the power consumption of MAC protocols, the MAC and physical layer model (MAPLAP) [11] is considered. A node in WSNs is modeled as a probabilistic state machine including the transmit (TX), receive (RX), monitor (MN), acquire (AQ) and sleep (SP) states as shown in Fig. 4.3. A transceiver node is in one of these five states at any given time instant. In the transmit and receive states, the node transmits and receives packets respectively. The acquire states always precedes the receive state to represent the compute and power intensive timing, phase or frequency acquisition. The

node senses the channel in the monitor state. Finally, in the sleep state, the majority of the node is powered off to economize energy consumption. Transition from one state to the other states consumes a nonzero turnaround power. However, the turnaround power is here assumed to be negligiable.

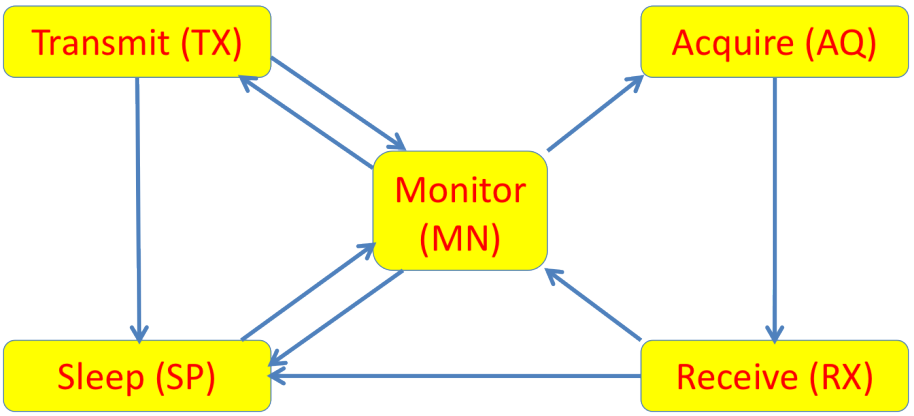

FIGURE 4.3: State diagram of MAPLAP model

4.3.2.2 Channel Model

A channel model is required to analyze performances of MAC protocols. In our work, the Gilbert-Elliot channel as shown in Fig. 4.4 is considered. It consists of two states: good state (G) and bad state (B) with the BER p_G and p_B respectively. The transition probability from G to B and from B to G is p_{GB} and p_{BG} respectively.

The average probability of being in G and B are:

$$\pi_G = \frac{p_{BG}}{p_{BG} + p_{GB}}, \tag{4.1}$$

$$\pi_B = \frac{p_{GB}}{p_{BG} + p_{GB}}. \tag{4.2}$$

Therefore, the average BER of the channel is:

$$P_b = \pi_G p_G + \pi_B p_B. \tag{4.3}$$

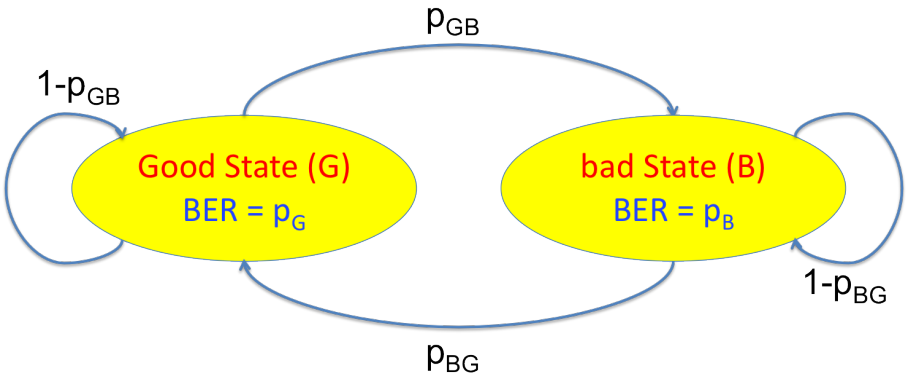

FIGURE 4.4: Gilbert-Elliot channel model

4.3.3 Energy consumption analysis

In our system, we assume that each node has n neighbors and only one potential destination node. RTS0, RTS1 and RTS2 have the same packet length. RTS (including RTS0, RTS1 and RTS2), CTS, DATA, ACK, WB and BZ take T_{RTS}, T_{CTS}, T_{DATA}, T_{ACK}, T_{WB} and T_{BZ} seconds to transmit. The propagation delay and decoding time at R1 are assumed to be negligible compared to the transmission time. All packets except for BZ include a preamble for bit synchronization that takes T_a seconds. T is the wakeup period of nodes. The network traffic is assumed to have Poisson distribution with mean of λ packets per second per node.

Let P_{tx}, P_{rx}, P_{aq}, P_{mn} and P_{sp} be the power consumption levels of the transmit, receive, acquire, monitor and sleep states. Let δ_{tx}, δ_{rx}, δ_{aq}, δ_{mn} and δ_{sp} be the average time of being in the above states for one successful communication. We assume that only one channel is used to transmit all the packets and all transmissions are performed over slow fading channel.

For the transmission from node i to node j, the expected number of WBs transmitted in one second, $E[N_{WB}]$ is

$$E[N_{WB}] = (1 - p_{by})(1 - \lambda^{'}(E[W] + 2MT_{RTS} + 2T_{CTS} + 2T_{DATA} + 2T_{ACK}))/T, \tag{4.4}$$

where $\lambda' = \lambda/(\pi_G(1 - p_{co}))$ is the scaled traffic load due to retransmissions of the entire session caused by channel fading which is represented by the average probability being in good state π_G, and collision rate p_{co}; $p_{by} = 1 - \Big(1 - \big(E[N_{WB}]T_{WB} + \lambda(T_{RTS} + T_{CTS} +$

$T_{DATA} + T_{ACK})\big)\Big)^n$ is the probability that a node detects the channel to be busy before transmitting a WB and backs off until T seconds later.

Let p_{RTS} be the probability that an RTS is successfully responded with a CTS and p_{WB} be the probability that a WB fails to be received. Then, the collision rate p_{co} is derived as

$$p_{co} = 1 - (1 - p_{WB})p_{RTS}. \tag{4.5}$$

There are cases that source nodes do not receive a WB properly:

- The destination node may find the channel to be busy and back off with probability p_{by}.
- WB is lost due to fading channel with probability $(1 - \pi_G)$.

So, the probability of WB failure is

$$p_{WB} = 1 - (1 - p_{by})\pi_G. \tag{4.6}$$

Similarly, there are four cases in which the source node does not receive a CTS corresponding to its RTS, given the WB is correctly received:

- The source node finds the channel with probability p_{by}, then it backs off and does not transmit RTS.
- RTS gets collision with the other RTSs in the M RTS slots or is not selected by the destination node when there are more than one source node try to establish the connection with the destination node with the probability p_1.
- The corresponding CTS may collide with probability $p_2 = 1 - (1 - T_{WB}/T)^{n-1}$.
- The RTS or CTS may be corrupted by channel fading with probability $(1 - \pi_G)$.

Therefore, the probability p_{RTS} is

$$p_{RTS} = (1 - p_{by})(1 - p_1)(1 - p_2)\pi_G. \tag{4.7}$$

The channel monitor time until a source node successfully receives a WB is

$$E[W] = (\frac{1}{2T}(T - T_{WB})^2 + \frac{p_{WB}}{1 - p_{WB}}T)/p_{RTS}. \tag{4.8}$$

Calculation of p_1: assuming that in WSNs, there are maximum 3 neighbor nodes of the destination nodes can generate a DATA in T seconds. It is reasonable because WSNs are low rate networks. The probability of receiving k RTSs every time a node wakes up is

$$Pr(n = k) = \frac{(\lambda T)^k}{k!}e^{-\lambda T}. \tag{4.9}$$

Focusing on one particular source node, if none of the neighbor nodes of the destination generated DATA in the past T seconds (probability $Pr(n = 0)$), the source node of interest is alway selected by the destination node with probability 1. Let

$$n_0 = Pr(n = 0)1.$$

If one of the destination node 's neighbors generated a DATA in the past T seconds ($Pr(n = 1)$), the probability that the two RTSs do not collide is $\frac{M-1}{M}$ ($M \geq 2$). If they not collide, the probability of the source node is selected is 1/2. So,

$$n_1 = Pr(n = 1)\frac{M - 1}{M}\frac{1}{2}.$$

In the scenario that two of the destination node 's neighbors generated a DATA in the past T seconds ($Pr(n = 2)$). If all three RTSs do not collide (probability $\frac{M-2}{M}\frac{M-1}{M}1$, $M \geq 3$), the source node of interest is selected with probability 1/3. In the second case, the other two RTSs collide while the RTS of interest is safe. This happens with probability $\frac{1}{M}\frac{M-1}{M}1$, $M \geq 2$. In this case the source node is selected with probability 1. Then, the probability that the source receives a CTS is

$$n_2 = Pr(n = 2)\big(\frac{(M - 2)(M - 1)}{M^2}\frac{1}{3} + \frac{M - 1}{M^2}1\big).$$

Then, the overall probability of an RTS being responded by a CTS is approximated by:

$$\begin{aligned} p_1 &= n_0 + n_1 + n_2 \\ &= e^{-\lambda T} + \lambda e^{-\lambda T}\frac{M-1}{M}\frac{1}{2} + \frac{(\lambda T)^2}{2}e^{-\lambda T}\big(\frac{(M-1)(M-2)}{M^2}\frac{1}{3} + \frac{M-1}{M^2}\big). \end{aligned} \tag{4.10}$$

These above expressions are reserved for a direct transmission from node i to node j. For cooperative transmission, the source node firstly makes a connection with both the relay and destination nodes before transmitting a DATA. Therefore, the total energy consumption per successful transmission E_{total} for cooperative relay system with RIC-MAC can be approximated from the above expressions and can be expressed as follows:

$$\begin{aligned} \delta_{tx} =& 2E[N_{WB}]T_{WB} + \lambda^{'}((2T_{RTS} + 2T_{CTS} + 2T_{BZ})/p_{RTS} \\ &+ 2T_{DATA} + T_{ACK}), \end{aligned} \tag{4.11}$$

$$\begin{aligned} \delta_{rx} =& 2E[N_{BZ}]T_{BZ} + \lambda^{'}((3T_{WB} + 3T_{RTS} + 2T_{CTS})/p_{RTS} \\ &+ 3T_{DATA} + T_{ACK} - (\frac{8}{p_{RTS}} + 4)T_a), \end{aligned} \tag{4.12}$$

$$\delta_{aq} = \lambda^{'}((8/p_{RTS} + 4)T_a), \tag{4.13}$$

$$\begin{aligned} \delta_{mn} =& 2E[N_{BZ}]MT_{RTS} + 2(E[N_{WB}] - E[N_{BZ}])T_{BZ} \\ &+ 3\lambda^{'}E[W], \end{aligned} \tag{4.14}$$

$$\delta_{sp} = 1 - \delta_{tx} - \delta_{rx} - \delta_{aq} - \delta_{mn}, \tag{4.15}$$

$$E_{total} = \delta_{tx}P_{tx} + \delta_{rx}P_{rx} + \delta_{aq}P_{aq} + \delta_{mn}P_{mn} + \delta_{sp}P_{sp}, \tag{4.16}$$

where the expected number of BZ that a node receives in one second is $E[N_{BZ}] = \lambda^{'}/p_{RTS} + n\lambda^{'}(T_{CTS} + T_{BZ})/T$.

In RIC-MAC, the average latency L of a successful transmission (including retransmissions if necessary) is derived as

$$L = 2T_{WB} + 2MT_{RTS} + 2T_{CTS} + \frac{3E_W}{1-p_{f5}} + \frac{p_{f5}}{1-p_{f5}}T + 2T_{bz}, \tag{4.17}$$

with $p_{f5} = 1 - p_{RTS}(1-p_{by})\pi_G$, the handshake failure rate.

4.3.4 Adaptive RIC-MAC

In RIC-MAC, while the S-R1 link is established and both nodes are waiting for D (i.e. case 1), the S-D communication may fail due to the fading channel or collisions. In this case, power is wasted at S and R1. The same kind of power is wasted in case 2 if the S-R1 connection is failed while S and D are waiting. The adaptive RIC-MAC is proposed to reduce this power waste.

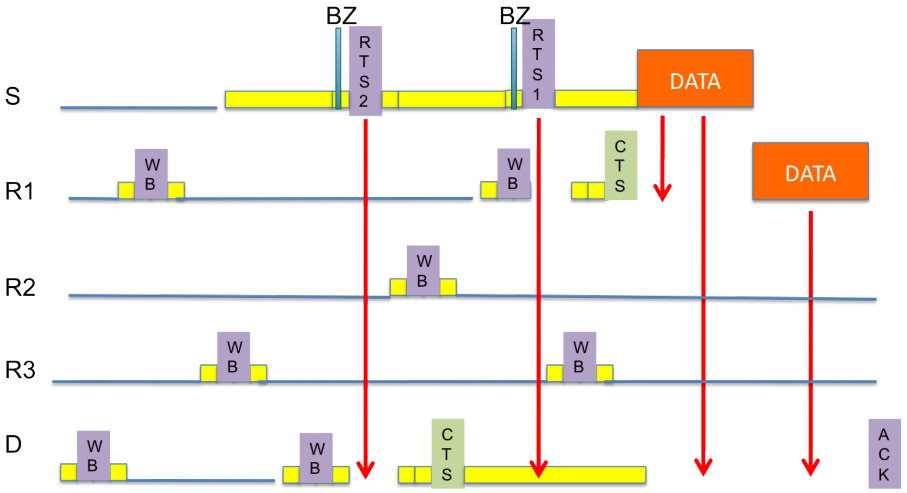

FIGURE 4.5: Adaptive RIC-MAC protocol for cooperative relay systems

In adaptive RIC-MAC as shown in Fig. 4.5, the relay is adaptively chosen depending on the channel and the wakeup time. In order to reduce the power due to monitoring the channel, S only connects to the relay if the S-D link is successfully connected. After the S-D link is established, S will make a connection with the relay that wakes up right after S receives CTS from D. If this connection is failed, S will automatically choose another relay that wakes up next. In dense WSNs, we can assume that S can choose a relay that wakes up right after D without difficulty and therefore, the S-R1 connection is always successful. In that case, the expected waiting time of the adaptive RIC-MAC can be approximated as the same as the expected waiting time of a SISO transmission. The energy consumption analysis of adaptive RIC-MAC is the same as RIC-MAC, except that (4.11), (4.12) and (4.14) need to be modified as

$$\begin{aligned}\delta_{tx} =&(E[N_{WB}]+1)T_{WB}+\lambda^{'}((2T_{RTS}+2T_{CTS}\\&+2T_{BZ})/p_{RTS}+2T_{DATA}+T_{ACK}),\end{aligned} \tag{4.18}$$

$$\begin{aligned}\delta_{rx} =&(E[N_{BZ}]+1)T_{BZ}+\lambda^{'}((3T_{WB}+3T_{RTS}\\&+2T_{CTS})/p_{RTS}+3T_{DATA}+T_{ACK}-(\frac{8}{p_{RTS}}+4)T_a),\end{aligned} \tag{4.19}$$

$$\begin{aligned}\delta_{mn} =&(E[N_{BZ}]+1)MT_{RTS}+(E[N_{WB}]-E[N_{BZ}])T_{BZ}\\&+\lambda^{'}E[W].\end{aligned} \tag{4.20}$$

The latency of adaptive RIC-MAC is modified as

$$L = 2T_{WB}+2MT_{RTS}+2T_{CTS}+\frac{E_W}{1-p_{f5}}+\frac{p_{f5}}{1-p_{f5}}T+2T_{bz}. \tag{4.21}$$

4.4 Energy model

The evaluation of energy consumption of the systems is based on some parameters (radio transceiver power, antenna gain, sensitivity, etc.) extracted from the PowWow WSN platform developed at INRIA [87] or typical energy model which are presented in Chapter 2. In this study, the radio part is considered and the power due to digital signal processing is neglected.

The total energy consumption per bit of the multi-hop SISO E^b_{h-SISO}, and cooperative relay E^b_{coop}, can be calculated based on the total energy consumption per bit of SISO transmission E^b_{SISO}

$$E^b_{h-SISO} = hE^b_{SISO}, \tag{4.22}$$

$$E^b_{coop} = E^b_{sr_1d}+E^b_{r_1d}, \tag{4.23}$$

where h is the number of SISO hops, $E^b_{sr_1d} = (P_T(d_{sd})+2P_R)/R_b$ is the energy consumption when S simultaneously transmits data to R1 and D and $E^b_{r_1d} = E^b_{SISO}$ is the energy consumption needed to forward data from R1 to D.

4.5 Simulation results

Whereas RIC-MAC is used for the cooperative relay system, RICER5b [74] is used for SISO and multi-hop SISO systems, since RICER5b can be considered as a reference for receiver-initiated MAC protocols. The simulations are done using a strong fading

channel model with the parameters as in Tab. 4.1. BZ and DATA have a respective need respectively 4 and 230 bits while all other packets use 60 bits. The wakeup period T is modified depending on the traffic load to get the region of interest in which the energy consumption decreases with increasing latency. Number of RTS slots is $M = 2$ and neighbor nodes is $n = 7$.

DATA length	230 bits
RTS, CTS, ACK, WB length	60 bits
BZ length	4 bits
Number of neighbors	$n = 7$
Number of potential destination nodes	1
Number of RTS slots	$M = 2$
Channel G to B transition probability	$p_{GB} = 0.35$
Channel B to G transition probability	$p_{BG} = 0.65$

TABLE 4.1: Simulation parameters

4.5.1 BER performance

For a fair comparison, it is assumed that the total received power at the destination for all systems is the same as the receive power at the destination for the SISO system. This means that for the cooperative relay system, the energy allocated to each symbol at the source and the relay is halved. Note that, for the multi-hop SISO and cooperative relay systems, the relays are uniformly distributed between the source and the destination. It is shown in Fig. 4.6 that the cooperative relay system has better BER performance than the SISO, 2-hop and 3-hop systems in high SNR regions.

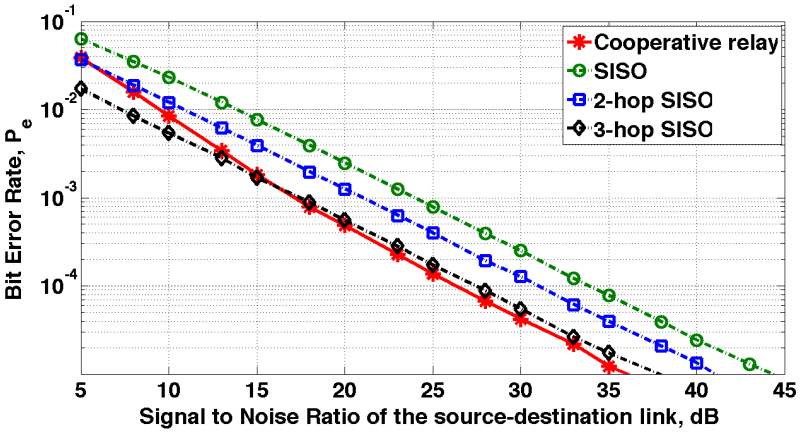

FIGURE 4.6: BER performance of single-hop, multi-hop and cooperative relay systems

4.5.2 Typical energy model

The comparison of energy consumption between SISO and cooperative relay systems is given based on a typical artificial energy model [64] considering ideal (Fig. 4.7) or real MAC protocols (Fig. 4.8). Fig. 4.7 shows that with an ideal MAC protocol, the cooperative relay system can get an energy gain of 60% in comparison with SISO system at a transmission distance $d_{sd} = 30m$. However, Fig. 4.8 shows that regardless of latency, cooperative relay system has no energy gain as compared to SISO system when using a real MAC protocol. This demonstrates a significant impact of the MAC protocol on the total energy consumption of the system.

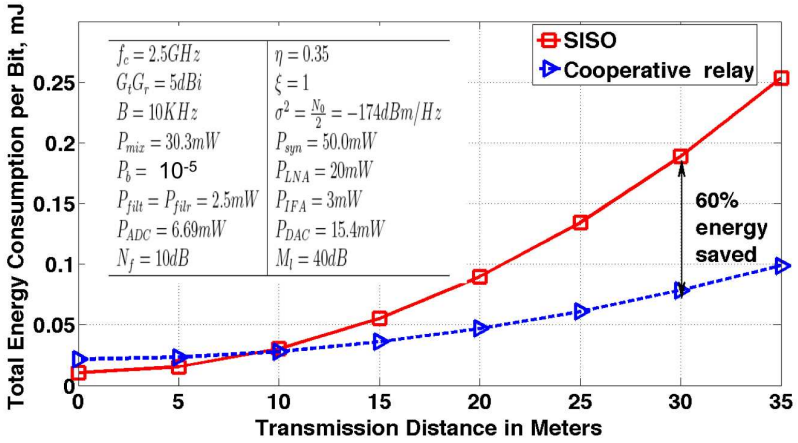

FIGURE 4.7: Comparison of energy consumption between single-hop and cooperative relay using an ideal MAC protocol (typical energy model)

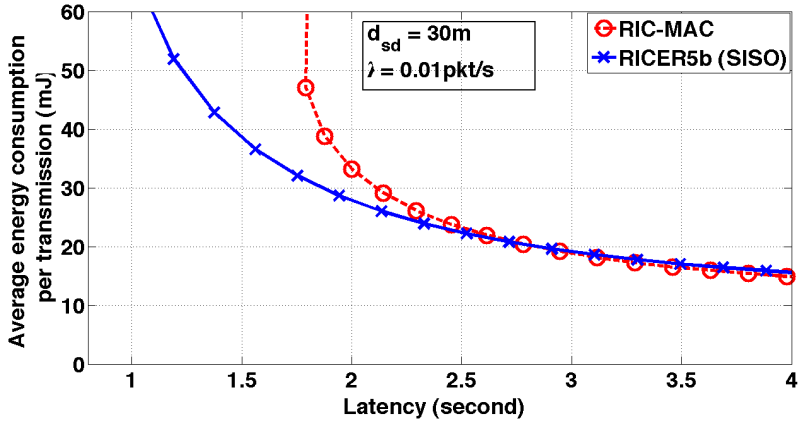

FIGURE 4.8: Comparison of energy consumption between single-hop and cooperative relay using real MAC protocols (typical energy model)

4.5.3 Energy model based on a real platform

The impact of the MAC protocol can be clearly demonstrated through a typical energy model. However, this does not give us a precise estimation since it is practically impossible to perform a successful transmission at any distance. Considering a real platform, e.g. PowWow, Fig. 4.9 shows that each model has a maximum transmission distance depending on the desired BER, the maximum transmit power of the transceiver, i.e. CC2420 and the transmission protocol. Considering the PowWow platform, a direct SISO system with $BER = 10^{-5}$ has a maximum transmission distance of only $14.5m$. The energy consumption comparison between SISO and cooperative relay when $d_{sd} > 14.5m$ is somehow meaningless. Since only 3-hop SISO and cooperative relay can get a transmission distance over $30m$, they will be used to make a comparison on energy consumption. Using an ideal MAC protocol, the cooperative relay system translates into a 33% energy consumption gain in comparison with the 3-hop SISO system (Fig. 4.9).

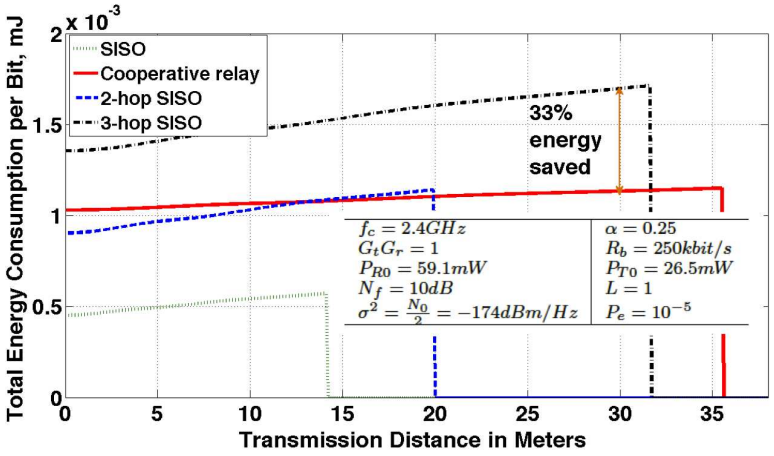

FIGURE 4.9: Comparison of energy consumption between single-hop and cooperative relay using an ideal MAC protocol (energy models based on PowWow platform)

The energy consumption for cooperative and non-cooperative MAC protocols are given in Fig. 4.10 (at low traffic load) and Fig. 4.11 (at high traffic load). Thanks to channel diversity of the cooperative relay system, the source S can still communicate with the destination D for a distance $d_{sd} = 30m$. This due to the fact with the help of the transmission from R1, the whole cooperative relay system can get the desired $BER = 10^{-5}$ for $d_{sd} = 30m$. The transmit power P_{tx} is calculated based on the results in Fig. 4.6 and the energy model in Section 4.4. Regardless of the latency, the energy gain of cooperative relay over SISO decreases when using real MAC protocols, i.e. 28% (Fig.

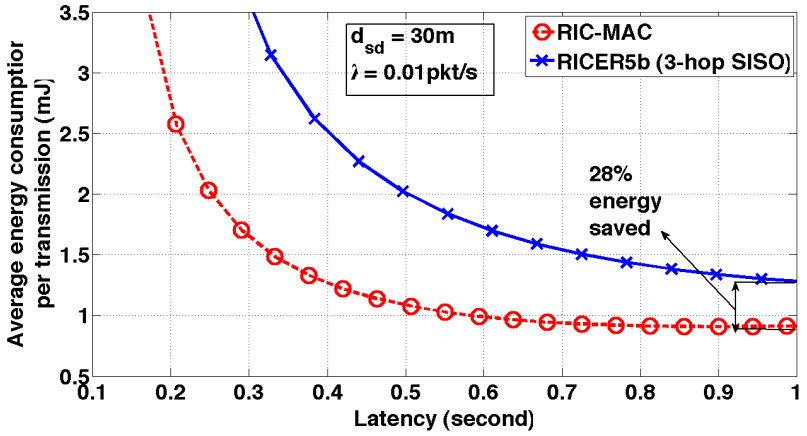

FIGURE 4.10: Comparison of energy consumption between single-hop and cooperative relay using real MAC protocols (energy models based on PowWow platform) in low traffic load networks

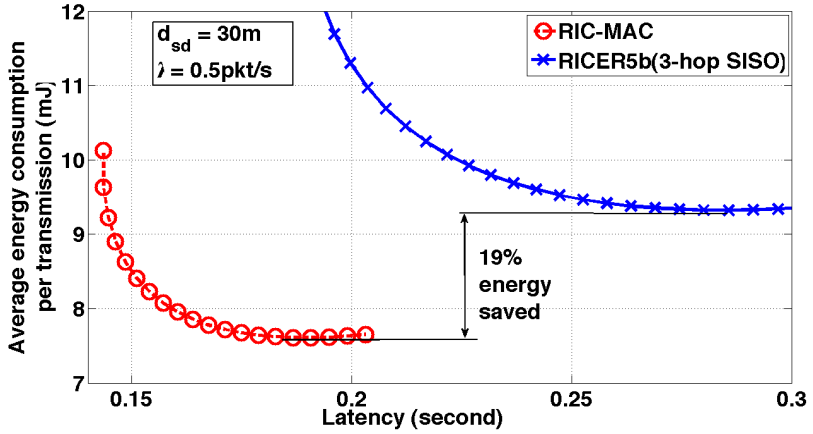

FIGURE 4.11: Energy consumption with real MAC protocol (PowWow platform) in high traffic load networks

4.10) instead of 33% (Fig. 4.9). As the traffic load increases (e.g. $\lambda = 0.5$) this gain is only 19% (Fig. 4.11). The complex MAC protocol of the cooperative relay system with many packet transmissions for establishing the rendez-vous between nodes, obviously gets into trouble for high traffic load. So, unlike the consideration on energy consumption with an ideal MAC protocol in which cooperative relay system always gets energy gain over SISO system in long range transmission distance, our results show that the energy gain is significantly affected by MAC protocols and traffic load. However, the precise evaluation of energy consumption on a real platform (i.e. PowWow) still confirms the interest of cooperative relay system over SISO and multi-hop SISO system. For the rest of this chapter, unless other statement, the powwow energy model will be used for all the simulations.

4.5.4 Effect of traffic load on latency and energy

The effect of traffic load on RIC-MAC is shown in Fig. 4.12. With a fixed wakeup period T (second), when the traffic load increases, the energy consumption increases as well. However, the latency is almost the same which means that RIC-MAC is robust to traffic load variations in terms of latency.

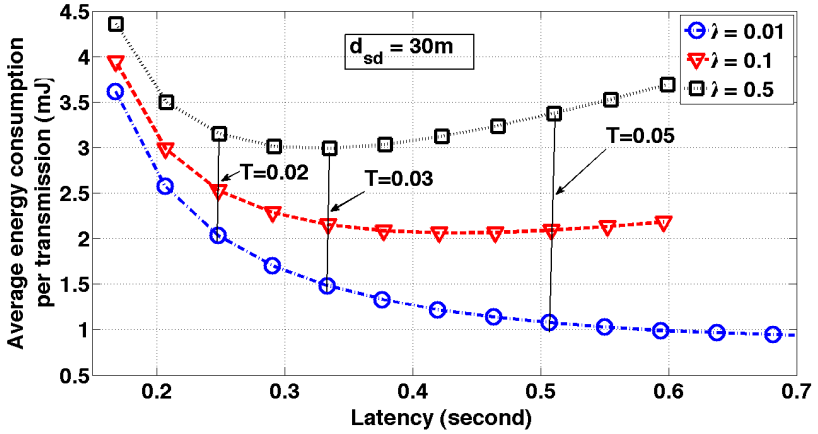

FIGURE 4.12: Effect of traffic load on RIC-MAC protocol

4.5.5 RIC-MAC vs. adaptive RIC-MAC

As discussed above, the MAC protocol plays an important role in the total energy consumption of the system. Therefore, a careful MAC protocol design for the cooperative relay system is critical to minimize the energy consumption in WSNs. With a simple modification, the use of the proposed adaptive RIC-MAC translates into a 50% energy consumption gain as shown in Fig. 4.13.

4.6 Conclusion

In the present chapter, a thorough consideration on the energy consumption of physical and MAC layers is presented. A low-power cooperative MAC protocol based on receiver-initiated schemes, RIC-MAC, is proposed. Unlike most of the articles in literature, we show that by considering real MAC protocol, the energy gain of cooperative relay system over SISO system is decreased in comparison with ideal MAC protocol. This energy gain is also affected by the traffic load of the networks. When considering with a real platform,

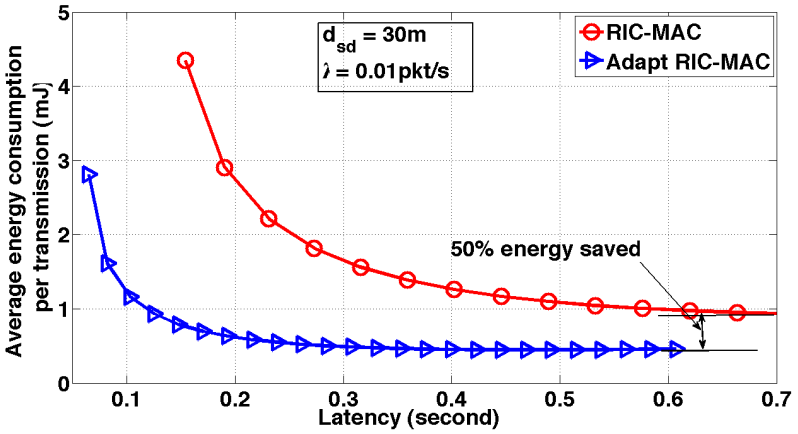

FIGURE 4.13: Energy consumption of RIC-MAC vs. adaptive RIC-MAC

the cooperative relay system still gets 28% energy gain in low traffic load and 19% in high traffic load over multi-hop SISO system as $d_{sd} = 30m$. These results confirm the interest of using cooperative relay techniques in WSNs to minimize the total energy consumption, thus to increase the life time of the networks. RIC-MAC is also shown to be robust to traffic load in terms of latency. In addition, with an adaptive relay selection, adaptive RIC-MAC can help us save 50% energy consumption in comparison with RIC-MAC.

Conclusion and future works

This thesis proposed the fDSTC protocol, in which there is an added inter-relay communication phase. The relays exchange data with each other before forwarding the signals to the destination. Firstly, the performances of the fDSTC protocol were considered and evaluated through single-antenna systems. In terms of BER, outage probability, spectral efficiency, diversity order and energy efficiency, the fDSTC protocol always outperforms the cDSTC protocol

- When using NR-relays, bounds and then a closed-form of the ASEP for the fDSTC protocol were derived. By simulations, it was shown that the fDSTC protocol gets an average signal to noise ratio (SNR) gain of $3.7dB$. On the other hand, using R-relays a closed-form expression of error probability of the fDSTC protocol, conditioned to the channel, was also derived. In addition, a huge average SNR gain of $18.1dB$ is obtained as compared to the cDSTC protocol.

- The relative distance of relays plays an important role in the BER performance of a relay model [12]. In fact, when the distance of relays between source and destination changes, the BER performance of the whole system will also change. In this thesis, simulations taking account of this effect showed that the required SNR of the system at $BER = 10^{-5}$ for the cDSTC protocol may vary from $27.5dB$ to $48dB$ (R-relays) or from $18dB$ to $24.3dB$ (NR-relays) when the relays move from the source to the destination. This huge variation may affect the performance of the whole system (in the case of mobile networks). However, with the fDSTC protocol, this effect can be reduced up to 75%.

- In the fDSTC protocol, there is an inter-relay transmission, the effect of the distance between the relays on the whole performance of the system was also considered. The simulation results showed that this distance only needs to be smaller than

one fifth of the transmission distance to guarantee the performance of the system. On the other hand, the suitable power allocation among the source and the relays was also shown to be able to further increase the BER performance of the fDSTC protocol.

- Besides, the fDSTC protocol requires more transmissions as compared to the cDSTC protocol, which will result in some rate loss. Therefore, the outage probability of the protocols was also considered to have a thorough view on this phenomenon. At the same spectral efficiency, the fDSTC protocol was shown to have better outage probability in high SNR regions due to the increased diversity order. Using automatic gain control (AGC) at the relays, the same result as [24] was found, i.e. the cDSTC protocol cannot get full diversity. By contrast, in this thesis the fDSTC protocol was shown to achieve full diversity in case of NR-relays. In case of R-relays, even if the fDSTC protocol cannot obtain full diversity, it still helps us to increase the system diversity order in comparison with the cDSTC protocol.

- The better performance of the fDSTC protocol over the cDSTC protocol comes from the communication between the relays. Since the relays also need power to exchange data, it is very important to consider the total power consumption of the protocols. Therefore, the total energy consumption per bit of the protocols as the function of the transmission distance was derived. On the one hand, using the typical energy model [64], the fDSTC protocol was shown to be energy-efficient in long-range transmissions. With R-relays, the fDSTC protocol can save 50% of the total energy consumption when the transmission distance between the source and destination $d_{sd} = 25m$. Otherwise, using the fDSTC protocol with NR-relays, 20% of the total energy consumption is saved when $d_{sd} = 270m$. On the other hand, with a real energy model the fDSTC protocol was also shown to have longer maximum transmission distance than the cDSTC protocol.

Secondly, the fDSTC protocol was exploited in multi-antenna systems to evaluate its performances. The association between the fDSTC protocol and MIMO systems (i.e. MFCR) still achieves better performances than those of the association between the cDSTC protocol and MIMO systems (i.e. MSCR).

- In terms of BER performance, MFCR was shown to be better than MSCR whatever type of relays is used (e.g. NR-relays or R-relays). However, unlike in single-antenna systems, using the fDSTC protocol in multi-antenna systems can not help to get higher system diversity order. Therefore, that MFCR needs more time slots for its whole transmission makes it less spectral efficiency than MSCR. In addition, the synchronization error of the DSTC transmission from the relays to the destination was shown to have less significant impact on the BER performance of the system.

- In terms of energy efficiency, the total energy consumption of MFCR and MSCR was thoroughly considered and calculated through the two energy models (i.e. typical and real energy model). A mathematical analysis on the total energy consumption was derived to show the best cooperative strategy to increase energy efficiency. In spite of complicated transmission protocol, MFCR was shown to be the most interesting model for long transmission distances.

Finally, a cross-layer design for cooperative relay systems was considered in terms of energy efficiency. RIC-MAC and adaptive RIC-MAC protocols were proposed for low-power cooperative relay wireless networks. Under the view of cross-layer, the energy gain of cooperative relay system over SISO and multi-hop SISO systems decreases due to the complexity of MAC protocols for cooperative relay systems. In addition, this energy gain was shown to be considerably affected by the traffic load of the networks. However, using a real energy model, this thesis still confirms the interest of cooperative relay system over SISO and multi-hop SISO systems (i.e. 28% energy gain in low traffic load and 19% energy gain in high traffic load as $d_{sd} = 30m$). When considering the effect of the traffic load on the energy consumption per packet and the latency, we see that RIC-MAC is a robust MAC protocol to traffic load in terms of latency. In addition, when associating with an adaptive relay selection, the adaptive RIC-MAC protocol can help us to save more than 50% energy consumption in comparison with RIC-MAC.

Future works

Association between the fDSTC protocol and relay selection technique

Besides the existing advanced techniques (i.e. relay selection, power allocation and two-way relays) in the literature which were shown to be able to further improve the performances of cooperative relay systems, this thesis presented a new technique based on the inter-communication between relays, which was also shown to be capable of increasing the cooperative relay systems' performances. However as shown in case of R-relays, the data exchange between the relays of the fDSTC protocol can not help to achieve the maximum diversity order. Fortunately, the inter-communication between relays can be combined with the other advanced techniques (e.g. power allocation, relay selection, etc.) without difficulty to overcome this problem. A first attempt in associating the fDSTC protocol with relay selection technique as shown in Fig. 4.14 illustrates that the full diversity order can be achieved in case of R-relays.

Here, we associate the relay selection technique in case of R-relays, called SR-relays, with the fDSTC protocol to improve its performance. For SR-relays, if the quality of the links between the source and the relays is smaller than a certain threshold, the source simply continues its transmission to the destination in the forms of repetition with twice the transmit power to make sure that the received power at the destination is equal to the case when the two relays forward signals to the destination. Otherwise, if the quality is larger than the threshold, the relays decode the signals and then use DSTC to forward the signals to the destination.

The approximation and simulation results for the fDSTC protocol association with relay selection technique, SR-fDSTC, in terms of outage probability is shown in Fig. 4.14. Since the SR-fDSTC protocol can achieve maximum diversity order (i.e. the third order) as compared to the second order of the R-fDSTC protocol, it has more spectral efficiency than the R-fDSTC protocol.

Energy and latency tradeoff

Due to the inter-communication between relays, the fDSTC protocol needs more time slots than the cDSTC protocol for a whole communication, thus leading to a higher

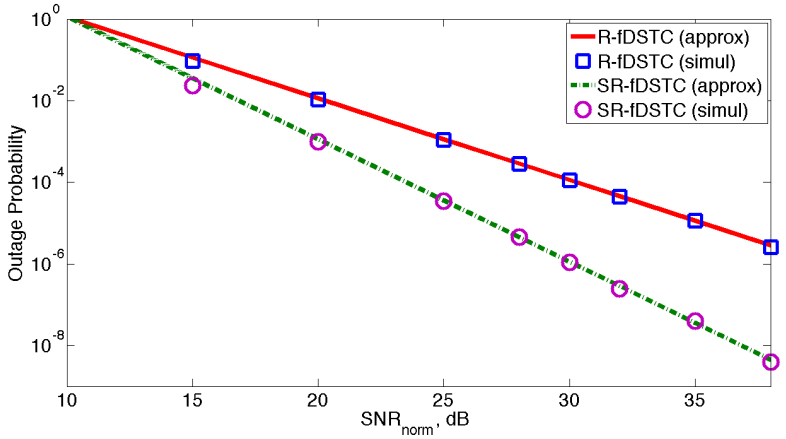

FIGURE 4.14: Outage probability versus SNR_{norm}, small, fixed R regime ($R = 1$), for statistically symmetric networks, i.e. $\sigma_{ij}^2 = 1$

latency. Although, the time slots used for the protocols are taken into account in the outage probability analysis, the thorough effect of the transmission protocol on latency are not still figured out. In addition, recently an interesting issue of energy-latency tradeoff for opportunistic relay and cooperative MIMO in multi-hop networks is considered in [103, 117–119]. They give significant guide for consideration of the energy-latency tradeoffs of the fDSTC protocol in future works.

Multiple-relay systems

Although, the fDSTC protocol is shown to outperform the cDSTC in not only single-antenna systems but also multi-antenna systems, the extension of the fDSTC protocol in systems with multiple relays (e.g. the number of relays is greater than 3) seems to be impossible due to the complicated transmission protocol. However, with the multiple-relay systems, the fDSTC protocol can be combined with repetition-based cooperative relay protocols, called hybrid cooperative relay protocol, to improve the system performances. The transmission protocol of the hybrid cooperative relay protocol for a 3-relay systems is shown in Fig. 4.15. In the first phase, source simultaneously transmits signal to relays and destination. The first relay will forward the received signal to the destination and the other relays in the second phase. Finally, the remaining two-relays will forward their signals to the destination using DSTC protocol.

The hybrid cooperative relay protocol can be deployed in the multiple-relay systems without difficulty. However, it still rests many problems needing to study such as how

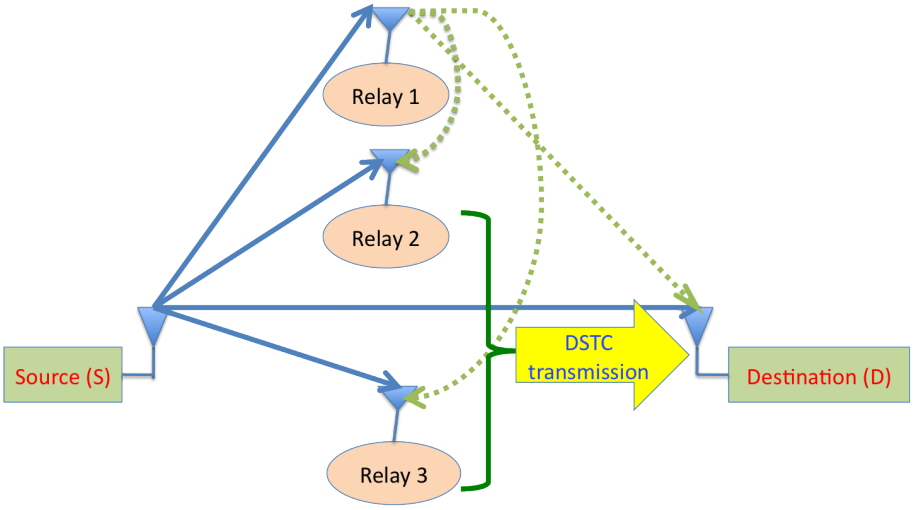

FIGURE 4.15: Hybrid cooperative relay protocol

to decide the number of relays consecutively forwarding signal and the number of relays simultaneously, how to select the relays, etc... That reserves for future works.

Cooperative MAC

Concerning the cooperative MAC protocols, this thesis proposed two MAC protocols for low-power cooperative wireless networks with or without association with relay selection technique (i.e. RIC-MAC and adaptive RIC-MAC). However, the thorough effect of the number of potential relays is not considered. In addition, there is a lack of a comparison between the proposed cooperative MAC protocols with the existing cooperative MAC protocols in the literature. Moreover, energy-efficiency considerations on a real MAC simulator (e.g. ns2, Omnet++, Opnet++, WSIM, etc.) also need to be carefully studied. On the other hand, the other advanced techniques such as power allocation and two-way relays should be associated with the cooperative MAC protocol to further improve the system performance. For example, it is firstly observed that MAC protocols belonging to RICER family seems to be a suitable candidate for two-way relays where two sources simultaneously communicate with one relay. Finally, RIC-MAC and adaptive RIC-MAC are designed only for repetition-based cooperative relay system with only one relay node. Cooperative MAC protocol with the extension of multiple relay nodes should be considered in case of DSTC-based or repetition-based cooperative relay systems.

Appendix A

Bounds on ASEP of the NR-fDSTC protocol

Proof of (2.14)

To obtain the lower bound ASEP using MGF-based approach, we need to find the MGF of $\Gamma(v,t) = \frac{vt}{v+t+1}$, where v and t are two independent random variables with the probability density function (PDF)

$$f_v(v) = \frac{1}{v_0^2} v e^{-\frac{v}{v_0}} \tag{A-1}$$

$$f_t(t) = \frac{1}{t_0} e^{-\frac{t}{t_0}} \tag{A-2}$$

The cumulative distribution function (CDF) of $\Gamma(v,t)$ is found for $\gamma > 0$ based on [53]

$$\begin{aligned} F_\Gamma(\gamma) = 1 &- \frac{2\sqrt{\gamma^2+\gamma}}{\sqrt{p}}\Big(1+\frac{\gamma}{t_0}\Big)e^{-\frac{\sigma}{p}\gamma}K_1\Big(\frac{2}{\sqrt{p}}\sqrt{\gamma^2+\gamma}\Big) \\ &- \frac{2}{p}(\gamma^2+\gamma)e^{-\frac{\sigma}{p}\gamma}K_0\Big(\frac{2}{\sqrt{p}}\sqrt{\gamma^2+\gamma}\Big) \end{aligned} \tag{A-3}$$

where $\sigma = t_0 + v_0$, $p = t_0 v_0$, and $K_l(.)$ denotes the modified Bessel function of the second kind with order l.

The PDF of $\Gamma(v,t)$ is found by taking the derivative of $F_\Gamma(\gamma)$ with respect to γ and using [18, Eq. 9.6.26]

$$\begin{aligned} f_\Gamma(\gamma) =& \frac{2}{p\sqrt{p}}\Big(-(\frac{p}{t_0}-\sigma-1)+(\frac{\sigma}{t_0}+2)\gamma\Big)e^{-\frac{\sigma}{p}\gamma}K_1\Big(\frac{2}{\sqrt{p}}\sqrt{\gamma^2+\gamma}\Big) \\ &+\frac{2}{p^2}\Big((\frac{2p}{t_0}+\sigma)\gamma^2+(\frac{p}{t_0}+\sigma)\gamma\Big)e^{-\frac{\sigma}{p}\gamma}K_0\Big(\frac{2}{\sqrt{p}}\sqrt{\gamma^2+\gamma}\Big) \end{aligned} \tag{A-4}$$

The moment generating function (MGF) is derived by using its definition and using the change of variable $\gamma \to \gamma_1 - 1/2$

$$\begin{aligned} M_\Gamma(s) =& e^{\alpha/2}\Big[\frac{2}{p\sqrt{p}}\Big((\frac{p}{t_0}-\sigma+\frac{\sigma}{2t_0})\frac{\delta J_0}{\delta\beta}+(\frac{\sigma}{t_0}+2)\frac{\delta^2 J_0}{\delta\alpha\delta\beta}\Big) \\ &+\frac{2}{p^2}\Big((\frac{2p}{t_0}+\sigma)\frac{\delta^2 J_0}{\delta\alpha^2}+\frac{p}{t_0}\frac{\delta J_0}{\delta\alpha}-\frac{\sigma}{4}J_0\Big)\Big] \end{aligned} \tag{A-5}$$

where $\alpha = (\sigma - ps)/p$, $\beta = 2/\sqrt{p}$ and

$$\begin{aligned} J_0 &= \int_{1/2}^{\infty} e^{-\alpha\gamma_1}K_0\big(\beta\sqrt{\gamma_1^2-(1/2)^2}\big) \\ &= \frac{1}{2c}\Big[e^{-\frac{c}{2}}E_1\Big(\frac{\alpha-c}{2}\Big)-e^{\frac{c}{2}}E_1\Big(\frac{\alpha+c}{2}\Big)\Big] \end{aligned} \tag{A-6}$$

with $c = \sqrt{\alpha^2-\beta^2}$, $Re\{s\} < \sigma/p + 2/\sqrt{(}p)$ and $E_1(.)$ the exponential integral function defined as [18, Eq. 5.1.1]. Note that J_0 is derived by using the integrand in [120, Eq. 646].

Taking the derivative of J_0 with respect to α or/and β with the respective order, we can get

$$\begin{aligned} \frac{\delta J_0}{\delta\alpha} =& -\frac{\alpha}{4c^3}(2+c)e^{-\frac{c}{2}}E_1\Big(\frac{\alpha-c}{2}\Big)+\frac{e^{\frac{-\alpha}{2}}}{c^2} \\ &+\frac{\alpha}{4c^3}(2-c)e^{\frac{c}{2}}E_1\Big(\frac{\alpha+c}{2}\Big) \end{aligned} \tag{A-7}$$

$$\begin{aligned} \frac{\delta J_0}{\delta\beta} =& \frac{\beta}{4c^3}(2+c)e^{-\frac{c}{2}}E_1\Big(\frac{\alpha-c}{2}\Big)-\frac{\alpha}{\beta c^2}e^{\frac{-\alpha}{2}} \\ &-\frac{\beta}{4c^3}(2-c)e^{\frac{c}{2}}E_1\Big(\frac{\alpha+c}{2}\Big) \end{aligned} \tag{A-8}$$

$$\begin{aligned} \frac{\delta^2 J_0}{\delta\alpha^2} =& \frac{\alpha^2}{c^5}(1+\frac{c}{2}+\frac{\beta^2}{2\alpha^2}+\frac{\beta^2 c}{4\alpha^2}+\frac{c^2}{8})e^{-\frac{c}{2}}E_1\Big(\frac{\alpha-c}{2}\Big) \\ &+\frac{\alpha^2}{c^5}(-1+\frac{c}{2}-\frac{\beta^2}{2\alpha^2}+\frac{\beta^2 c}{4\alpha^2}-\frac{c^2}{8})e^{\frac{c}{2}}E_1\Big(\frac{\alpha+c}{2}\Big) \\ &+\frac{1}{c^4}(-\frac{c^2}{2}-3\alpha)e^{\frac{-\alpha}{2}} \end{aligned} \tag{A-9}$$

$$\begin{aligned}\frac{\delta^2 J_0}{\delta\alpha\delta\beta} =& \frac{1}{c^5}(-\frac{3}{2}\alpha\beta - \frac{3}{4}\alpha\beta c - \frac{1}{8}\alpha\beta c^2)e^{-\frac{c}{2}}E_1\Big(\frac{\alpha - c}{2}\Big) \\ &+ \frac{1}{c^5}(\frac{3}{2}\alpha\beta - \frac{3}{4}\alpha\beta c + \frac{1}{8}\alpha\beta c^2)e^{\frac{c}{2}}E_1\Big(\frac{\alpha + c}{2}\Big) \\ &+ \frac{1}{c^4}(\frac{\alpha^2}{\beta} + \frac{\alpha c^2}{2\beta} + 2\beta)e^{\frac{-\alpha}{2}}\end{aligned} \tag{A-10}$$

Appendix B

Closed-form of ASEP of the NR-fDSTC protocol

Proof of (2.20)

To approximate the closed-form ASEP of the NR-fDSTC protocol, we need to find the MGF of $\Gamma(v,t) = \frac{vt}{v+t+1}$, where v and t are two independent random variables with respective probability density functions (pdf) $f_v(v) = \frac{1}{v_0^2} v e^{-\frac{v}{v_0}}$, and $f_t(t) = \frac{1}{t_0^2} t e^{-\frac{t}{t_0}}$.

The cumulative distribution function (cdf) of $\Gamma(v,t)$ is found for $\gamma > 0$ based on [53]

$$\begin{aligned} F_\Gamma(\gamma) = 1 - 2\sqrt{\frac{\gamma^2+\gamma}{p}}\Big(1 + \frac{\gamma\sigma}{p} + \frac{2\gamma^2+\gamma}{p}\Big)e^{-\frac{\sigma}{p}\gamma} K_1\Big(\frac{2}{\sqrt{p}}\sqrt{\gamma^2+\gamma}\Big) \\ - 2\frac{\gamma^2+\gamma}{p}\Big(1+\frac{\gamma\sigma}{p}\Big)e^{-\frac{\sigma}{p}\gamma} K_0\Big(\frac{2}{\sqrt{p}}\sqrt{\gamma^2+\gamma}\Big), \end{aligned} \tag{B-1}$$

with $\sigma = t_0 + v_0$, $p = t_0 v_0$, and $K_l(.)$ the modified Bessel function of the second kind with order l.

The pdf of $\Gamma(v,t)$ is found by taking the derivative of $F_\Gamma(\gamma)$ and using [18, Eq. 9.6.26]

$$\begin{aligned} f_\Gamma(\gamma) = &\frac{2}{p^2\sqrt{p}}\gamma\sqrt{\gamma^2+\gamma}\Big(4\sigma\gamma + \sigma^2 + 2\sigma - 2p\Big)e^{-\frac{\sigma}{p}\gamma} K_1\Big(\frac{2}{\sqrt{p}}\sqrt{\gamma^2+\gamma}\Big) \\ &+ \frac{2}{p^2}\gamma\Big((\frac{\sigma^2}{p}+4)\gamma^2 + (\frac{\sigma^2}{p}+4)\gamma + 1\Big)e^{-\frac{\sigma}{p}\gamma} K_0\Big(\frac{2}{\sqrt{p}}\sqrt{\gamma^2+\gamma}\Big). \end{aligned} \tag{B-2}$$

The MGF is then derived by using its definition and using the change of variable $\gamma \to \gamma_1 - 1/2$

$$\begin{aligned} M_\Gamma(s) =& e^{\alpha/2}\Big[\frac{2}{p\sqrt{p}}\Big(-(1-\frac{\sigma^2}{p})\frac{\delta J_0}{\delta\beta} + (\frac{\sigma^2}{p} - \frac{2\sigma}{p} - 2)\frac{\delta^2 J_0}{\delta\alpha\delta\beta} - \frac{4\sigma}{p}\frac{\delta^3 J_0}{\delta\beta\delta\alpha^2}\Big) \\ &+ \frac{2}{p^2}\Big(-(\frac{\sigma^2}{p}+4)\frac{\delta^3 J_0}{\delta\alpha^3} - \frac{1}{2}(\frac{\sigma^2}{p}+4)\frac{\delta^2 J_0}{\delta\alpha^2} + \frac{\sigma^2}{p}\frac{\delta J_0}{\delta\alpha} - \frac{\sigma^2}{8p}J_0\Big)\Big], \end{aligned} \tag{B-3}$$

where $\alpha = (\sigma - ps)/p$, $\beta = 2/\sqrt{p}$ and

$$J_0 = \int_{1/2}^{\infty} e^{-\alpha\gamma_1} K_0\big(\beta\sqrt{\gamma_1^2 - (1/2)^2}\big) = \frac{1}{2c}\Big[e^{-\frac{c}{2}}E_1\Big(\frac{\alpha - c}{2}\Big) - e^{\frac{c}{2}}E_1\Big(\frac{\alpha + c}{2}\Big)\Big] \tag{B-4}$$

with $c = \sqrt{\alpha^2 - \beta^2}$, $Re\{s\} < \sigma/p + 2/\sqrt{(}p)$ and $E_1(.)$ the exponential integral function defined as [18, Eq. 5.1.1]. Note that J_0 is derived by using the integrand in [120, Eq. 646].

The first and second order derivatives of J_0 with respect to α or/and β, $\frac{\delta J_0}{\delta\beta}$, $\frac{\delta^2 J_0}{\delta\alpha\delta\beta}$, $\frac{\delta^2 J_0}{\delta\alpha^2}$ and $\frac{\delta J_0}{\delta\alpha}$ can be found in Appendix A. The third order derivatives of J_0, $\frac{\delta^3 J_0}{\delta\beta\delta\alpha^2}$ and $\frac{\delta^3 J_0}{\delta\alpha^3}$ can be directly derived

$$\begin{aligned} \frac{\delta^3 J_0}{\delta\alpha^3} =& \frac{\alpha}{c^7}(-3\alpha^2 - \frac{3}{2}\alpha^2 c - \frac{9}{2}\beta^2 - \frac{9}{4}\beta^2 c - \frac{3}{8}\alpha^4 + \frac{3}{8}\beta^4 - \frac{1}{16}\alpha^2 c^3)e^{-\frac{c}{2}}E_1\Big(\frac{\alpha - c}{2}\Big) \\ &+ \frac{\alpha}{c^7}(3\alpha^2 - \frac{3}{2}\alpha^2 c + \frac{9}{2}\beta^2 - \frac{9}{4}\beta^2 c + \frac{3}{8}\alpha^4 - \frac{3}{8}\beta^4 - \frac{1}{16}\alpha^2 c^3)e^{\frac{c}{2}}E_1\Big(\frac{\alpha + c}{2}\Big) \\ &+ \frac{1}{c^6}(\frac{5}{2}\alpha^3 + 11\alpha^2 + 4\beta^2 + \frac{1}{2}\alpha^4 - \frac{3}{2}\alpha^2\beta^2 - \frac{5}{2}\alpha\beta^2 + \frac{1}{4}\beta^4)e^{\frac{-\alpha}{2}} \end{aligned} \tag{B-5}$$

$$\begin{aligned} \frac{\delta^3 J_0}{\delta\beta\delta\alpha^2} =& \frac{1}{c^7}(6\beta\alpha^2 + 3\alpha^2\beta c + \frac{5}{8}\alpha^4\beta - \frac{1}{2}\alpha^2\beta^3 + \frac{3}{2}\beta^3 - \frac{1}{8}\beta^5 + \frac{3}{4}\beta^3 c + \frac{1}{16}\alpha^2\beta c^3)e^{-\frac{c}{2}}E_1\Big(\frac{\alpha - c}{2}\Big) \\ &+ \frac{1}{c^7}(-6\beta\alpha^2 + 3\alpha^2\beta c - \frac{5}{8}\alpha^4\beta + \frac{1}{2}\alpha^2\beta^3 - \frac{3}{2}\beta^3 + \frac{1}{8}\beta^5 + \frac{3}{4}\beta^3 c + \frac{1}{16}\alpha^2\beta c^3)e^{\frac{c}{2}}E_1\Big(\frac{\alpha + c}{2}\Big) \\ &+ \frac{1}{c^6}(-13\alpha\beta + \frac{1}{4}\alpha^3\beta - \frac{2\alpha^3}{\beta} - \frac{\alpha^4}{\beta} - \frac{9}{2}\alpha^2\beta + \frac{3}{2}\beta^3 - \frac{\alpha^5}{4\beta})e^{\frac{-\alpha}{2}} \end{aligned} \tag{B-6}$$

Appendix C

Closed-form error probability of the R-fDSTC protocol

Proof of (2.25)

In this appendix, the closed-form error probability of the R-fDSTC protocol is derived based on the decoding of the combined signals at destination $y_d[2k]$. Let $w_{2k} = Re\{y_d[2k]\}$, so

$$\begin{aligned} w_{2k} &= \gamma_{sd}x[2k] + \gamma_{r_1d}\hat{x}_{r_1}[2k] + \gamma_{r_2d}\hat{x}_{r_2}[2k] \\ &- \frac{\sqrt{\epsilon_{r_1}\epsilon_{r_2}}Re\{h^*_{r_1d}h_{r_2d}\}}{N_{r_2d}}\hat{x}_{r_1}[2k+1] + \frac{\sqrt{\epsilon_{r_1}\epsilon_{r_2}}Re\{h^*_{r_1d}h_{r_2d}\}}{N_{r_1d}}\hat{x}_{r_2}[2k+1] + z'_{y_d}[2k], \end{aligned} \tag{C-1}$$

where $z'_{y_d}[2k] = Re\{z_{y_d}[2k]\}$.

Let the following events be defined

$$\mathcal{E}_{1,1} \equiv \{x[2k] = 1, x[2k+1] = 1\}; \quad \mathcal{E}_{1,-1} \equiv \{x[2k] = 1, x[2k+1] = -1\}$$

$$\mathcal{E}_{-1,1} \equiv \{x[2k] = -1, x[2k+1] = 1\}; \quad \mathcal{E}_{-1,-1} \equiv \{x[2k] = -1, x[2k+1] = -1\}$$

$$\mathcal{H}_1 \equiv \{\hat{x}_{r_1}[2k] = x[2k], \hat{x}_{r_2}[2k] = x[2k]; \hat{x}_{r_1}[2k+1] = \hat{x}_{r_2}[2k+1]\}$$

$$\mathcal{H}_2 \equiv \{\hat{x}_{r_1}[2k] = x[2k], \hat{x}_{r_2}[2k] = -x[2k]; \hat{x}_{r_1}[2k+1] = \hat{x}_{r_2}[2k+1]\}$$

$$\mathcal{H}_3 \equiv \{\hat{x}_{r_1}[2k] = -x[2k], \hat{x}_{r_2}[2k] = x[2k]; \hat{x}_{r_1}[2k+1] = \hat{x}_{r_2}[2k+1]\}$$

$$\mathcal{H}_4 \equiv \{\hat{x}_{r_1}[2k] = -x[2k], \hat{x}_{r_2}[2k] = -x[2k]; \hat{x}_{r_1}[2k+1] = \hat{x}_{r_2}[2k+1]\}$$

$$\mathcal{H}_5 \equiv \{\hat{x}_{r_1}[2k] = x[2k], \hat{x}_{r_2}[2k] = x[2k]; \hat{x}_{r_1}[2k+1] = -\hat{x}_{r_2}[2k+1]\}$$

$$\mathcal{H}_6 \equiv \{\hat{x}_{r_1}[2k] = x[2k], \hat{x}_{r_2}[2k] = -x[2k]; \hat{x}_{r_1}[2k+1] = -\hat{x}_{r_2}[2k+1]\}$$

$$\mathcal{H}_7 \equiv \{\hat{x}_{r_1}[2k] = -x[2k], \hat{x}_{r_2}[2k] = x[2k]; \hat{x}_{r_1}[2k+1] = -\hat{x}_{r_2}[2k+1]\}$$

$$\mathcal{H}_8 \equiv \{\hat{x}_{r_1}[2k] = -x[2k], \hat{x}_{r_2}[2k] = -x[2k]; \hat{x}_{r_1}[2k+1] = -\hat{x}_{r_2}[2k+1]\}$$

The error probability, conditioned to the channel, is given by

$$P_{2k} = \frac{1}{4}\sum_{m=1}^{8} \mathcal{P}(\mathcal{H}_m) \times \Big[\mathcal{P}\{w_{2k} > 0/\mathcal{E}_{-1,1}, \mathcal{H}_m\} + \mathcal{P}\{w_{2k} > 0/\mathcal{E}_{-1,-1}, \mathcal{H}_m\} \\ \mathcal{P}\{w_{2k} < 0/\mathcal{E}_{1,1}, \mathcal{H}_m\} + \mathcal{P}\{w_{2k} < 0/\mathcal{E}_{1,-1}, \mathcal{H}_m\}\Big], \tag{C-2}$$

where the probability of the event $\mathcal{H}_m$ depends on the error probabilities at relays p^j_{2k} and p^j_{2k+1} $(j \in \{r_1, r_2\})$ (2.26)

$$\mathcal{P}(\mathcal{H}_m) = \begin{cases} (1-p^{r_1}_{2k})(1-p^{r_2}_{2k})\Big[(1-p^{r_1}_{2k+1})(1-p^{r_2}_{2k+1}) + p^{r_1}_{2k+1}p^{r_2}_{2k+1}\Big], & \text{m=1} \\ (1-p^{r_1}_{2k})p^{r_2}_{2k}\Big[(1-p^{r_1}_{2k+1})(1-p^{r_2}_{2k+1}) + p^{r_1}_{2k+1}p^{r_2}_{2k+1}\Big], & \text{m=2} \\ p^{r_1}_{2k}(1-p^{r_2}_{2k})\Big[(1-p^{r_1}_{2k+1})(1-p^{r_2}_{2k+1}) + p^{r_1}_{2k+1}p^{r_2}_{2k+1}\Big], & \text{m=3} \\ p^{r_1}_{2k}p^{r_2}_{2k}\Big[(1-p^{r_1}_{2k+1})(1-p^{r_2}_{2k+1}) + p^{r_1}_{2k+1}p^{r_2}_{2k+1}\Big], & \text{m=4} \\ (1-p^{r_1}_{2k})(1-p^{r_2}_{2k})\Big[p^{r_1}_{2k+1}(1-p^{r_2}_{2k+1}) + (1-p^{r_1}_{2k+1})p^{r_2}_{2k+1}\Big], & \text{m=5} \\ (1-p^{r_1}_{2k})p^{r_2}_{2k}\Big[p^{r_1}_{2k+1}(1-p^{r_2}_{2k+1}) + (1-p^{r_1}_{2k+1})p^{r_2}_{2k+1}\Big], & \text{m=6} \\ p^{r_1}_{2k}(1-p^{r_2}_{2k})\Big[p^{r_1}_{2k+1}(1-p^{r_2}_{2k+1}) + (1-p^{r_1}_{2k+1})p^{r_2}_{2k+1}\Big], & \text{m=7} \\ p^{r_1}_{2k}p^{r_2}_{2k}\Big[p^{r_1}_{2k+1}(1-p^{r_2}_{2k+1}) + (1-p^{r_1}_{2k+1})p^{r_2}_{2k+1}\Big], & \text{m=8} \end{cases} \tag{C-3}$$

and

$$\mathcal{P}\{w_{2k} < 0/\mathcal{E}_{1,1}, \mathcal{H}_1\} = \mathcal{P}\Big\{\gamma_{r_1 d} + \gamma_{r_2 d} + \gamma_{sd} + z'_{y_d}(2k) < 0\Big\} \\ = \frac{1}{2}\operatorname{erfc}(\sqrt{\gamma_{r_1 d} + \gamma_{r_2 d} + \gamma_{sd}}) = \frac{1}{2}\operatorname{erfc}(\beta_{2k}).$$

Using the same approach, we can derive the other terms in (C-2)

$$\mathcal{P}\{w_{2k} < 0/\mathcal{E}_{1,-1}, \mathcal{H}_1\} = \frac{1}{2}\operatorname{erfc}(\beta_{2k});$$

$$\mathcal{P}\{w_{2k} < 0/\mathcal{E}_{1,1}, \mathcal{H}_2\} = \frac{1}{2}\operatorname{erfc}(\delta_{2k}); \quad \mathcal{P}\{w_{2k} < 0/\mathcal{E}_{1,-1}, \mathcal{H}_2\} = \frac{1}{2}\operatorname{erfc}(\delta_{2k});$$

$$\mathcal{P}\{w_{2k} < 0/\mathcal{E}_{1,1}, \mathcal{H}_3\} = \frac{1}{2}\operatorname{erfc}(\lambda_{2k}); \quad \mathcal{P}\{w_{2k} < 0/\mathcal{E}_{1,-1}, \mathcal{H}_3\} = \frac{1}{2}\operatorname{erfc}(\lambda_{2k});$$

$$\mathcal{P}\{w_{2k} < 0/\mathcal{E}_{1,1}, \mathcal{H}_4\} = \frac{1}{2}\operatorname{erfc}(\phi_{2k}); \quad \mathcal{P}\{w_{2k} < 0/\mathcal{E}_{1,-1}, \mathcal{H}_4\} = \frac{1}{2}\operatorname{erfc}(\phi_{2k});$$

$$\mathcal{P}\{w_{2k} < 0/\mathcal{E}_{1,1}, \mathcal{H}_5\} = \frac{1}{2}\operatorname{erfc}(\beta_{2k} + \theta_{2k}); \quad \mathcal{P}\{w_{2k} < 0/\mathcal{E}_{1,-1}, \mathcal{H}_5\} = \frac{1}{2}\operatorname{erfc}(\beta_{2k} - \theta_{2k});$$

$$\mathcal{P}\{w_{2k} < 0/\mathcal{E}_{1,1}, \mathcal{H}_6\} = \frac{1}{2}\operatorname{erfc}(\delta_{2k} + \theta_{2k}); \quad \mathcal{P}\{w_{2k} < 0/\mathcal{E}_{1,-1}, \mathcal{H}_6\} = \frac{1}{2}\operatorname{erfc}(\delta_{2k} - \theta_{2k});$$

$$\mathcal{P}\{w_{2k} < 0/\mathcal{E}_{1,1}, \mathcal{H}_7\} = \frac{1}{2}\operatorname{erfc}(\lambda_{2k} + \theta_{2k}); \quad \mathcal{P}\{w_{2k} < 0/\mathcal{E}_{1,-1}, \mathcal{H}_7\} = \frac{1}{2}\operatorname{erfc}(\lambda_{2k} - \theta_{2k});$$

$$\mathcal{P}\{w_{2k} < 0/\mathcal{E}_{1,1}, \mathcal{H}_8\} = \frac{1}{2}\operatorname{erfc}(\phi_{2k} + \theta_{2k}); \quad \mathcal{P}\{w_{2k} < 0/\mathcal{E}_{1,-1}, \mathcal{H}_8\} = \frac{1}{2}\operatorname{erfc}(\phi_{2k} - \theta_{2k}),$$

where β_{2k}, δ_{2k}, λ_{2k}, ϕ_{2k} and θ_{2k} are given in (21). Note that we have $\mathcal{P}\{w_{2k} < 0/\mathcal{E}_{1,-1}, \mathcal{H}_m\} = \mathcal{P}\{w_{2k} > 0/\mathcal{E}_{-1,-1}, \mathcal{H}_m\}$ and $\mathcal{P}\{w_{2k} < 0/\mathcal{E}_{1,1}, \mathcal{H}_m\} = \mathcal{P}\{w_{2k} > 0/\mathcal{E}_{-1,1}, \mathcal{H}_m\}$. That leads to all terms in (C-2) which therefore give rise to (2.25).

Appendix D

Outage probability of MSCR

Proof of (3.25)

It is not difficult to show that the density function of a random variable which is the sum of two independent exponential random variables can be derived as follow

$$p_w(w) = \lambda^2 w e^{-\lambda w} \tag{D-1}$$

where $w = x + y$ and $p_x(x) = \lambda e^{-\lambda x}$, $p_y(y) = \lambda e^{-\lambda y}$.

Proof:

$$\begin{aligned} p_w(w) &= \int_0^w \lambda e^{-\lambda x} \lambda e^{-\lambda(w-x)} dx \\ &= \lambda^2 e^{-\lambda w} \int_0^w e^{-(\lambda-\lambda)x} dx \\ &= \lambda^2 e^{-\lambda w} x \Big|_0^w \\ &= \lambda^2 w e^{-\lambda w} \quad \blacksquare \end{aligned} \tag{D-2}$$

By calculating the cumulative density function of $Pr(w < h(\delta))$, we can illustrate that

$$Pr[w < h(\delta)] \sim \frac{\lambda^2}{2} h^2(\delta) \tag{D-3}$$

Proof:

$$\begin{aligned} Pr[w < h(\delta)] &= \int_0^{h(\delta)} \lambda^2 w e^{-\lambda w} dw \\ &= 1 - e^{-\lambda h(\delta)} - \lambda h(\delta) e^{-\lambda h(\delta)} \\ &= 1 - \big(1 - \lambda h(\delta) + \frac{1}{2}\lambda^2 h^2(\delta) + o(h^3(\delta))\big) \\ &\quad - \lambda h(\delta)\big(1 - \lambda h(\delta) + \frac{1}{2}\lambda^2 h^2(\delta) + o(h^3(\delta))\big) \\ &= \frac{\lambda^2}{2} h^2(\delta) + o(h^3(\delta)) \quad \blacksquare \end{aligned} \tag{D-4}$$

Moreover, we can derive

$$Pr[\delta f(\frac{u}{\delta}, \frac{v}{\delta}) < h(\delta)] \sim \frac{\lambda_u^2 + \lambda_v^2}{2} h^2(\delta) \tag{D-5}$$

where u and v are two independent random variable with the respective density functions $p_u(u) = \lambda_u^2 u e^{-\lambda_u u}$ and $p_v(v) = \lambda_v^2 v e^{-\lambda_v v}$ with $\lambda_u \neq \lambda_v$

Proof :

$$\begin{aligned} &Pr[\delta f(\frac{u}{\delta}, \frac{v}{\delta}) < h(\delta)] = Pr[\frac{1}{u} + \frac{1}{v} + \frac{\delta}{uv} \geqslant \frac{1}{h(\delta)}] \\ &\geqslant Pr[\frac{1}{u} + \frac{1}{v} \geqslant \frac{1}{h(\delta)}] \geqslant Pr[\max(\frac{1}{u}, \frac{1}{v}) \geqslant \frac{1}{h(\delta)}] \\ &= 1 - \Big(1 - Pr[u < h(\delta)]\Big)\Big(1 - Pr[v < h(\delta)]\Big) \\ &= 1 - \Big(1 - \frac{\lambda_u^2}{2} h^2(\delta) + o(h^3(\delta))\Big)\Big(1 - \frac{\lambda_v^2}{2} h^2(\delta) + o(h^3(\delta))\Big) \\ &= \frac{\lambda_u^2 + \lambda_v^2}{2} h^2(\delta) + o(h^3(\delta)) \end{aligned} \tag{D-6}$$

Therefore, we illustrated

$$\lim_{h(\delta)\to 0} inf \frac{1}{h(\delta)^2} Pr[\delta f(\frac{u}{\delta}, \frac{v}{\delta}) < h(\delta)] \geqslant \frac{\lambda_u^2 + \lambda_v^2}{2} \tag{D-7}$$

To prove the other direction, let $l > 1$ be a fixed constant

$$\begin{aligned} &Pr[\delta f(\frac{u}{\delta}, \frac{v}{\delta}) < h(\delta)] = Pr[\frac{1}{u} + \frac{1}{v} + \frac{\delta}{uv} \geqslant \frac{1}{h(\delta)}] \\ &= \int_0^{lh(\delta)} Pr\Big[\frac{1}{u} > \frac{\frac{1}{h(\delta)} - \frac{1}{v}}{1 + \frac{\delta}{v}}\Big] p_v(v)dv \\ &\quad + \int_{lh(\delta)}^{\infty} Pr\Big[\frac{1}{u} > \frac{\frac{1}{h(\delta)} - \frac{1}{v}}{1 + \frac{\delta}{v}}\Big] p_v(v)dv \\ &\leqslant \int_0^{lh(\delta)} p_v(v)dv + \int_{lh(\delta)}^{\infty} Pr\Big[\frac{1}{u} > \frac{\frac{1}{h(\delta)} - \frac{1}{v}}{1 + \frac{\delta}{v}}\Big] p_v(v)dv \\ &= A + B \end{aligned} \tag{D-8}$$

But

$$A \leqslant \int_0^{lh(\delta)} \lambda_v^2 v dv = \frac{\lambda_v^2}{2} l^2 h^2(\delta) \tag{D-9}$$

To bound the second term of (D-8), let $k > l$ be another fixed constant, and note that

$$\begin{aligned} B &= \int_{kh(\delta)}^{\infty} Pr\Big[\frac{1}{u} > \frac{\frac{1}{h(\delta)} - \frac{1}{v}}{1 + \frac{\delta}{v}}\Big] p_v(v)dv \\ &\quad + \int_{lh(\delta)}^{kh(\delta)} Pr\Big[\frac{1}{u} > \frac{\frac{1}{h(\delta)} - \frac{1}{v}}{1 + \frac{\delta}{v}}\Big] p_v(v)dv \\ &\leqslant Pr\Big[\frac{1}{u} > \frac{1 - \frac{1}{k}}{h(\delta) + \frac{\delta}{k}}\Big] \int_{kh(\delta)}^{\infty} p_v(v)dv \\ &\quad + \lambda_v^2 \int_{lh(\delta)}^{kh(\delta)} Pr\Big[\frac{1}{u} > \frac{\frac{1}{h(\delta)} - \frac{1}{v}}{1 + \frac{\delta}{v}}\Big] v dv \\ &\leqslant Pr\Big[\frac{1}{u} > \frac{1 - \frac{1}{k}}{h(\delta) + \frac{\delta}{k}}\Big] + \lambda_v^2 \int_{lh(\delta)}^{kh(\delta)} Pr\Big[\frac{1}{u} > \frac{\frac{1}{h(\delta)} - \frac{1}{v}}{1 + \frac{\delta}{v}}\Big] v dv \end{aligned} \tag{D-10}$$

where the first term comes from the fact that $Pr\Big[\frac{1}{u} > \frac{\frac{1}{h(\delta)} - \frac{1}{v}}{1 + \frac{\delta}{v}}\Big]$ is non increasing in v and $\int_{kh(\delta)}^{\infty} p_v(v)dv \leqslant 1$. And since $e^{-\lambda_v v} \leqslant 1 \quad (v \geqslant 0)$, the second term is derived.

Now, based on the result of (D-9), the first term of (D-10) satisfies

$$\begin{aligned} Pr\Big[\frac{1}{u} > \frac{1 - \frac{1}{k}}{h(\delta) + \frac{\delta}{k}}\Big] &= Pr\Big[u \leqslant \frac{h(\delta) + \frac{\delta}{k}}{1 - \frac{1}{k}}\Big] \\ \leqslant \frac{\lambda_u^2}{2}\Big(\frac{h(\delta) + \frac{\delta}{k}}{1 - \frac{1}{k}}\Big)^2 &= \frac{\lambda_u^2}{2} h^2(\delta)\Big(\frac{1 + \frac{\delta}{kh(\delta)}}{1 - \frac{1}{k}}\Big)^2 \end{aligned} \tag{D-11}$$

By a change of variable $z = \frac{v}{h(\delta)}$, the second term of (D-10) can be derived as follow

$$\begin{aligned}
&\lambda_v^2 \int_{lh(\delta)}^{kh(\delta)} Pr\Big[\frac{1}{u} > \frac{\frac{1}{h(\delta)} - \frac{1}{v}}{1+\frac{\delta}{v}}\Big] v dv \\
&= h^2(\delta)\lambda_v^2 \int_l^k Pr\Big[u \leqslant \frac{h(\delta)+\frac{\delta}{z}}{1-\frac{1}{z}}\Big] z dz \\
&\leqslant h^2(\delta)\lambda_v^2 \int_l^k \frac{\lambda_u^2}{2}\Big(\frac{h(\delta)+\frac{\delta}{z}}{1-\frac{1}{z}}\Big)^2 z dz \\
&= h^4(\delta)\lambda_v^2 \int_l^k \frac{\lambda_u^2}{2}\Big(\frac{1+\frac{\delta}{zh(\delta)}}{1-\frac{1}{z}}\Big)^2 z dz \\
&= h^4(\delta) C\big(\delta, h(\delta), l, k\big)
\end{aligned} \tag{D-12}$$

where $C\big(\delta, h(\delta), l, k\big)$ remains finite for any $k > l > 1$ as $\delta \to 0$

Combining (D-9), (D-11), and (D-12), we have

$$\begin{aligned}
&Pr[\delta f(\frac{u}{\delta}, \frac{v}{\delta}) < h(\delta)] \\
&\leqslant \frac{\lambda_v^2}{2} l^2 h^2(\delta) + \frac{\lambda_v^2}{2} h^2(\delta)\Big(\frac{1+\frac{\delta}{kh(\delta)}}{1-\frac{1}{k}}\Big)^2 + h^4(\delta) C\big(\delta, h(\delta), l, k\big)
\end{aligned} \tag{D-13}$$

So, we can conclude

$$\lim_{h(\delta)\to 0} sup \frac{1}{h(\delta)^2} Pr[\delta f(\frac{u}{\delta}, \frac{v}{\delta}) < h(\delta)] \leqslant \frac{\lambda_u^2}{2} + \frac{\lambda_v^2}{2} \tag{D-14}$$

By particularly choosing l arbitrarily close to 1 and k enough large. Note that, we assumme $h(\delta) \to 0$ and $\frac{\delta}{h(\delta)} \to constant$ as $\delta \to 0$ ■

To derive the outage probability of MSCR, the following expression must be proved

$$Pr[r + \delta f(\frac{u}{\delta}, \frac{v}{\delta}) < h(\delta)] \sim \frac{(\lambda_u^2 + \lambda_v^2)\lambda_r^2}{24} h^4(\delta) \tag{D-15}$$

with r random variable having the density function $p_r(r) = \lambda_r^2 r e^{-\lambda_r r}$

Proof : let $g = \delta f(\frac{u}{\delta}, \frac{v}{\delta})$ we have

$$\begin{aligned} & Pr[r + g < h(\delta)] \\ & = Pr[g < h(\delta) - r] \\ & = \int_0^{h(\delta)} Pr[g < h(\delta) - r] p_r(r) dr \\ & = h^2(\delta) \int_0^1 Pr[g < h(\delta)(1 - r^{'})] \lambda_r^2 r' e^{-\lambda_r h(\delta) r^{'}} dr^{'} \\ & = h^4(\delta) \int_0^1 (1 - r')^2 \frac{Pr[g < h(\delta)(1 - r^{'})]}{(h(\delta)(1 - r'))^2} \lambda_r^2 r' e^{-\lambda_r h(\delta) r^{'}} dr^{'} \end{aligned} \tag{D-16}$$

Using (D-7) we have

$$\begin{aligned} & \lim_{h(\delta) \to 0} inf \frac{1}{h(\delta)^4} Pr[r + g < h(\delta)] \\ & \geqslant \frac{\lambda_u^2 + \lambda_v^2}{2} \lambda_r^2 \int_0^1 (1 - r')^2 r' dr^{'} = \frac{\lambda_u^2 + \lambda_v^2}{2} \lambda_r^2 \frac{1}{12} \end{aligned} \tag{D-17}$$

Using (D-14) we can demonstrate

$$\lim_{h(\delta) \to 0} sup \frac{1}{h(\delta)^4} Pr[r + g < h(\delta)] \leqslant \frac{\lambda_u^2 + \lambda_v^2}{2} \lambda_r^2 \frac{1}{12} \tag{D-18}$$

So (D-15) is proved ■

Appendix E

Outage probability of MFCR

Proof of (3.28)

Let x and y two random variables respectively having the density functions $p_x(x) = \lambda^2 x e^{-\lambda x}$ and $p_y(y) = \lambda^2 y e^{-\lambda y}$. The densifty function of $w = x + y$ is the convolution of $p_x(x)$ and $p_y(y)$ and can be derived as

$$p_w(w) = \frac{1}{6}\lambda^4 w^3 e^{-\lambda w} \tag{E-1}$$

By calculating the cumulative density function of $Pr(w < h(\delta))$, we can illustrate that

$$Pr[w < h(\delta)] \sim \frac{\lambda^4}{4!} h^4(\delta) \tag{E-2}$$

Proof : We have

$$\begin{aligned} Pr[w < h(\delta)] &= \frac{1}{6}\lambda^4 \int_0^{h(\delta)} w^3 e^{-\lambda w} dw \\ &= -\frac{\lambda^3 w^3}{6} e^{-\lambda w}\Big|_0^{h(\delta)} - \frac{\lambda^2 w^2}{2} e^{-\lambda w}\Big|_0^{h(\delta)} - \lambda w e^{-\lambda w}\Big|_0^{h(\delta)} \\ &\quad - e^{-\lambda w}\Big|_0^{h(\delta)} \\ &= 1 - \Big(1 + \lambda h(\delta) + \frac{\lambda^2 h^2(\delta)}{2} + \frac{\lambda^3 h^3(\delta)}{6}\Big) e^{-\lambda h(\delta)} \end{aligned} \tag{E-3}$$

Using $e^{-\lambda h(\delta)} = 1 - \lambda h(\delta) + \frac{1}{2}\lambda^2 h^2(\delta) - \frac{1}{6}\lambda^3 h^3(\delta) + \frac{1}{24}\lambda^4 h^4(\delta) + o(h^5(\delta))$, we can derive (E-3) without difficulty. ■

However, we illustrate that

$$Pr[\delta f(\frac{w}{\delta}, \frac{v}{\delta}) < h(\delta)] \sim \frac{\lambda_v^2}{2} h^2(\delta) \quad (h(\delta) \to 0) \tag{E-4}$$

where v and w is random variables with the respective density functions

$$p_v(v) = \lambda_v^2 v e^{-\lambda v}$$

$$p_w(w) = \frac{1}{6}\lambda_w^4 w^3 e^{-\lambda_w w}$$

Proof : we have

$$\begin{aligned}
&Pr[\delta f(\frac{w}{\delta}, \frac{v}{\delta}) < h(\delta)] = Pr[\frac{1}{w} + \frac{1}{v} + \frac{\delta}{wv} \geqslant \frac{1}{h(\delta)}] \\
&\geqslant Pr[\frac{1}{w} + \frac{1}{v} \geqslant \frac{1}{h(\delta)}] \geqslant Pr[\max(\frac{1}{w}, \frac{1}{v}) \geqslant \frac{1}{h(\delta)}] \\
&= 1 - Pr[w \geqslant h(\delta)] Pr[v \geqslant h(\delta)] \\
&= 1 - \Big(1 - Pr[w < h(\delta)]\Big)\Big(1 - Pr[v < h(\delta)]\Big) \\
&= 1 - \Big(1 - \frac{\lambda_w^4}{4!} h^4(\delta) + o(h^5(\delta))\Big)\Big(1 - \frac{\lambda_v^2}{2} h^2(\delta) + o(h^3(\delta))\Big) \\
&= \frac{\lambda_v^2}{2} h^2(\delta) + o(h^3(\delta))
\end{aligned} \tag{E-5}$$

Therefore, it is proved that

$$\lim_{h(\delta)\to 0} inf \frac{1}{h(\delta)^2} Pr[\delta f(\frac{w}{\delta}, \frac{v}{\delta}) < h(\delta)] \geqslant \frac{\lambda_v^2}{2} \tag{E-6}$$

Similar to method using in Appendix D, the other direction of (E-6) can be proved. That means, we can derive

$$\lim_{h(\delta)\to 0} sup \frac{1}{h(\delta)^2} Pr[\delta f(\frac{w}{\delta}, \frac{v}{\delta}) < h(\delta)] \leqslant \frac{\lambda_v^2}{2} \tag{E-7}$$

So (E-4) is proved. ■

The above results can help us to determine the outage probability of MFCR which is given by

$$Pr[r + \delta f(\frac{w}{\delta}, \frac{v}{\delta}) < h(\delta)] \sim \frac{\lambda_v^2 \lambda_r^2}{4!} h^4(\delta) \quad (h(\delta) \to 0) \tag{E-8}$$

with r random variable having the density function $p_r(r) = \lambda_r^2 r e^{-\lambda r}$

Proof :

Using [Eq. D-17, Appendix D] and (E-6) we have

$$\begin{aligned} &\lim_{h(\delta)\to 0} inf \frac{1}{h(\delta)^4} Pr[r + g < h(\delta)] \\ &\geqslant \frac{\lambda_v^2}{2}\lambda_r^2 \int_0^1 (1-r')^2 r' dr' = \frac{\lambda_v^2}{2}\lambda_r^2 \frac{1}{12} \end{aligned} \tag{E-9}$$

Similarly, combining [Eq. D-18, Appendix D] and (E-7) we can illustrate

$$\lim_{h(\delta)\to 0} sup \frac{1}{h(\delta)^4} Pr[r + g < h(\delta)] \leqslant \frac{\lambda_v^2}{2}\lambda_r^2 \frac{1}{12} \tag{E-10}$$

So (E-8) is proved ■

Bibliography

[1] G. Moore, "Cramming more components onto integrated circuits," *IEEE Solid-State Circuits Newsletter*, vol. 11, no. 5, pp. 32–35, Apr. 1965.

[2] K. Lahiri, A. Raghunathan, S. Dey, and D. Panigrahi, "Battery-driven system design: a new frontier in low power design," in *Proceedings of International Conference on VLSI Design*, pp. 261–267, 2002.

[3] R. Mangharam, R. Rajkumar, S. Pollin, F. Catthoor, B. Bougard, L. Van der Perre, and I. Moeman, "Optimal fixed and scalable energy management for wireless networks," in *Proceedings of IEEE INFOCOM*, vol. 1, pp. 114–125, Mar. 2005.

[4] J. Huang and S. Signell, "On spectral efficiency of low-complexity adaptive MIMO systems in rayleigh fading channel," *IEEE Transactions on Wireless Communications*, vol. 8, no. 9, pp. 4369–4374, Sept. 2009.

[5] S. Alamouti, "A simple transmit diversity technique for wireless communications," *IEEE Journal on Selected Areas in Communications*, vol. 16, no. 8, pp. 1451–1458, Oct. 1998.

[6] A. Sendonaris, E. Erkip, and B. Aazhang, "User cooperation diversity: part I. system description," *IEEE Transactions on Communications*, vol. 51, no. 11, pp. 1927–1938, Nov. 2003.

[7] ——, "User cooperation diversity: part II. implementation aspects and performance analysis," *IEEE Transactions on Communications*, vol. 51, no. 11, pp. 1939–1948, Nov. 2003.

[8] J. N. Laneman and G. W. Wornell, "Distributed space-time-coded protocols for exploiting cooperative diversity in wireless networks," *IEEE Transactions on Information Theory*, vol. 49, no. 10, pp. 2415–2425, Oct. 2003.

[9] J. N. Laneman, G. W. Wornell, and D. N. C. Tse, "Cooperative diversity in wireless networks: Efficient protocols and outage behavior," *IEEE Transactions on Information Theory*, vol. 50, no. 12, pp. 3062–3080, Dec. 2004.

[10] T.-D. Nguyen, O. Berder, and O. Sentieys, "Cooperative MIMO schemes optimal selection for wireless sensor networks," in *Proceedings of IEEE 65th Vehicular Technology Conference (VTC)*, pp. 85–89, Apr. 2007.

[11] E.-Y. Lin, J. Rabaey, and A. Wolisz, "Power-efficient rendez-vous schemes for dense wireless sensor networks," in *Proceedings of IEEE International Conference on Communications (ICC)*, vol. 7, pp. 3769–3776, Jun. 2004.

[12] J. N. Laneman and G. W. Wornell, "Energy-efficient antenna sharing and relaying for wireless networks," in *Proceedings of IEEE Wireless Communications and Networking Conference (WCNC)*, vol. 1, pp. 7–12, 2000.

[13] A. Bletsas, A. Khisti, D. Reed, and A. Lippman, "A simple cooperative diversity method based on network path selection," *IEEE Journal on Selected Areas in Communications*, vol. 24, no. 3, pp. 659–672, Mar. 2006.

[14] Z. Jingmei, Z. Qi, S. Chunju, W. Ying, Z. Ping, and Z. Zhang, "Adaptive optimal transmit power allocation for two-hop non-regenerative wireless relaying system," in *Procedings of IEEE 59th Vehicular Technology Conference (VTC)*, vol. 2, pp. 1213–1217, May 2004.

[15] M. Ju and I.-M. Kim, "Relay selection with ANC and TDBC protocols in bidirectional relay networks," *IEEE Transactions on Communications*, vol. 58, no. 12, pp. 3500–3511, Dec. 2010.

[16] M. K. Simon and M. S. Alouini, *Digital Communication over Fading Channels*, New York, NY: John Wiley & Sons, Inc., 2000.

[17] P. Anghel, G. Leus, and M. Kavehl, "Multi-user space-time coding in cooperative networks," in *Proceedings of IEEE International Conference on Acoustics, Speech, and Signal Processing (ICASSP)*, vol. 4, pp. 73–76, Apr. 2003.

[18] M. Abramowitz and I. A. Stegun, *Handbook of Mathematical Functions with Formulas, Graphs, and Mathematical Tables*. New York, NY: Dover Publications, ninth ed., 1970.

[19] K. Seddik, A. Sadek, W. Su, and K. Liu, "Outage analysis of multi-node amplify-and-forward relay networks," in *Proceedings of IEEE Wireless Communications and Networking Conference (WCNC)*, vol. 2, pp. 1184–1188, Apr. 2006.

[20] G. Sharma, V. Ganwani, U. Desai, and S. Merchant, "Performance analysis of maximum likelihood decode and forward cooperative systems in rayleigh fading," in *Proceedings of IEEE International Conference on Communications(ICC)*, pp. 1–5, Jun. 2009.

[21] V. Tarokh, H. Jafarkhani, and A. Calderbank, "Space-time block coding for wireless communications: performance results," *IEEE Journal on Selected Areas in Communications*, vol. 17, no. 3, pp. 451–460, Mar 1999.

[22] Y. Jing and B. Hassibi, "Distributed space-time coding in wireless relay networks," *IEEE Transactions on Wireless Communications*, vol. 5, no. 12, pp. 3524–3536, Dec. 2006.

[23] Y. Jing and H. Jafarkhani, "Using orthogonal and quasi-orthogonal designs in wireless relay networks," *IEEE Transactions on Information Theory*, vol. 53, no. 11, pp. 4106–4118, Nov. 2007.

[24] B. Maham, A. Hjorungnes, and G. Abreu, "Distributed GABBA space-time codes in amplify-and-forward relay networks," *IEEE Transactions on Wireless Communications*, vol. 8, no. 4, pp. 2036–2045, Apr. 2009.

[25] B. Hassibi and B. Hochwald, "High-rate codes that are linear in space and time," *IEEE Transactions on Information Theory*, vol. 48, no. 7, pp. 1804 –1824, jul 2002.

[26] G. Freitas de Abreu, "GABBA codes: Generalized full-rate orthogonally decodable space-time block codes," in *Proceedings of Thirty-Ninth Asilomar Conference on Signals, Systems and Computers*, pp. 1278–1283, Nov. 2005.

[27] M. Vajapeyam and U. Mitra, "Performance analysis of distributed space-time coded protocols for wireless multi-hop communications," *IEEE Transactions on Wireless Communications*, vol. 9, no. 1, pp. 122–133, Jan. 2010.

[28] S. Barbarossa and G. Scutari, "Distributed space-time coding strategies for wide-band multihop networks: regenerative vs. non-regenerative relays," in *Proceedings of IEEE International Conference on Acoustics, Speech, and Signal Processing (ICASSP)*, vol. 4, pp. 501–504, May 2004.

[29] J. G.Proakis, *Digital Communication*. Fourth Edition, McGraw Hill International Edition, ISBN 0-07-232111-3, 2001.

[30] G. Scutari and S. Barbarossa, "Distributed space-time coding for regenerative relay networks," *IEEE Transactions on Wireless Communications*, vol. 4, no. 5, pp. 2387– 2399, Sept. 2005.

[31] P. Anghel and M. Kaveh, "On the performance of distributed space-time coding systems with one and two non-regenerative relays," *IEEE Transactions on Wireless Communications*, vol. 5, no. 3, pp. 682–692, Mar. 2006.

[32] Y. Chen, G. Yu, P. Qiu, and Z. Zhang, "Power-aware cooperative relay selection strategies in wireless ad hoc networks," in *Proceedings of IEEE 17th International Symposium on Personal, Indoor and Mobile Radio Communications (PIMRC)*, pp. 1–5, Sept. 2006.

[33] K.-S. Hwang and Y.-C. Ko, "An efficient relay selection algorithm for cooperative networks," in *Proceedings of IEEE 66th Vehicular Technology Conference*, pp. 81–85, Oct. 2007,.

[34] C.-L. Wang and S.-J. Syue, "An efficient relay selection protocol for cooperative wireless sensor networks," in *Proceedings of IEEE Wireless Communications and Networking Conference (WCNC)*, pp. 1–5, Apr. 2009.

[35] A. Bletsas, A. Khisti, and M. Win, "Opportunistic cooperative diversity with feedback and cheap radios," *IEEE Transactions on Wireless Communications*, vol. 7, no. 5, pp. 1823–1827, May 2008.

[36] A. Tajer and A. Nosratinia, "Opportunistic cooperation via relay selection with minimal information exchange," in *Proceedings of IEEE International Symposium on Information Theory (ISIT)*, pp. 1926–1930, Jun. 2007.

[37] E. Beres and R. Adve, "Selection cooperation in multi-source cooperative networks," *IEEE Transactions on Wireless Communications*, vol. 7, no. 1, pp. 118–127, Jan. 2008.

[38] R. Tannious and A. Nosratinia, "Spectrally-efficient relay selection with limited feedback," *IEEE Journal on Selected Areas in Communications*, vol. 26, no. 8, pp. 1419–1428, Oct. 2008.

[39] F. A. Onat, Y. Fan, H. Yanikomeroglu, and H. V. Poor, "Threshold-based relay selection for detect-and-forward relaying in cooperative wireless networks," *EURASIP Journal on Wireless Communications and Networking*, pp. 1–13, Apr. 2010.

[40] L. Sun, T. Zhang, L. Lu, and H. Niu, "Cooperative communications with relay selection in wireless sensor networks," *IEEE Transactions on Consumer Electronics*, vol. 55, no. 2, pp. 513–517, May 2009.

[41] W. Su, A. Sadek, and K. Liu, "SER performance analysis and optimum power allocation for decode-and-forward cooperation protocol in wireless networks," in *Proceedings of IEEE Wireless Communications and Networking Conference (WCNC)*, vol. 2, pp. 984– 989, Mar. 2005.

[42] J. Luo, R. Blum, L. Cimini, L. Greenstein, and A. Haimovich, "Decode-and-forward cooperative diversity with power allocation in wireless networks," *IEEE Transactions on Wireless Communications*, vol. 6, no. 3, pp. 793–799, Mar. 2007.

[43] W.-J. Huang, Y.-W. Hong, and C.-C. Kuo, "Lifetime maximization for amplify-and-forward cooperative networks," *IEEE Transactions on Wireless Communications*, vol. 7, no. 5, pp. 1800–1805, May 2008.

[44] K. Vardhe, D. Reynolds, and B. Woerner, "Joint power allocation and relay selection for multiuser cooperative communication," *IEEE Transactions on Wireless Communications*, vol. 9, no. 4, pp. 1255–1260, Apr. 2010.

[45] B. Rankov and A. Wittneben, "Spectral efficient protocols for half-duplex fading relay channels," *IEEE Journal on Selected Areas in Communications*, vol. 25, no. 2, pp. 379–389, Feb. 2007.

[46] I. Krikidis, "Relay selection for two-way relay channels with MABC DF: A diversity perspective," *IEEE Transactions on Vehicular Technology*, vol. 59, no. 9, pp. 4620–4628, Nov. 2010.

[47] C. Y. Lee and G. U. Hwang, "Fair and minimal power allocation in a two-hop relay network for QoS support," *IEEE Transactions on Wireless Communications*, vol. 10, no. 11, pp. 3864–3873, Nov. 2011.

[48] F. Ke, S. Feng, and H. Zhuang, "Relay selection and power allocation for cooperative network based on energy pricing," *IEEE Communications Letters*, vol. 14, no. 5, pp. 396–398, May 2010.

[49] S. Talwar, Y. Jing, and S. Shahbazpanahi, "Joint relay selection and power allocation for two-way relay networks," *IEEE Signal Processing Letters*, vol. 18, no. 2, pp. 91–94, Feb. 2011.

[50] L. Song, "Relay selection for two-way relaying with amplify-and-forward protocols," *IEEE Transactions on Vehicular Technology*, vol. 60, no. 4, pp. 1954–1959, May. 2011.

[51] M. Zhou, Q. Cui, R. Jantti, and X. Tao, "Energy-efficient relay selection and power allocation for two-way relay channel with analog network coding," *IEEE Communications Letters*, vol. 16, no. 6, pp. 816–819, Jun. 2012.

[52] T. Cover and A. Gamal, "Capacity theorems for the relay channel," *IEEE Transactions on Information Theory*, vol. 25, no. 5, pp. 572–584, Sept. 1979.

[53] V. Emanian, P. A. Anghel, and M. Kaveh, "Multi-user spatial diversity in a shadow-fading environment," in *Proceedings of IEEE Vehicular Technology Conference (VTC)*, pp. 573–576, 2002.

[54] M. Yuksel and E. Erkip, "Diversity in relaying protocols with amplify and forward," in *Proceedings of IEEE Global Telecommunications Conference (GLOBECOM)*, vol. 4, pp. 2025–2029, Dec. 2003.

[55] H. Min, S. Lee, K. Kwak, and D. Hong, "Effect of multiple antennas at the source on outage probability for amplify-and-forward relaying systems," *IEEE Transactions on Wireless Communications*, vol. 8, no. 2, pp. 633–637, May. 2010.

[56] A. Bou Saleh, S. Redana, B. Raaf, T. Riihonen, J. Hamalainen, and R. Wichman, "Performance of amplify-and-forward and decode-and-forward relays in LTE-advanced," in *Proceedings of IEEE 70th Vehicular Technology Conference (VTC)*, pp. 1–5, Sept. 2009.

[57] O. Bulakci, S. Redana, B. Raaf, and J. Hamalainen, "System optimization in relay enhanced LTE-advanced networks via uplink power control," in *Proceedings of IEEE 71st Vehicular Technology Conference (VTC)*, pp. 1–5, May. 2010.

[58] S. Barbarossa and G. Scutari, "Distributed space-time coding for multi-hop networks," in *Proceedings of IEEE International Conference on Communications (ICC)*, vol. 2, pp. 916–920, Jun. 2004.

[59] P. Anghel and M. Kaveh, "Exact symbol error probability of a cooperative network in a rayleigh-fading environment," *IEEE Transactions on Wireless Communications*, vol. 3, no. 5, pp. 1416–1421, Sept. 2004.

[60] J. Hu and N. Beaulieui, "Performance analysis of decode-and-forward relaying with selection combining," *IEEE Communications Letters*, vol. 11, no. 6, pp. 489–491, Jun. 2007.

[61] P. A. Anghel, G. Leus, and M. Kaveh, "Distributed space-time cooperative systems with regenerative relays," *IEEE Transactions on Wireless Communications*, vol. 5, no. 11, pp. 3130–3140, Nov. 2006.

[62] D. Gunduz, M. Khojastepour, A. Goldsmith, and H. Poor, "Multi-hop MIMO relay networks: diversity-multiplexing trade-off analysis," *IEEE Transactions on Wireless Communications*, vol. 9, no. 5, pp. 1738–1747, May. 2010.

[63] H. Wicaksana, S. Ting, M. Motani, and Y. Guan, "On the diversity-multiplexing tradeoff of amplify-and-forward half-duplex relaying," *IEEE Transactions on Communications*, vol. 58, no. 12, pp. 3621–3630, Dec. 2010.

[64] S. Cui, A. Goldsmith, and A. Bahai, "Energy-efficiency of MIMO and cooperative MIMO techniques in sensor networks," *IEEE Journal on Selected Areas in Communications*, vol. 22, no. 6, pp. 1089–1098, Aug. 2004.

[65] R. Fantini, D. Sabella, and M. Caretti, "Energy efficiency in LTE-advanced networks with relay nodes," in *Proceedings of IEEE 73rd Vehicular Technology Conference (VTC Spring)*, pp. 1–5, May 2011.

[66] H. Kim and T. Chen, "A study of energy efficient transparent relay using cooperative strategy," in *Proceedings of IEEE 73rd Vehicular Technology Conference (VTC Spring)*, pp. 1 –5, may 2011.

[67] G. de Oliveira Brante, M. Kakitani, and R. Souza, "Energy efficiency analysis of some cooperative and non-cooperative transmission schemes in wireless sensor networks," *IEEE Transactions on Communications*, vol. 59, no. 10, pp. 2671–2677, Oct. 2011.

[68] L. Q. V. Tran, O. Berder, and O. Sentieys, "Non-regenerative full distributed space-time codes in cooperative relaying networks," in *Proceedings of IEEE Wireless Communications and Networking Conference (WCNC)*, pp. 1529–1533, Mar. 2011.

[69] L. Zheng and D. Tse, "Diversity and multiplexing: a fundamental tradeoff in multiple-antenna channels," *IEEE Transactions on Information Theory*, vol. 49, no. 5, pp. 1073–1096, May 2003.

[70] T. Melly, E. Le Roux, F. Peng, D. Ruffieux, N. Raemy, F. Giroud, A. Ribordy, and V. Peiris, "Wisenet: Design of a low-power RF CMOS receiver chip for wireless applications," in *CSEM Scientific and Technical Report*, page 25, 2002.

[71] M. Otis, I. Chee, R. Lu, N. Pletcher, S. Gambini, and J. Rabaey, *Low-power electronics design*. CRC Press, Dec. 2003.

[72] T. H. Lee, *The Design of CMOS Radio-Frequency Integrated Circuits*. Cambridge Univ. Press, Cambridge, UK, 1998.

[73] A. El-Hoiydi and J.-D. Decotignie, "Wisemac: an ultra low power MAC protocol for the downlink of infrastructure wireless sensor networks," in *Proceedings of Ninth International Symposium on Computers and Communications*, vol. 1, pp. 244–251, Jun. 2004.

[74] E.-Y. Lin, J. Rabaey, S. Wiethoelter, and A. Wolisz, "Receiver initiated rendezvous schemes for sensor networks," in *Proceedings of IEEE Global Telecommunications Conference (GLOBECOM)*, vol. 5, pp. 3117–3122, Dec. 2005.

[75] T. D. Nguyen, O. Berder, and O. Sentieys, "Impact of transmission synchronization error and cooperative reception techniques on the performance of cooperative MIMO systems," *IEEE International Communication Conference (ICC)*, pp. 460–4605, May 2008.

[76] T.-D. Nguyen, O. Berder, and O. Sentieys, "Cooperative MISO and relay comparison in energy constrained WSNs," in *Proceedings of IEEE 71st Vehicular Technology Conference (VTC Spring)*, pp. 1–5, May 2010.

[77] ——, "Energy-efficient cooperative techniques for infrastructure-to-vehicle communications," *IEEE Transactions on Intelligent Transportation Systems*, vol. 12, no. 3, pp. 659–668, Sept. 2011.

[78] C. Zhai, J. Liu, L. Zheng, and H. Xu, "Lifetime maximization via a new cooperative MAC protocol in wireless sensor networks," in *Proceedings of IEEE Global Telecommunications Conference (GLOBECOM)*, pp. 1–6, Dec. 2009.

[79] I. Stanojev, O. Simeone, Y. Bar-Ness, and D. H. Kim, "Energy efficiency of non-collaborative and collaborative Hybrid-ARQ protocols," *IEEE Transactions on Wireless Communications*, vol. 8, no. 1, pp. 326–335, Jan. 2009.

[80] W. Ye, J. Heidemann, and D. Estrin, "An energy-efficient MAC protocol for wireless sensor networks," in *Proceedings of IEEE INFOCOM*, vol. 3, pp. 1567–1576, 2002.

[81] A. Corporation, *http://www.atmel.com/, AVR Micro-controller AT90LS8535 Reference Manual.*

[82] R. M. Inc., *http://www.rfm.com/, ASH Transceiver TR1000 Data Sheet.*

[83] J. Polastre, J. Hill, and D. Culler, "Versatile low power media access for wireless sensor networks," in *Proceedings of the 2nd international conference on Embedded networked sensor systems*. New York, NY, USA: ACM, 2004, pp. 95–107.

[84] A. Ben Nacef, S.-M. Senouci, Y. Ghamri-Doudane, and A.-L. Beylot, "A cooperative low power MAC protocol for wireless sensor networks," in *Proceedings of IEEE International Conference on Communications (ICC)*, pp. 1–6, Jun. 2011.

[85] M. M. Alam, O. Berder, D. Menard, T. Anger, and O. Sentieys, "A hybrid model for accurate energy analysis of WSN nodes," *EURASIP Journal on Embedded Systemes*, vol. 4, pp. 1–16, Jan. 2011.

[86] Q. Wang, M. Hempstead, and W. Yang, "A realistic power consumption model for wireless sensor network devices," in *Proceedings of Sensor and Ad-hoc Communications and Networks (SECON)*, vol. 1, pp. 286–295, Sept. 2006.

[87] CAIRN/INRIA, *http://powwow.gforge.inria.fr/*.

[88] O. Berder, P. Quemerais, O. Sentieys, J. Astier, T. Nguyen, J. Menard, G. Le Mestre, Y. Le Roux, Y. Kokar, G. Zaharia, R. Benzerga, X. Castel, M. Himdi, G. El Zein, S. Jegou, P. Cosquer, and M. Bernard, "Cooperative communications between vehicles and intelligent road signs," in *Proceedings of 8th International Conference on ITS Telecommunications*, pp. 121–126, Oct. 2008.

[89] Chipcon, *Smart RF CC2420, 2.4GHz IEEE 802.15.4/ZigBee-ready RF Transceiver*.

[90] T. S. Rappaport, *Wireless Communications Principles and Practice*. Prentice Hall, ISBN 978-0130422323, 2002.

[91] Y. Li, B. Bakkaloglu, and C. Chakrabarti, "A system level energy model and energy-quality evaluation for integrated transceiver front-ends ," *IEEE Transactions on Very Large Scale Integration Systems*, vol. 15, no. 1, pp. 90–103, Jan. 2007.

[92] M. Yuksel and E. Erkip, "Diversity in relaying protocols with amplify and forward," in *Proceedings of Global Telecommunication Conference (GLOBECOM)*, vol. 4, pp. 2025–2029, Dec. 2003.

[93] V. Ganwani, B. Dey, and G. Sharma, "Performance analysis of amplify and forward based cooperative diversity in MIMO relay channels," in *Proceedings of Vehicular Technology Conference (VTC Spring)*, pp. 1–5, 2009.

[94] Y. Song, H. Shin, and E.-K. Hong, "MIMO cooperative diversity with scalar-gain amplify-and-forward relaying," *IEEE Transactions on Communications*, vol. 57, no. 7, pp. 1932–1938, Jul. 2009.

[95] S. Barbarossa and G. Scutari, "Distributed space-time coding for multi-hop networks," in *Proceedings of IEEE International Conference on Acoustics, Speech and Signal Processing (ICASSP)*, pp. 50–504, May 2004.

[96] K. G. Seddik, A. K. Sadek, W. Su, and K. R. Liu, "Outage analysis of multi-node amplify-and-forward relay networks," in *Proceedings of Wireless Communication and Networking Conference (WCNC)*, vol. 2, pp. 1184–1188, Apr. 2006.

[97] H. Wan, J.-F. Diouris, and G. Andrieux, "Time synchronization for cooperative communication in wireless sensor networks," *Wireless Personal Communications*, vol. 63, no. 4, pp. 977–993, Apr. 2012.

[98] H. Zhu and G. Cao, "RDCF: A relay-enabled medium access control protocol for wireless ad hoc networks," *IEEE Transactions on Mobile Computing*, vol. 5, no. 9, pp. 1201–1214, Sept. 2006.

[99] P. Liu, Z. Tao, S. Narayanan, T. Korakis, and S. S. Panwar, "Coopmac: A cooperative MAC for wireless lans," *IEEE Journal on Selected Areas in Communications*, vol. 25, no. 2, pp. 340–354, Feb. 2007.

[100] S. Zou, B. Li, H. Wu, Q. Zhang, W. Zhu, and S. Cheng, "A relay-aided media access (RAMA) protocol in multirate wireless networks," *IEEE Transactions on Vehicular Technology*, vol. 55, no. 5, pp. 1657–1667, Sept. 2006.

[101] J. Pathmasuritharam, A. Das, and A. Gupta, "Efficient multi-rate relaying (EMR) MAC protocol for ad hoc networks," in *Proceedings of IEEE International Conference on Communications (ICC)*, vol. 5, pp. 2947– 2951, May 2005.

[102] T. Korakis, Z. Tao, S. R. Singh, P. Liu, and S. S. Panwar, "Implementation of a cooperative MAC protocol: Performance and challenges in a real environment," *EURASIP Journal on Wireless Communications and Networking*, pp. 1– 19, Feb. 2009.

[103] J. Zhang, Q. Zhang, and W. Jia, "Vc-mac: A cooperative MAC protocol in vehicular networks," *IEEE Transactions on Vehicular Technology*, vol. 58, no. 3, pp. 1561–1571, Mar. 2009.

[104] T. Zhou, H. Sharif, M. Hempel, P. Mahasukhon, W. Wang, and T. Ma, "A novel adaptive distributed cooperative relaying MAC protocol for vehicular networks," *IEEE Journal on Selected Areas in Communications*, vol. 29, no. 1, pp. 72 –82, january 2011.

[105] H. Yang, H.-Y. Shen, and B. Sikdar, "A MAC protocol for cooperative MIMO transmissions in sensor networks," in *Proceedings of IEEE Global Telecommunications Conference (GLOBECOM)*, pp. 636–640, Nov. 2007.

[106] S. Moh, C. Yu, S.-M. Park, H.-N. Kim, and J. Park, "CD-mac: Cooperative diversity MAC for robust communication in wireless ad hoc networks," in *Proceedings of IEEE International Conference on Communications (ICC)*, pp. 3636–3641, Jun. 2007.

[107] S. Moh and C. Yu, "A cooperative diversity-based robust MAC protocol in wireless ad hoc networks," *IEEE Transactions on Parallel and Distributed Systems*, vol. 22, no. 3, pp. 353–363, Mar. 2011.

[108] Z. Yang, Y.-D. Yao, X. Li, and D. Zheng, "A TDMA-based mac protocol with cooperative diversity," *IEEE Communications Letters*, vol. 14, no. 6, pp. 542–544, Jun. 2010.

[109] Y. Zhou, J. Liu, C. Zhai, and L. Zheng, "Two-transmitter two-receiver cooperative MAC protocol: Cross-layer design and performance analysis," *IEEE Transactions on Vehicular Technology*, vol. 59, no. 8, pp. 4116–4127, Oct. 2010.

[110] M. Buettner, G. V. Yee, E. Anderson, and R. Han, "X-mac: a short preamble MAC protocol for duty-cycled wireless sensor networks," in *Proceedings of the 4th international conference on Embedded networked sensor systems*. New York, NY, USA: ACM, 2006, pp. 307–320.

[111] T. Ahsin and S. Ben Slimane, "Energy efficiency using cooperative relaying," in *Proceedings of IEEE 22nd International Symposium on Personal Indoor and Mobile Radio Communications (PIMRC)*, pp. 1698–1702, Sept. 2011.

[112] N. Guan, Y. Zhou, H. Liu, L. Tian, and J. Shi, "An energy efficient cooperative multicast transmission scheme with power control," in *Proceedings of IEEE Global Telecommunications Conference (GLOBECOM)*, pp. 1–5, Dec. 2011.

[113] J. Feng, R. Zhang, S. Ng, and L. Hanzo, "Relay selection for energy-efficient cooperative media access control," in *Proceedings of IEEE Wireless Communications and Networking Conference (WCNC)*, pp. 287–292, Mar. 2011.

[114] Y. Qi, R. Hoshyar, M. Imran, and R. Tafazolli, "The energy efficiency analysis of HARQ in hybrid relaying systems," in *Proceedings of IEEE 73rd Vehicular Technology Conference (VTC Spring)*, pp. 1–5, May 2011.

[115] A. Crismani, F. Babich, and L. Hanzo, "Cross-layer solutions for cooperative medium access control protocols," in *Proceedings of IEEE 71st Vehicular Technology Conference (VTC Spring)*, pp. 1–5, May 2010.

[116] J. Alonso-Zarate, E. Stavrou, A. Stamou, P. Angelidis, L. Alonso, and C. Verikoukis, "Energy-efficiency evaluation of a medium access control protocol for cooperative ARQ," in *Proceedings of IEEE International Conference on Communications (ICC)*, june 2011, pp. 1–5.

[117] R. Zhang and J.-M. Gorce, "Lower bound of energy-delay tradeoff of cooperative MIMO communications," in *Proceedings of IEEE International Conference on Communications (ICC)*, pp. 1–6, May 2010.

[118] J. Gorce, R. Zhang, K. Jaffrè ands Runser, and C. Goursaud, "Energy, latency and capacity trade-offs in wireless multi-hop networks," in *Proceedings of IEEE 21st International Symposium on Personal Indoor and Mobile Radio Communications (PIMRC)*, pp. 2757–2762, Sept. 2010.

[119] P. Ferrand, C. Goursaud, and J. Gorce, "Energy-delay tradeoffs in a linear sequence of relay channels," in *Proceedings of IEEE Wireless Communications and Networking Conference (WCNC)*, pp. 1140–1145, Apr. 2012.

[120] I. S. Rappaport and I. M. Ryzhik, *Table of Integrals, Series and Products*. San Diego, CA: Academic Press, fifth ed., 1994.

VU :

Le Directeur de thèse

VU :

Le Responsable de l'École Doctorale

VU pour autorisation de soutenance

Rennes, le

Le Président de l'Université de Rennes 1

Guy Cathelineau

VU après soutenance pour autorisation de publication :

Le Président de Jury,